SYNTHESIS AND CHARACTERIZATION OF NOVEL GREEN CHEMICALS FROM RICE HUSKS AND THEIR TECHNOLOGICAL APPLICATIONS IN ENVIRONMENTAL POLLUTION CONTROL

KUNGU RAPHAEL EMMANUEL

DOCTOR OF PHILOSOPHY

(Environmental Technology)

JOMO KENYATTA UNIVERSITY OF

AGRICULTURE AND TECHNOLOGY

2021

Synthesis and characterization of novel green chemicals from rice husks and their technological applications in environmental pollution control in Kenya

Raphael Emmanuel Kungu

A Thesis Submitted in Fulfillment of the Requirements for the Degree of Doctor of Philosophy in Environmental Technology of the Jomo Kenyatta University of Agriculture and Technology

2021

DECLARATION

This thesis is my original work and has not been presented for award of degree in any other University.

Signature.....Date……

.

Reg. EET40-5347/2016 Raphael Emmanuel Kungu

This thesis has been submitted for examination with our approval as university supervisors.

Signature.....Date……

.

Dr. Paul Njogu, PhD

JKUAT, Kenya

Signature.....Date……

.

Prof. Robert Kinyua, PhD

JKUAT, Kenya

DEDICATION

This work is first and foremost dedicated to the Almighty God Who cares for us, inspires, and blesses our work. Secondly, the work is dedicated with total respect and appreciation to my late loving parents Kungu (Wa Muthitu) and Wanjiku (Wa Ranjoni) for their prayers, nurture, and sacrifices to educate me. Finally, I dedicate this work to my wife Jacqueline Wanjiru and children; Beatrice Wanjiku, Susan Gitiri, James Kungu for their understanding and encouragement that enabled me to succeed in this work.

ACKNOWLEDGEMENT

I deeply acknowledge the contributions of my supervisors Dr. P. Njogu and Professor R. Kinyua of Jomo Kenyatta University of Agriculture and Technology. I sincerely thank Jomo Kenyatta University of Agriculture and Technology (JKUAT) for offering me the opportunity to pursue my studies and for providing me with the ever encouraging and ready to assist academic mentors. I thank and acknowledge the support I received from the National Research Fund from the innovation fund 2015/2016 financial year. I also thank Dr. P. Karanja, the Food Science department for giving me space to do my experiments in the Food Science laboratory. I acknowledge the assistance of S.K. Mwaura (Research assistant) who helped me in all the field and laboratory work, Amos Kamau (Msc. Student), Dr. Jane Mburu, Chemistry department, Kenyatta University, Chris Agata, KIRDI and Peter, Mines and Geology for offering me invaluable assistance. I also acknowledge the support I got from my family members and friends especially my wife Jacqueline Wanjiru. I thank you and I will forever remain indebted to you. God bless you all.

May the Almighty Father also bless you.

TABLE OF CONTENTS

LIST OF TABLES

LIST OF FIGURES

LIST OF PLATES

LIST OF APPENDICES

ABBREVIATIONS AND ACRONYMS

AAS	Atomic absorption spectroscopy
AC	Activated carbon
AFR	Air flow rate
ANOVA	Analysis of variance
AOAC	Association of official analytical chemists
ARH	Acid treated rice husk
ASTM	American society for testing and materials
BAS	Biogenic amorphous silica
BRHA	Black rice husk ash
CAS	Chemical abstracts service
CHP	Combined heat and power system
CMC	Ceramic matrix composites
COGEN	Co-generation of heat and power
CRH	Calcined rice husk
CTAB	Cetrimonium bromide
DC	Direct current
DI	Deionized H_2O
DTGS	Deuterated triglycine sulfate
EDS	Energy-dispersive spectroscopy
EDXRF	Energy-dispersive X-ray florescence
ENR	Epoxidized natural rubber
USEPA	United states environmental protection agency
eV	Electron Volt

FCR	Fuel consumption rate
FT-IR	Fourier transformation infra-red spectroscopy
GOK	Government of Kenya
HDPE	High-density polyethylene
HV	Heating value
ICP	Inductively coupled plasma emission spectrometer
IE	Industry ecology
IOP	Institute of Physics
IR	Infra-red
ISO	International Organization for Standardization
JKUAT	Jomo Kenyatta University of agriculture and technology
KBr	Potassium bromide
KEBS	Kenya bureau of standards
KIRDI	Kenya industrial research and development Institute
KS	Kenya standard
LBDA	Lake basin development authority
LLDPE	Linear low-density polyethylene
MCM	Mobil Composition of Matter
MJ	Mega Joule
MSD	Material safety data
MSW	Municipal solid waste
MWNT	Multi-walled carbon nanotubes
NCPB	National cereals and produce board

NIB	National irrigation board
NRI	Natural Resources Institute
OPB1	Openly burnt sample1
PAC	Powdered activated carbon
PBH	Parboiled husks
PCL	Polycaprolactone
PDMS	Phenyldimethylchlorosilane
PEG	Polyethylene glycol
PPL	Plane polarized light
RH	Rice husk
RHA	Rice Husk Ash
RHAC	Rice Husk Activated carbon
RH-ash	Rice husks ash
RRH	Raw Rice Husk
SAR	Stoichiometric air of husks
SBA	Santa Barbara (Amorphous type) mesoporous silica
SEM	Scanning Electronic Microscope
SG	Silica gel
SS	**S**tainless steel
SWNT	Single-walled carbon nanotubes
TEOS	Tetraethylorthosilicate
TGA	Thermal gravimetric analysis
TMCS	Trimethylchlorosilane
TPR	Thermoplastic Rubber

TXRF	Total X-ray Fluorescence
UNEP	United Nations Environment Program
UNIDO	United Nations Industrial Development Organization
USA	United States of America
WMT	Waste Management Theory
WRHA	White Rice Husk Ash
XPL	Cross polarized light
XRD	X-ray diffraction

ABSTRACT

Rice husks (RH) are products of rice milling. Waste management of RH creates health and environmental problems. Wastewater discharges lead to serious environmental problems. The goal of the study was to synthesize and characterize industrial chemicals using RH, test their technological application in wastewater treatment especially lead, chromium and cadmium removal in water. RH was collected from rice millers in Kirinyaga County, whereas wastewater samples were collected from tea factory in Kiambu County, Kenya, A oxidation reactor for converting RH to RHA was developed. Optimum conditions for sodium silicate (SS) and silica gel (SG) production were determined by separately leaching with 0.5 M HCl and 0.5 M H_2SO_4. Silica (S) obtained was reacted with 1 M, 2 M, 3 M NaOH to find optimum conditions for SS production. SS solutions were further reacted with 3 M HCl each to determine ideal conditions for silica gel (SG) production. To prepare RHACs, RH was carbonized and residual char activated with sodium hydroxide (NaOH) and phosphoric acid (H_3PO_4). Resulting SS, SG, and RHACs samples were analyzed and characterized using TXRF, SEM, XRD, and infrared spectroscopy. Heavy metal removal efficiency of RHACs was tested by mixing aliquots of wastewater; adsorbent (RHAC), centrifuged at 4500 rpm then using UV spectrophotometry (765 nm). Removal efficiency and kinetics of removal of Pb, Cd, and Cr using RHACs evaluated using AA spectroscopy. RH had a moisture content of 7.07 ± 0.63 %. Percent ash content ranged from 23.43 ± 0.77 to 22.17 ± 0.48. Leaching (0.5 M HCl) RH and thermal treatment at 600 °C yielded the best % SiO_2 and removed the most metallic impurities (P_2O_5, K_2O, CaO, MnO, ZnO). To determine the optimum conditions for the conversion of RHA to SS and SG, RH was converted to RHA at different temperatures (400, 500, 600 °C), 60 g leached RHA was then reacted with 300 mL of 1 M, 2 M, 3 M NaOH. Infrared spectroscopy analysis indicated HCl leaching availed more silicon dioxide. Post leaching RHA yielded 97.37 SiO_2 % (water), 99.17 SiO_2 % (HCl), and 99.02 SiO_2 % (H_2SO_4) silicon dioxide respectively. SS (Liquid neutral) from RH analyzed at KEBs compared well with KS2350:2012 Standard. Results show NaOH-RHACs were more efficient in total phenols removal. The total phenolic removal efficiency from factory tea wastewater was 72-77 % for NaOH-RHACs compared to 2.6% for H_3PO_4-RHACs. Langmuir correlation coefficient R^2 (0.99) for Pb (II), Cd (II) and Cr (ll) removal using NaOH and H_3P0_4-RHACs indicated monolayer adsorption. Kinetic pseudo-second-order R^2 (0.90) values indicated electron transfer between solution and adsorbent. Processing of RH wastes into innovative novel chemicals that have industrial applications is a sustainable approach of managing the wastes. Silica, silica gel and RHACs can be manufactured from RH due its high silica content. Such chemicals find wide spread applications in wastewater management. This development of wastewater treatment chemicals can mitigate the problems caused by heavy metal pollutants.

CHAPTER ONE

INTRODUCTION

1.1 Background to the study

Rice is a grass seed from *Oryza sativa* (Asian rice) species or *Oryza glaberrima* species also known as African rice. Rice is grown widely across the globe and is usually a staple food for many people (Seck, 2012). It is key to food security in many areas of the world mainly in the Caribbean, Asia, and Africa. According to Atera et al (2018), 400 million metric tons of milled rice are produced annually in the world. Unlike maize and wheat consumed as human and livestock feed, rice remains the most favored grain globally for human consumption.

In Kenya, rice is mostly grown mainly in the counties of Tana River (Tana delta, Msambweni), Kisumu (Ahero, West Kano, Kuria), Migori, Kirinyaga (Mwea), and Busia (Bunyala) by small-scale farmers. As reported by Majiwa et al. (2018), there are four main rice mills with varying capacities across Kenya. Rice mills in the Mwea sub-county can produce 24 metric tons per hour while those in Tana delta and LBDA have milling capacities of 3 and 3.5 metric tons per hour respectively. The main rice traders are the National Cereals and Produce Board (NCPB) and Lake Basin Development Authority (LBDA) in Ahero, Mwea, and Kibos. National Irrigation Board (NIB), Capwell Industries, and Mwea Farmers' Multipurpose Cooperative Society supply the major supermarkets in Kenya. According to Gewona (2018), Kenya has about 95% of its rice grown through irrigation. Areas like the Yala swamp region near Lake Victoria, LBDA, and Mwea in central Kenya contribute to 78% of all irrigated farms. Rice farming plays a vital role in poverty alleviation especially its integral role in the economic status of the country (Inoue, et al., 2013). There is increased acceptance that rice and its products are a strategic commodity to fuel economic growth and also contribute towards poverty reduction and hunger in Kenya. Because of this, Kenya has embarked on a program to boost its rice production capacity.

Rice husk (or hull) is the outer layer of rice, which is separated from the rice grains during the process of milling. Rice grain consists of 20% rice husk by weight. Gummert and Rickman (2006) indicated how rice husks were considered agro-wastes, being dumped or burnt on landfills. However, rice husk is now considered an economically viable agro-waste, which can assist in controlling environmental pollution. Some enterprising companies are turning it into various products not only for the eco-conscious marketplace but also for the industrial sector (Santiaguel, 2013).

In Kenya, the production of rice has resulted in increased production of rice husks, which are considered agro-wastes (GOK, 2009). Additionally, rice husk management in the country has not been viable and sustainable and has majorly been via open burning which has led to environmental pollution as well as the release of greenhouse gases. Further, there is a proposition by UNEP for countries to recover valuable materials from the waste stream to enhance waste to wealth conversion (Singhania, Agarwal, Kumar, & Sukumaran, 2017). This recommendation is in tandem with Vision 2030 that aspires Kenya to become an industrialized Nation supported through small and micro enterprises (GOK, 2013).

Njogu et al (2015), reports that rice husk once incinerated produces rice husk ash that contains high heat content that can be processed and utilized for industrial purposes. Rice husks ash (RHA) has 80% silica content, which can be converted to sodium silicate, and other silica-related products (Adam, Appaturi, & Iqbal, 2012). Sodium silicate, which can be produced from rice husk ash (RHA), has many applications in soap and detergent production (Hemalatha, Hemasruthi, Priya, Gayathri, & Kavinilavu, 2018). The heat generated during the burning of rice husks can also be used to produce electricity (Lubis, 2018). In addition, rice husks can be used in the production of activated carbon (Menya, Olupot, Storz, Lubwama, & Kiros, 2018).

1.1.1 Kenya National Rice Development Strategy (2008-2018)

Kenya's national rice development strategy was formulated to bring attention to the growing of rice because it was found to have great potential in improving overall

food security and in promoting the economic status of Kenya (GOK, 2009). The main components of the strategy include,

i. Minimizing and eliminating post-harvest losses
ii. Enhancing farmers access to credit and high-quality inputs
iii. Expanding cultivation areas
iv. Offering extension support services
v. Setting up a National Stakeholders Forum
vi. Promoting human resource development as well as effective monitoring and

1.1.2 Global and local rice growing.

In 2018/2019, world production of milled rice was 495.9 million metric tons. China, India, and Indonesia were the top rice-producing countries. China is the world's largest rice producer with 35 % of total world production, which is 148 million metric tons (Durand-Morat, 2021). Low-acreage farmers mainly produce Kenyan rice. Rice milling produces rice husks, which worsen environmental pollution issues, thus it is very important to explore ways of generating chemical materials from rice husks to curtail accumulation and subsequently environmental pollution (Gakungu, 2011).

Rice is the primary food source for over three billion people, influencing complex production ecosystems that relate to issues of global concern, such as food security, poverty alleviation, preservation of cultural heritage, and sustainable development (Van Nguyen & Ferrero, 2006). About 800 million people in the world are suffering from malnutrition due to limited possibilities for expanding rice-growing areas, declining yields, and low returns from production. Rice growth rates are declining in yield due to soil fertility depletion and climate change. Rice farming in Kenya remains an important activity due to its positive impact on increasing household food security, raising farmers' income (Atera, Onyancha, & Majiwa, 2018). Demand for rice in Kenya outstrips its production, a gap filled through imports. Challenges include providing improved rice varieties that are attractive to farmers and

consumers, land and water use management, market information, and extension services, reducing risks caused by poor weather conditions, and reduction of competition from cheap rice imports.

Figure 1.1 below shows the global rice production forecast for 2018/19. Countries in the Asia region produced the most rice.

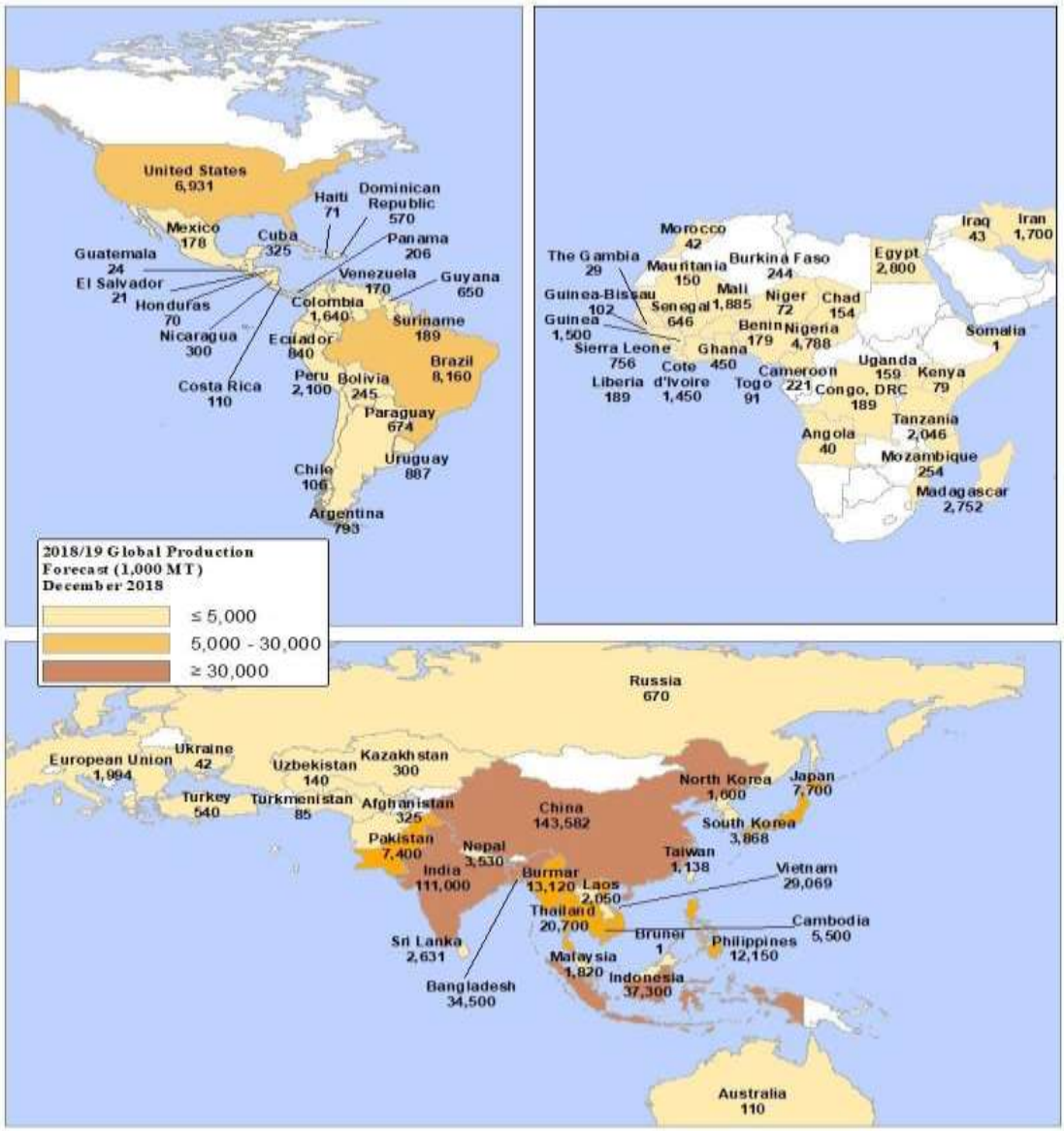

Figure 1.1: Areas in the world growing rice (production forecast for the market year 2018/19)

Source: **(Childs, 2019)**

Figure 1.2 below shows the main rice-growing area, Mwea in the central area, Kenya. Farmers practice low acreage rice farming in this area.

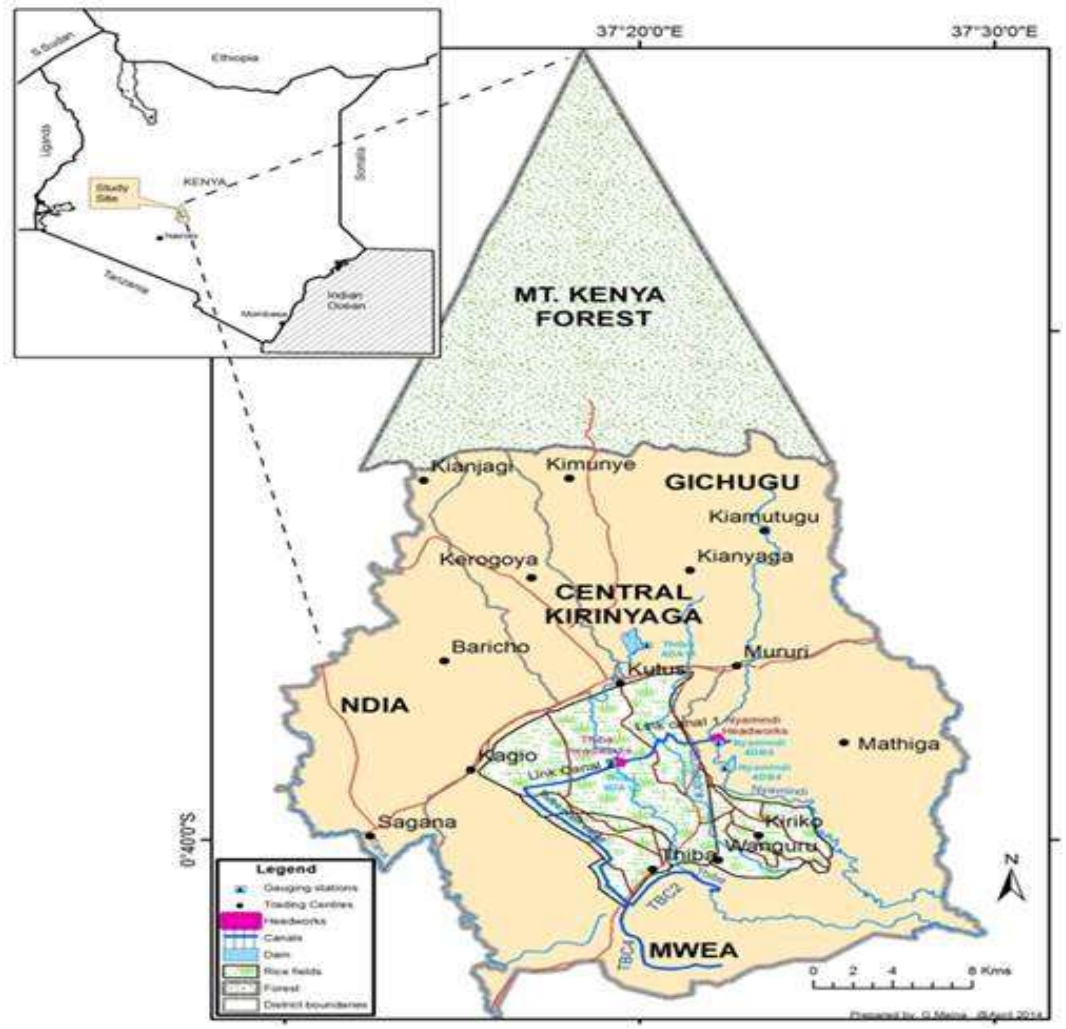

Figure 1.2: Mwea rice-growing area, Kenya.

Source: (Wanja, et al., 2019)

To manage disposed rice husks waste, governments and organizations are trying to reduce waste disposal costs by sales of recovered materials. Energy generation from burning rice husks is also an option (Kumar, et al., 2017)

Unfortunately, waste collection systems are not efficient while disposal systems are generating more pollution. Traditional methods for managing rice husk waste included land filling, incineration, open dumping, and open-air burning. Some of these methods were unsustainable due to limited land area for expansion, potential environmental risks, and increased disposal costs (Singh, Solanki, Ghosh, & Pal, 2020). This has shifted focus to research for more sustainable rice husk waste management strategies with growing interest in chemical treatment of wastes, with a specific interest in resource/energy recovery (Oladejo, Shi, Luo, Yang, & Wu, 2019).

According to Pode (2016) plant biomass (rice husks) use to produce low-cost grade solar silicon has been investigated by relatively few research groups. The design of sustainable and least-cost solid waste management systems is the focus today. This should be done while considering a variety of management processes that can control environmental pollution.

1.2 Statement of the problem

Disposal of rice husks in most developing countries is through open dumping. Public health and environmental quality concerns provide the impetus needed to develop and implement sustainable approaches to waste management (Njogu, Kinyua, Muthoni, & Nemoto, 2015). Rice husk disposal is a problem in rice-growing areas worldwide including Kenya. Current disposal methods of open burning and open dumping create environmental and public health problems. The conversion of rice husks into valuable industrial chemicals would help to solve this disposal. Water pollution is a serious environmental problem. Water pollution can be controlled using rice husk-derived carbons. Preventing waste and water pollution using rice husks are the objectives of this particular study.

1.3 Justification of the study

This study contributes to Kenya's vision 2030 especially Agenda three (3) manufacturing. Industrial development will result from this study. The creation of small industries producing industrial chemicals which otherwise would be imported will contribute to industrial growth by creating a value addition chain. The use of

rice husk waste will create positive multiplier effects in other economic activities. For sustainable development, the needs of future generations must be met (Basuki, 2015). Integrating the environment in socio-economic planning and management by chemically processing rice husks for various products that can increase incomes and thus lift the living standard of many citizens would meet the above goal.

Synthesis of industrial chemicals using rice husks (wastes) would be using local materials in an environmentally sound manner. Designing safer chemicals from the natural world as opposed to the use of fossil unsafe products is recommended in the green chemistry principles (Beach, Cui, & Anastas, 2009). It would also boost economic activity in all rice-growing areas and contribute to industrial development. Extra income from sales of green chemicals would improve the economic status of farmers and locals. The challenge of solid waste processing and upgrading to generate energy and to promote industrial growth is real (Gakungu, 2011).

Wastewater discharges are a serious environmental problem. Rice husk-derived carbons are potentially low-cost adsorbents. Rice husk-derived activated carbons (RHAC) were tested for efficiency in environmental pollution control and subsequently used to control environmental pollution. The proposed use will ensure effective utilization of rice husks waste resulting in a cleaner environment. There will be also an improvement in the industrial sector due to enhanced employment especially to the youths. It is expected to boost the economic growth of all rice-growing areas.

This study will also add to the research database on rice husk management in the country. Physio- and biochemical properties of rice husk are based on geographical location so although we have data on rice husks we do not have any information on local rice husk-derived chemical products. This includes; use of potentiality, their characteristics, and viabilities as chemical industry substitutes.

1.4 Null hypothesis

i. Green industrial chemicals (sodium silicate (Na_2SiO_3), silica gel (SG), activated carbon (AC)) derived from agro-wastes (rice husks) are not significantly different from commercial ones.
ii. The color removal efficiencies of RHACs are not significantly different from commercial ones.
iii. The lead, cadmium and chromium removal efficiencies on wastewater by RHACs obey the Langmuir and Freundlich isotherms.

1.5 Objectives

1.5.1 Main objective

To synthesis and characterize novel green chemicals from rice husks and test their technological applications in environmental pollution control in Kenya.

1.5.2 Specific objectives

i. To determine the ash content, volatile organic compounds, particle size distribution, and moisture content of rice husks from local mills in Mwea, Kenya
ii. To design and fabricate a small-scale silica extraction oxidation reactor for conversion of rice husks to RHA.
iii. To develop and optimize a chemical conversion process of RHA to sodium silicate, silica gel, and activated carbon using green chemistry strategies and approaches.
iv. To determine the kinetics of removal efficiencies of synthesized activated carbon on colour and heavy metals removals in wastewater.

1.6 Scope and limitation of study

(i) Scope of the study

1. The study was conducted using rice husks from Mwea, Kirinyaga County. Sampling was done in March 2017, possible seasonal variations were not considered.
2. Removal efficiencies and kinetics of removal of Priority Pollutants with RHACs were limited to lead (II), cadmium (II), and chromium (IV) metallic ions.
3. Characterizations of silica, sodium silicate solution, silica gel, and rice husk-derived activated carbons samples were limited to FTIR spectroscopy, X-Ray Diffraction spectroscopy, UV spectroscopy, AA spectroscopy, and Scanning electron microscope.

(ii) Limitation of study

Kenya Bureau of Standards (KEBS) has reference KEBs standard (KS 2350: 2012) applicable to neutral, acidic, and alkaline sodium silicate Solutions. There are no reference standards for silica gel and rice husk-derived activated carbons in Kenya.

1.7 Significance of the study

1. Processing RH wastes into innovative novel chemicals is a sustainable approach to managing the wastes in rice-growing areas.

2. Silica, silica gel, and RHACs from RH will create a value addition chain, which increases economic activity thus raising incomes in the rice-growing areas.

3. The novel chemicals from RH reduce the need to import similar commercial chemicals abroad thus creating industries locally.

4. The sustainable RH waste management system created from the study will reduce human and environmental problems in rice-growing areas.

5. The development of wastewater treatment chemicals will mitigate public health and environmental problems caused by organic phenolic and heavy metal pollution.

6. The study will create new data which will be used by other researchers to carry out related research.

CHAPTER TWO

LITERATURE REVIEW

2.1 Introduction

This chapter section presents a review of literature on the chemistry of rice husks, utilization, and chemical conversion of rice husks to chemical products. Characterization methods of the novel products are discussed. Technological applications of the synthesized chemicals in wastewater treatment are also reviewed.

2.2 Rice production in Kenya

Rice is a very popular food crop in the world. Globally, 500 million metric tons of rice are milled annually (Atera et al., 2018). The total area under rice cultivation globally is expected to rise by 1.5% (153 - 158.6 million hectares) (Skorbiansky, 2018). Unlike maize and wheat which are consumed as human and livestock feed, rice remains the most popular grain globally for human consumption (Awika, 2011).

According to Kenya National Rice Development Strategy 2008 – 2018**,** rice was introduced from Asia and first grown in Kenya in 1907. It now supports 500,000 rural households in activities and businesses like agro-chemical enterprises, machinery ownership and operators, millers, and general trading. In 2017, paddy rice production for Kenya was 81,198 tons. From 1968 - 2017 the production has been rising ending at 81,198 tons in 2017 (Atera et al., 2018).

2.1.1 Rice Husks Management in Kenya

Rice husks pose a waste management issue in the rice-growing regions since they are considered of low economic value. The husk is formed from hard materials (opaline silica and lignin) which also protects the seed during growth.

Due to its grain composition, the husk is considered a by-product that creates disposal and pollution problems. Rice husks are dumped or burned after being considered agro-wastes (Gummert & Rickman, 2006). Most rice husks are burnt in

the open. This has increased environmental pollution from the release of toxic and greenhouse gases. The husk is inedible due to its high silica content.

Rice husks present a serious agro-waste management since

i. Rice husks do not burn easily on open flame unless air is blown through the husk.
ii. Moisture uptake by rice husks is difficult making it resistant to fungal decomposition.

The traditional methods for managing rice husk waste in Kenya have included landfilling, incineration, open dumping, and open-air burning. Newer methods have included rice husks gasification to syngas for cooking, electricity generation, making rice husk charcoal, rice husk soil composite, ceiling boards, and cement manufacturing (Njogu et al., 2015).

De Sousa et al (2009) states that most rice varieties have approximately 20 % of rice hull, which contains fibrous materials and silica; but the specific amount of each component depends on the climate and geographic location of the rice crop.

High silica (SiO_2) content in rice husks slows decomposition in the field. It is poor fodder and also bulky and dusty when handling. It has a low bulk density of only 70-110 kg/m³, 145 kg/m³ when vibrated or 180 kg/m³ in form of briquettes or pellets (Gewona, 2018). It is thus un-economical to store and transport because of its large volume.

2.2 Chemistry of Rice Husks

Rice husk has different chemical compositions depending on geographic location. RHA is gray and contains high amounts of amorphous silica. It has high pozzolanic activity and is used in cement production. The moisture content of rice husks ranges from 8.68-10.44 wt. %, while its bulk density ranges from 86-114 kg/m3 (Kabir, Shabbir,&Elahi,2014).

Table 2.1 shows the properties of rice husks based on geographical location.

Table 2.1: Overview of the physical- and bio-chemical properties of rice husk based on geographical location

Geographical location	Biochemical analysis (% db)			Proximate analysis (% db)			Ultimate analysis (% dab)					Reference
	Lignin	Hemicellulose	Cellulose	Ash	VM	FC	C	H	O	N	S	
China	-	-	-	16.64	67.63	16.89	37.65	5.13	36.20	1.63	0.18	(Liu, Gu, & Zhou, 2016)
Malaysia	26.10	21.25	42.45	11.98	74.54	12.11	-	-	-	-	-	(Naqvi, Uemura, Osman, & Yusup, 2015)
Sierra Leone	24.95-31.41	18.10-21.35	25.89-35.50	18.20-4.60	63.00-70.20	12.40-14.50	38.70-44.50	4.70-5.51	31.50-35.20	0.40-0.51	0.014-0.025	(Mansary & Ghaly, 1997)
-	26.91	22.18	34.56	10.54	-	-	42.43	5.82	40.63	0.58	-	(Liou & Wu, 2009)
Uruguay	-	-	-	17.20	-	-	48.30	0.50	44.40	6.80	0.00	(Deiana, et al., 2008)
*Uganda	10.58-13.47	11.39- 19.97	31.03-36.54	15.87-25.56	58.78-66.37	14.77-17.75	29.98-34.48	4.46-5.59	40.48-43.36	0.36-0.63	0.005-0.041	(Olupot, Candia, Menya, & Walozi, 2016)
Colombia	35.84	24.50	39.65	21.86	63.65	14.49	33.80	4.90	40.20	1.40	0.01	(Marrugo, Valdés, & Chejne, 2016)
Japan	-	-	-	12.70-22.00	-	-	35.2-41.2	4.6-5.4	34.8-42.1	0.4	0.6-0.7	(Kumagai, Shimizu, Toida, & Enda, 2009)
India	-	-	-	16.81	64.72	18.48	-	-	-	-	-	(Kalderis, Bethanis, Paraskeva, & Diamadopoulos, 2008)
Egypt	20.00	21.00	35.00	19.00	-	-	-	-	-	-	-	(Toniazzo, Fierro, Braghiroli, Amaral, & Celzard, 2013)

Bangladesh	-	-	-	11.38	71.56	17.06	38.48	6.60	44.05	-	-	(Hossain, Islam, Rahman, Kader, & Haniu, 2017)
**Portugal	-	-	-	11.70-15.60	59.90-61.90	14.70-15.90	38.80-40.00	4.60-5.00	29.60-31.70	0.80-1.30	0.30	(Casaca & Costa, 2009)
Thailand	-	-	-	17.90	72.80	9.30	48.90	6.20	44.10	0.80	-	(Wannapeera, Worasuwannarak, & Pipatmanomai, 2008)
Tanzania	-	-	-	26.20	59.20	14.60	45.60	4.50	33.40	0.19	0.02	(Mhilu, 2014)
Pakistan	40.16	11.14	38.35	15.22	59.04	25.74	44.13	5.01	50.40	0.39	0.07	(Danish, Naqvi, Farooq, & Naqvi, 2015)
South Korea	-	-	-	12.98	73.73	13.28	55.13	6.43	38.43	0.01	0.00	(Kook, et al., 2016)
India	20.30	26.70	34.80	17.89	76.84	5.26	39.45	6.49	52.98	0.83	0.25	(Prakash & Sheeba, 2016)

Note: db.-dry basis; dab-dry ash-free basis; ** implies the composition of rice husks is expressed on a wet basis (wb %)

Source: Menya et al. (2018).

Harvested rice weight (paddy) has about 22 % hull, this means our planet is accumulating high volumes of this scaly residue. Incineration of rice husks produces 17-20 % ash. RHA is composed of about 87-93% opaline silica and other metallic oxides (Menya, et al., 2018). The physical and chemical properties of rice husks are dependent on geographic location. A high concentration of silica as found in rice husks is rare in plant fibers (Fernandes, et al., 2017).

According to Ong et al. (2012), the rice hull has the lowest percentage of total digestible nutrients of all cereal by-products (less than 10 %). Also reporting a drawback of rice husk usefulness, Balamurugan, and Saravanan (2012) stated "Nowhere could we ever find a cereal by-product so low in protein and available carbohydrates and yet, at the same time, so high in crude fiber, crude ash, and silica." Due to its high fiber, crude ash, and silica, rice husks cannot be used as animal fodder, however, value-added products can be obtained from rice husks due to their high ash and silica content. Organic products like furfural have been produced from rice husks. Incineration of rice husks produces white rice husk ash (WRHA) and carbonized rice husks (CRH) depending on whether combustion is complete or not (Ugheoke & Mamat, 2012). In either form, rice husk has some applications. Among the uses reported are pozzolan in the cement industry (Waswa-Sabuni, Syagga, Dulo, & Kamau, 2003), aerogels (Chen, et al., 2013), SiC (Zemnukhova & Nikolenko, 2011), porous carbon (Bryant, et al., 2011), zeolites (Klunk, et al., 2020) and cordierite (Chen, et al., 2013).

Martin (2007) reports making insulating refractories with rice husks. The product characteristics are dependent on the processing route or method used. It has been shown that different methods of silica preparation from rice husks produce different morphology, structure, and reactivity (Uhrlandt, 2006).

Wang and Zhuang (2017) report that rice husks are insoluble in water, have good chemical stability, possess a granular structure, have high mechanical strength, and possess a unique chemical composition. In rice-growing areas, rice husks are locally available, renewable, and more efficient in heavy metals remediation. Rice husks

make good adsorbent material for treating heavy metals pollution from wastewater (Alalwan, Kadhom, & Alminshid, 2020).

2.3 Rice husk utilization

Globally rice husks are used as follows: low-cost material for making carbide SiC whiskers used to reinforce ceramic cutting tools, in brewing beer to increase the lautering ability of mash also convertible to fertilizers (Alweendo et al., 2019). Using vermicomposting techniques, parboiled husks (PBH) are used as substrate or medium for gardening, including certain hydro-cultures. Rice husks are also used to make particleboards and cardboard. Silica present in rice husks makes particleboards less attractive to termites (Ciannamea, Marin, Ruseckaite, & Stefani, 2017).

Rice husks have 17-26 % ash, which is higher than in other fuels (wood 0.2-2 %, coal 12.2 %). Rice husks are a good renewable energy source with a high average calorific value of 3410 kcal/kg (Gewona et al., 2018). This implies large amounts of ash produced from energy generation require handling. Internationally rice husks are a source of silica with technological applications in industry (Patil, Dongre, & Meshram, 2014). Rice husks have found applications in thermal insulation, as absorbents for oils and chemicals, as soil ameliorants, and in the production of silicon (Prasad & Pandey, 2012). Because of availability, rice husks are used as the energy source for small applications, brick production, gasifiers, and rice dryers (Belonio, Ramos, Regalado, & Ocon, 2013). The cement industry uses rice husk ash (RHA) as a filler due to its high silica content (Kang, Hong, & Moon, 2019). Farmers also use rice husk ash as a soil conditioner (Singh, et al., 2019).

Figure 2.1 below shows how rice husks are used as an energy source in combustion and gasification. Burning rice husks emits CO_2 and generates heat energy. Controlled combustion of rice husks with limited air produces synthesis gas (syngas) in a gasifier reactor. Syngas gas is used for cooking, as a drying fuel, and in cogeneration systems to produce electricity (Breeze, 2017).

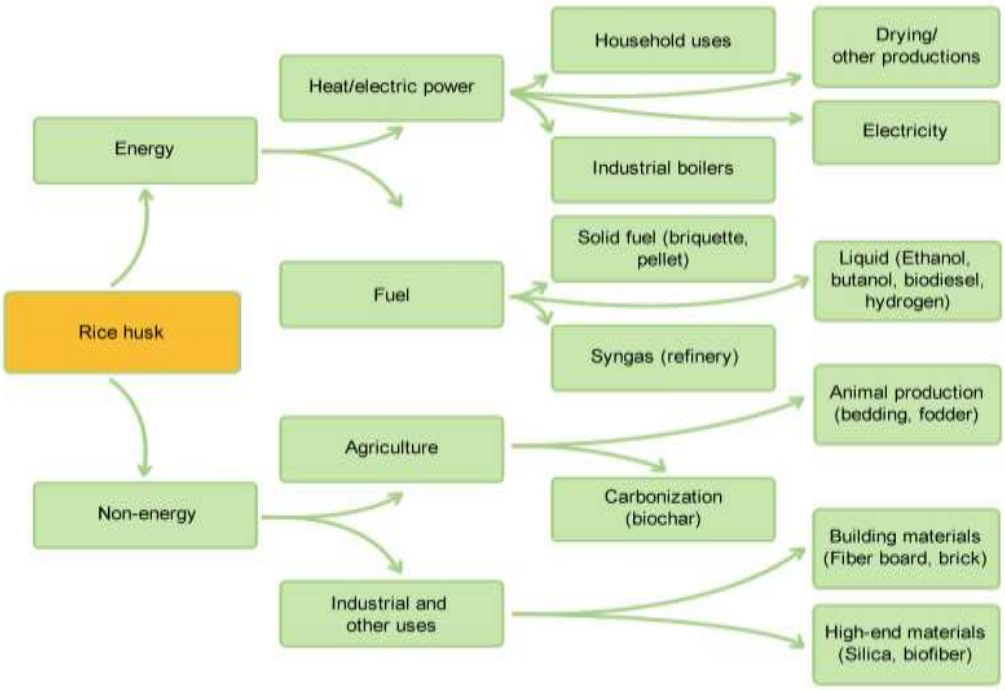

Figure 2.1: Common uses of rice husks.

Source. IRRI rice knowledge bank (RRI, 2014)

Solid fuel (that is loose form, briquettes, and pellets), carbonized rice husk produced after burning are common products of rice husks (Bajwa, Peterson, Sharma, Shojaeiarani, & Bajwa, 2018). Rice husk briquettes and pellets are also products of rice husks formed from densification. Densification increases the density of materials and their combustion performance (Bajwa, et al., 2018). Densified rice husks are used as fossil fuel substitutes. Under limited amounts of oxygen (O_2) and temperatures (less than 700°C), rice husks are decomposed into carbonized rice husks (Biochar). Activated carbons can be made from Biochar (Kalderis, Bethanis, Paraskeva, & Diamadopoulos, 2008).

2.4 Rice husks conversion to chemical products

According to (Soltani, Bahrami, Pech-Canul, & González, 2015), rice husk ash is a very good insulator especially in molten metal during slab caster. The temperature of molten metal in the ladle is around 1400 °C and above with temperatures dropping to

around 1250 °C when molten metal flows from ladle to tundish (Abdel, Hefny, & Chaghaby, 2007). Temperature gradient leads to choking and breakdown in the slab caster. Spreading rice husk ash as a coating over the molten metal in tundish and ladle maintains good insulation causing a constant temperature and hence reduces the breakdown time of the casting.

According to Ismail et al (2001), burnt RHA produces two quality grades of fillers, black rice husk ash (BRHA) and white rice husk ash (WRHA). WRHA contains 96 wt. % of silica, whereas BRHA has lower silica content which is approximately 54 wt. %. A substantial amount of carbon up to 44 wt. % is also present in WRHA. RHA is usually epoxidized with natural rubber (Epoxidized natural rubber (ENR), 50 mol. % epoxidation grade) using a two-roll, g-mercaptopropyl trimethoxysilane as coupling agent along with a filler.

According to Pode (2016), India a major rice-producing country uses the husks generated during milling as a fuel to produce energy via direct combustion or by gasification. Specific uses of RHA include; as an aggregate and filler for concrete and board production, as an economic substitute for micro silica/silica fumes, as an absorbent for oils and chemicals, soil ameliorants, source of silicon, insulation powder in steel mills, repellent in the form of vinegar-tar, release agent in the ceramics industry, and insulation material for homes and refrigerants (Nagrale, Hajare, & Modak, 2012).

In the past decade, RHA was used as a reinforcing filler to increase the strength of polymer composites. Polypropylene (PP) is one of the commodity plastics consuming a major proportion of these materials apart from high-density polyethylene (HDPE), polyester, among others. Rice husk ash has high silica content and is an easily available material, which can provide significant reinforcement to polymer matrix (Mohanty, Misra, & Hinrichsen, 2000).

The low degradation temperature of natural fibers is also a limitation while using them as filler in thermoplastic composites. Coupling agents and compatibilizers are effective in enhancing the bonding properties between polymer and fillers (Jayamani, Hamdan, Rahman, & Bakri, 2015). Studies show rice husks consist of 32.24-21.34 %

cellulose, 21.44 % hemicelluloses lignin, 15.05 % mineral ash, and approximately 96.34 % silica in its mineral ash (Banerjee, Barman, & Halder, 2017). Useful qualities of RHA relate to its chemical composition. Variation however is dependent on the source of RH and processing conditions. Oxides of AI, Mn, Fe, Na, Mg, K, Ca, and P occur in variable proportions in RHA in addition to silica. Carbon, sulfates, and traces of other elemental oxides have also been reported in RHA (Zhao, Tao, Yam, Mok, & Song, 2008).

To confirm the above, Sereda et al. (2003) synthesized a mix of WRHA filled natural rubber (NR)/ linear low-density polyethylene (LLDPE) blended with and without a compatibilizer with positive results. Siqueira et al. (2009) have prepared eco-composites using degradable polymer, polycaprolactone (PCL), and rice husks in India. Mixtures of polysiloxane network and RHA at a weight ratio of 4:1 respectively were pyrolyzed at 1000 ºC and 1600 ºC to obtain ceramic matrix composites (CMCs). Obtained without macroscopic defects, the CMCs were observed to reduce their initial porosity by polymeric infiltration cycles of polymeric precursor, improving their modulus and flexural strength up to 100 % (Siqueira, Yoshida, Pardini, & Schiavon, 2009).

A new recycling method for RHs and waste-expanded polystyrene was also developed by Ndazi et al. (2007) in South Africa, where they used a styrene solution of waste expanded polystyrene as a binder for rice husks-plastic composites, were water-resistant with strong flexural strength and suitable for building material applications.

Rice husk ash (RHA) main industrial uses are as a pozzolan in the cement and concrete industry. It is also used as an insulator in the steel industry. Sodium silicate uses include; component of detergents and soaps, silica gel production, load for medicines, inks, preparation of catalysts, and deflocculant in clay slurries, concrete hardening accelerator, and a refractory constituent (Chenier, 2012).

Crystalline properties of rice husk silica are strongly influenced by the temperature of formation and the duration of heating. There is also evidence that the level of impurities has a strong influence on the change of crystalline structure with

temperature (Khoshbin, Oruji, & Karimzadeh, 2018). This particular amorphous crystalline characteristic of rice husk silica which derives from its role in plant structure can only be maintained through the combustion process if the temperature of combustion is kept low. Precise temperatures vary but at above 500 °C, it seems some significant degradation will commence. However, it appears that even at temperatures over 1000 °C the amorphous structure can be retained provided the ash is quickly cooled. With increasing temperature, the silica structure progressively changes into cristobalite, tridymite, and quartz crystalline forms (James & Rao, 1992).

2.4.1 Silica from post-treatment of RHA

RHA typically contains impurities due to incomplete combustion of RH in air, or impurities within the melted silica. Post-treatment can improve the quality of RHA, but the quality of the final silica product is usually much lower than silica obtained from controlled calcination of pre-treated RH (Chen et al., 2013).

2.4.2 Base post-treatment of RHA

The unique solubility behavior of SiO_2 in base, very low solubility when pH<10 and increased solubility when pH>10, has been employed to extract SiO_2 from RHA by the alkaline dissolution followed by acid precipitation. Effect of type of acid or base used, pH value of gelation, and pre-acid washing of RHA on the purity and properties of the obtained SiO_2 gel was reported by Kalapathy et al. (2002). Silica xerogels of high purity from RHA were also successfully synthesized.

Berlin et al. (2011) used sulphuric acid and nitric acid in adjusting the sodium silicate solution pH value from RHA to obtain silica gels. Wang et al. (2008) boiled RHA from the calcination of RH at 600 °C for 4 hours in sodium hydroxide (NaOH) solution to obtain sodium silicate solution, subsequently neutralized by H_2SO_4 to form a silica hydrogel. Silica aerogel was then produced by supercritical carbon dioxide (CO_2) drying or by drying in the atmosphere after adding the appropriate amount of tetraethyl orthosilicate (TEOS) and washing successively by water and ethanol. The synthesized aerogels exhibited high surface area (597.7 and 500 m^2/g

respectively). Besides NaOH solution, Na_2CO_3 was also used to dissolve RHA because it can be recycled (Jang, Bhagiyalakshmi, Yun, & Anuradha, 2010).

Ammonium fluoride (NH_4F) was used to synthesis 50-60 nm silica powder by Ma et al. (2012). Rice husk ash was initially boiled in HCL solution. The acid-rinsed RHA was added into NH_4F solution to yield $(NH_4)_2SiF_6$ and was then filtered. NH_3 produced during the reaction was collected by water to form $NH_3 \cdot H_2O$. The filtrate was added to $NH_3 \cdot H_2O$ to yield silica precipitate and NH_4F solution. High-purity amorphous silica products were produced after washing and drying the precipitate. The NH_4F filtrate was collected and reactivated as the reactant. Although the main reagent, NH_4F, can be recycled, the corrosive nature of NH_4F is a negative factor during production.

Fernandes et al. (2017) have compiled a list of all recent experiments on rice husk acid leaching as shown in Table 2.2 below.

Table 2.2: Studies that investigated methods used to obtain and purify silica from rice husk ash.

Study	Objective	Summary of the method used	Main results
(Sankar, et al., 2016)	Production of Nano silicon powder from three kinds of rice husk.	• Open combustion of rice husk. • Acid leaching • Incineration under atmospheric conditions at 700ºC _	Spherical, amorphous silica particles of large specific surface area and composed only by Si and O from all kinds of rice husks.
(Bakar, Yahya, & Gan, 2016)	Investigating the ideal conditions to obtain high purity silica.	• Washing rice husks with water • Acid leaching • Incineration for 2h at 500, 600, 700, 800, and 900 °C under atmospheric conditions	All silica had amorphous particles, and rice husks leached with HCl produced the highest content of silica (99.582%) at 600 ºC...
(Ma, et al., 2012)	Development of a new, recycling-based technique to produce silica from RHA.	• Acid leaching of RHA • Extraction in a reactor with NH4F • Acid precipitation of silica	Spherical, complete amorphous silica particles measuring 50 - 60 nm in diameter and containing only Si and O, with a yield of 94.6%.
(Liou & Yang, 2011)	Investigating the effect of experimental conditions on the characteristics of the Nano silica obtained.	• Leaching of rice husk with water and thereafter HCl • Incineration • NaOH Extraction to form silicate • Precipitation	Best results with pH 3, silicate 0.15 M, the aging time of 12 h at 50ºC, with 99.48% purity silica.
(Fernandes, et al., 2017)	Evaluating the leaching of RHA with NaOH to obtain highly reactive colloidal silica.	• Extraction of silica with NaOH 1M • Precipitation using H2SO4 drop by drop	Best Si: Na mass ratio was 4:1, and highly reactive colloidal silica was obtained with minimal energy investment.
(Yalcin &	Obtaining high purity silica of	• Washing rice husks with	Amorphous silica particles of the maximum

Study	Objective	Summary of the method used	Main results
Sevinc, 2001)	large specific surface area and evaluating the competitiveness of silica from rice husk.	water • Chemical treatments (acid leaching, alkaline leaching) • Incineration at 600ºC under different conditions (static oven, airflow, argon flow, oxygen flow).	specific surface area of 321 m2/g 99.66% purity, dependent on treatment.
(Kalapathy, Proctor, & Shultz, 2002)	Investigated the efficacy of acid leaching of RHA before alkaline extraction and washing of silica obtained with water.	• Acid leaching • Extraction of silica with NaOH • Precipitation with HCl • Washing with water	Initial acid leaching did not improve purity, the washing with water reduced Na and K levels, and silica yield was excellent when extraction was carried out with 1MNaOH.
(Conradt, Pimkhaokham, & Leela-Adisorn, 1992)	Obtaining high purity silica of large specific surface area and evaluating the competitiveness of silica from rice husk.	• Washing rice husks with water • Different chemical treatments (acid leaching, alkaline leaching, and enzymatic digestion) • Incineration at 600ºC (static oven, air flow, steam)	Except for leaching with NaOH, all other treatments produced amorphous silica of large specific surface area, and high purity silica was obtained after acid leaching with HCl.
(Riveros & Garza, 1986)	To optimize the production of silica from rice husks.	• Washing rice husks with water • Acid leaching • Incineration • Leaching of RHA	Silica purity of 99.98% with three washing cycles, 6-h acid leaching, 6 leaching cycles with HCl 3% at 90ºC, and the main contaminant was Ca (100 ppm).

Source: (Fernandes, et al., 2017), https://doi.org/10.1590/1980-5373-MR-2016-1043-Accessed 12th December 2017

2.4.3 Chemistry of sodium silicate

Heating silica and sodium carbonate at temperatures above 1300°C is the common manufacturing process to form water-soluble glass referred to as water glass (solid sodium silicate). Iler (1979) presents these reactions as shown. **Equations 2.1-2.2** show the formation of solid sodium silicate from sodium sulphate and sodium carbonate respectively.

$$3SiO_2 + Na_2SO_4 + \tfrac{1}{2}C = \tfrac{1}{2}CO_2 + SO_2 + 3SiO_2.Na_20 \quad \text{....Equation 2.1}$$

$$3SiO_2 + Na_2CO_3 + \tfrac{1}{2}C = CO_2 + 3SiO_2 + 3SiO_2.Na_20 \quad \text{....Equation 2.2}$$

Sodium silicates are commercially produced as glasses having SiO_2: Na_20 molar ratios of 1.6-3.9. When sodium silicate is dissolved in water, different silicate species tend to dominate at varying pHs. Equilibrium equations describe which species dominate and are listed as shown in **Equation 2.3-2.7**:

$$SiO_2 + H_2O = Si(OH)_4 \quad \text{.....Equation 2.3}$$

$$Si(OH)_4 + HO^- = HSiO_3^- + 2H_2O \quad \text{.....Equation 2.4}$$

$$2HSiO_3^- = SiO_5^{2-} + H_2O \quad \text{..... Equation 2.5}$$

$$SiO_5^{2-} + H_2O = HSi_2O_6^{3-} + H^+ \quad \text{..... Equation 2.6}$$

$$HSiO_3^- + OH^- = SiO_3^{2-} + H_2O \quad \text{..... Equation 2.7}$$

Equilibrium constants for equations 3-7 are $10^{-9,8}$, $10^{-12,16}$, $10^{-9,8}$, $10^{-12,8}$, 2200 respectively. By using these equilibrium constants, it is possible to calculate the concentration of each silicate species at different pH (Iler, 1979).

2.4.4 Gel formation

At higher pH values, dimer species dominate but when the pH is reduced, silicate will react to form a gel through a polymerization process. To initiate gel formation, the pH has to be reduced to a value below 11 (Hamouda & Amiri, 2014).

The development of the gel can be described using the following steps:

a) Polymerization of monomer to polymer
b) Growth of particles
c) Linking of growing particles to form polymer chains and forming a gel

In solution, molecules will grow by linking to other silica molecules, resulting in polymer creation. Water molecules are captured and locked in a network of silicate molecules (Alothman, 2012).

There are many configurations of polymerization. The rate and extent of sodium silicate polymerization are affected by several factors. To understand and control gelation time, these factors must be taken into account.

Summary of which and how different factors affect gelation time is as follows:

1. pH: When the pH of solutions decreases, the process will move down.

2. Molar Ratio: An increase in silica ratio will result in a higher degree of polymerization.

3. Dilution rate: Dilution at constant pH will de-polymerize silica (process moves up).

4. Salts: act as catalysts and increase the rate of polymerization.

5. Temperature: Process is accelerated at higher temperatures.

The main factor controlling gelation time for sodium silicate is the pH of the solution. However, the above relationship is not linear for all pH values. Therefore, this correlation is extrapolated into several pH intervals, where a change in the pH will follow a certain trend (Stavland et al., 2011). This is outlined in Table 2.3, where the pH values of sodium silicate solution are decreased and the reduction, in given intervals, are also presented.

Table 2.3: Relation between pH range and gelation time of an aqueous sodium silicate

pH interval	Gelation time	Reason
$11 \leq pH < 14$	Does not gel	Solution is stable
$5.5 \leq pH < 11$	Decrease in gelation time	Reduction in negative charge
$2 \leq pH < 5.5$	Increase in gelation time	Catalyzed by OH^-
$0 \leq pH < 2$	Decrease in gelation time	Catalyzed by F^- from metal ions

Source: Stayland et al (2011)

2.4.5 Acid post-treatment of RHA

Acid leaching performed after calcination of RH is an effective method for metal impurities removal and produces high-purity silica. Real et al. (2006) used RHA which was obtained from the calcination of RH at 600 °C to produce amorphous RH silica by leaching with hydrochloric acid (HCl) solution. The product exhibited similar purity (about 99.5%) with silica synthesized from calcination of HCl treated RH.

The purity of silica obtained by post-treatment of the RHA method was 95.14%. This is higher than silica from RH without treatment (91.50%) and lower than that of silica obtained by pre-treatment (99.16%). The silica had the highest purity (99.66 %) if 3% (v/v) HCl was used for treatment before and after calcination of RH. Acid post-treatment removed most metal impurities, but the low specific surface area has limited its application (Adam, Appaturi, & Iqbal, 2012).

2.4.6 Gelling agents

The simplest way to reduce a solution's pH is to add acid. Such systems have been applied for many years and a lot of work has been done on optimizing silicate/acid systems for petroleum production purposes. Other chemicals have also been used as gelling agents, although acids are more common (Stavland et al., 2011).

2.4.6.1 Hydrochloric acid (HCl)

The addition of almost any acid will cause gelation of sodium silicate. Hydrochloric acid (HCl) is usually chosen as a gelation agent for many experiments. HCl is a good and cheap gelling agent for silicate systems. Concentrated acid (37 wt. %) has a pH value of 1. At the point, HCl is added to sodium silicate solution the pH value drops. However, the use of concentrated acid is limited because it causes immediate gelation in a mixture with sodium silicate. The biggest advantages of HCl as a gelling agent for silicate gels are price, availability, and little if any, damage to the environment (Chiarakorn, Areerob, & Grisdanurak, 2007).

2.4.6.2 Glyoxal

Glyoxal is the smallest double aldehyde (two aldehyde groups) with the chemical formula OCH-CHO. Mixtures of sodium silicate and Glyoxal were used as early as 1964 to form hard, cement-like coatings. Very hard substances have been created in the past by using high (around 50 wt. %) glyoxal concentrations. Such gels are extremely hard, cohesive, and water-insoluble. For casing and repair, hard substances created with high glyoxal concentration might be an alternative (Iler, 2009).

As mentioned, sodium silicate pH has to be reduced to a value below 11; an addition of a sufficient amount of glyoxal can achieve that. The reduction of pH is highly dependent on temperature and, therefore, this system has an advantage when gelation has to be delayed until it is injected deeply in a reservoir. Ideally, there should exist a system of sodium silicate cross-linked with glyoxal which would be close to stable, i.e. it would not gel at room temperatures, but once the necessary temperature is reached, it would form a strong and water-insoluble concentration and ions in dilution water (Stavland, et al., 2011). Parameters that have an effect here are sodium silicate concentration and glyoxal.

2.4.6.3 Esters

In reaction with water, esters produce acid and alcohol and, thereby, can initiate polymerization. Esters are derived by reacting an oxoacid with a hydroxyl

compound, such as an alcohol or phenol (Uhrlandt, 2006). Temperature plays an important role in ester hydrolysis as the reaction rate increases exponentially with an increase in temperature. By selecting specific esters and catalysts, a highly temperature-dependent system can be created and optimized. As discussed earlier, such systems have an advantage when gelation has to be delayed for deep gelant placement. A review of the available literature shows that similar systems have been created; however, no attempt to optimize these systems has been made (Yalcin & Sevinc, 2001).

2.5 Thermochemical and biochemical conversion technologies

Household energy, mainly for cooking, heating, and drying, are the most widely available technology. Biomass cook stoves, for instance, have hundreds of versions existing all over the world especially in Southeast Asia (Kshirsagar & Kalamkar, 2014). Meanwhile, pyrolysis and gasification have most technologies in the demonstration stage. These technologies are concentrated in Europe, the USA, Japan, and India.

Biochemical-oil applications at a research and development stage are distributed mainly in Europe, North America, and Japan (Govorushko, 2013). Co-generation of heat and power has been used for decades in various industries such as food processing, wood, textiles, pulp and paper, chemical, petrochemical industries, and others (Gyftopoulos, 2003).

A common trend is in the application of co-generation in industrial estates and buildings to cover all heat and/or cooling requirements. Having high energy requirements, these sectors represent a large market for cogeneration technology (Calvillo, Sánchez-Miralles, & Villar, 2016). In comparison with conventional generation, power (CHP) and combined heat systems have higher overall efficiency and reduce much more losses during operation.

The flowchart in Figure 2.2 maps out various conversion processes down to industrial products. End-users can use it as a guide on which technology to consider given their desire for particular energy products.

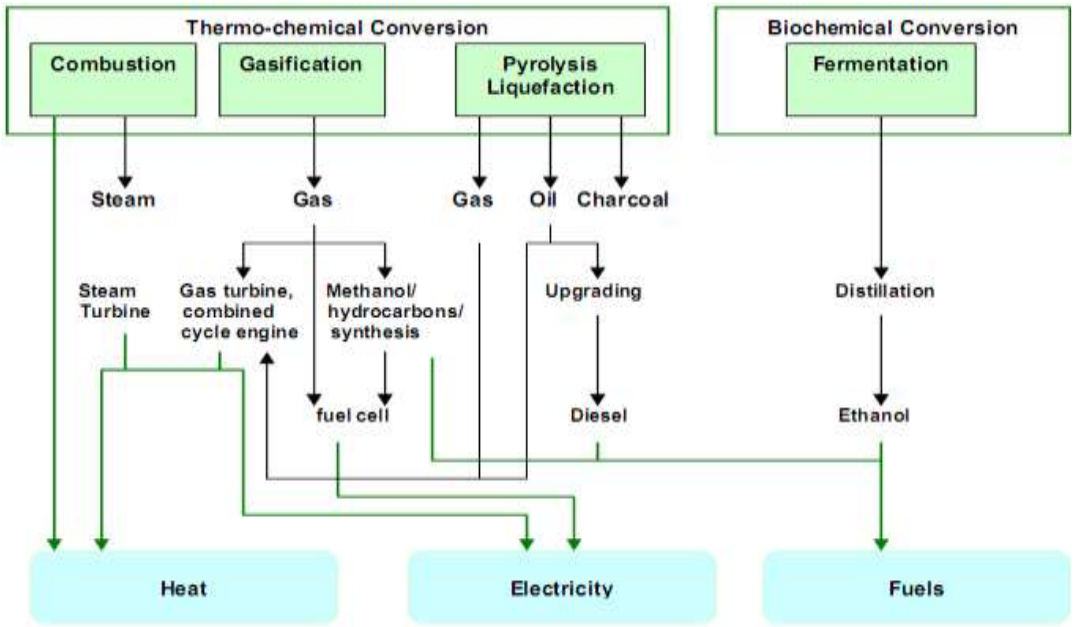

Figure 2.2: Conversion routes for cellulosic agricultural biomass Waste

Source: (Brumitt, 2015)

2.5.1 Gasification

Thermo-chemical conversion of organic materials at high temperatures with partial oxidation is called gasification. Organic matter or biomass is converted to combustible gases (mixture of CH_4, CO, and H_2) with char, water, and condensable gases as minor products.

Njogu et al (2015) produced syngas at temperatures between 450 °C and 750 °C with an injection of a limited supply of air, purified the gas using a series of gas cleaning and cooling devices. Rice husks were the feedstock, and were consumed at a rate of 25 - 32 kg/hr with a gas generation rate of 7.76 - 7.78 m^3/hr; this translates to a gas yield of 0.31 - 0.35 m^3/kg. Rice husks were initially broken down by heat to liquid volatile materials, gases, and char (containing high carbon content). The hot char then reacted with the gases (mainly CO_2 and H_2O) in a second step leading to product gases namely, CO, H_2, and CH_4 (Njogu et al., 2015).

Gas produced requires cleaning as it leaves the reactor due to pollution. This enables the gas to burn well in engines. The cleaned producer gas mixed with air can be used

in gas turbines (in large-scale plants), gasoline or diesel engines, and gas engines (Sridhar, et al., 2005). Figure 2.3 shows the basic steps involved.

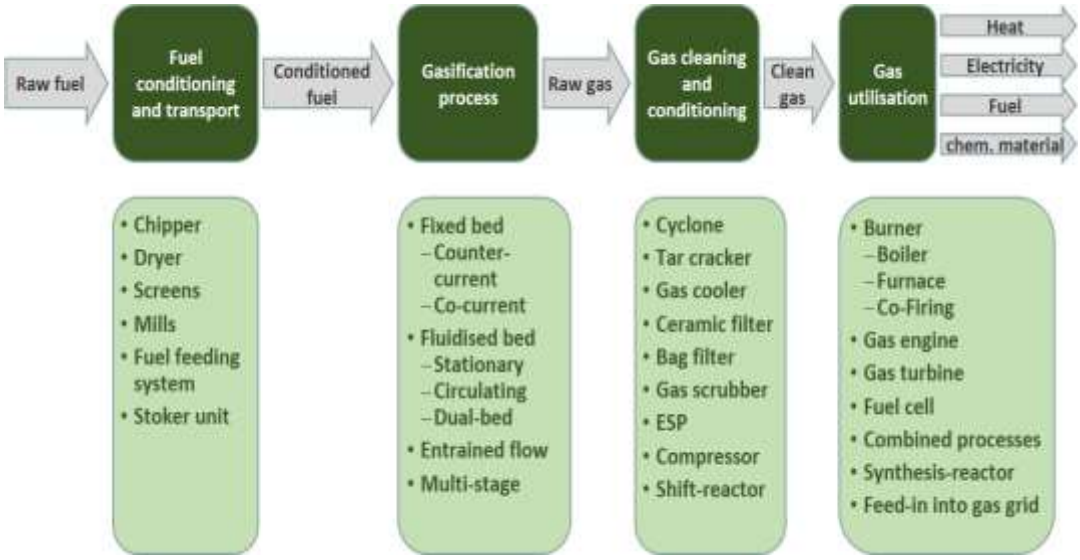

Figure 2.3: Basic process steps of a biomass gasification plant

Source:https://www.bios-bioenergy.at/index.php/en/technology-info/biomass-gasification-accessed

Carbon monoxide (CO), hydrogen (H_2), and methane (CH_4), mixed with carbon dioxide, nitrogen, and other incombustible gases are called syngas (producer gas). Heat values of syngas gas range between 4-20 MJ/m^3, depending on the carbon and hydrogen content of the biomass and the properties of the gasifier. Syngas was reported to have a composition of 16.5 % - 17.55 % CO, 14.5 % - 16.1 % CO_2, 4.1 % - 4.5 % H_2, 6.8 % - 7.2 % CH_4 and 17.9 % - 45.7 % N_2 among others (Njogu et al., 2015). The gas was used for direct heating applications and to run modified petrol engines. Air-based gasifiers typically produce syngas containing a relatively high concentration of nitrogen with a low heating value between 4-6 MJ/m^3. Gasifiers are usually available in small sizes, down to one or a few kW. For electricity generation, the size of installed systems in China has been reported to be between 200-1500 kW. The units are modular which means they can be combined to form larger power plants (Bergqvist, Wårdh, Das, & Ahlgren, 2007).

2.5.2 Combustion/incineration

External combustion offers the possibility to burn fuels in their natural form that is especially helpful in the case of “bad fuels” which would destroy internal combustion equipment. They are often referred to as direct combustion systems since no or little refinement of the fuel is made. The different types of technologies available for direct combustion represent 97 % of global bio-energy production and are promising for the near future (Demirbas, 2007). Producing heat and/or power from direct combustion from rice husks in both large and small-scale applications is common (Bergqvist & Wårdh, 2007).

In direct combustion systems, burnt biomass generates hot flue gases, which provide heat directly or fed into a boiler to generate steam. Direct combustion biomass that produces electricity through a steam turbine has a conversion efficiency of 15 % to 35 %, depending upon the manufacturer. Combined Heat and Power (CHP) systems can have an overall system efficiency of as much as 85 %. The efficiency of a direct combustion biomass system is influenced by several factors including biomass moisture content, combustion air distribution, and amounts, operating temperatures and pressures, fuel feed handling, distribution, mixing, and furnace retention time (Kontor, 2013). The main parts of a combustion-based biomass plant include a biomass-fired boiler that produces steam and a steam turbine that generates electricity.

2.5.3 Extraction of silica from rice husks

Silica is a valuable inorganic multipurpose chemical compound (Carmona, Oliveira, Silva, Mattoso, & Marconcini, 2013). It can exist in gel, crystalline, and amorphous forms. It is abundant material on the earth’s crust. However, the manufacture of pure silica is energy-intensive. A variety of industrial processes exist involving conventional raw materials (sand) which requires high furnace temperatures (more than 700 °C) (Carmona et al., 2013). Rice husks are the most silica-rich raw materials containing about 90-98 % silica (after complete combustion) among all agro-wastes (Todkar et al., 2016).

Using rice husk as boiler fuel generates RHA creating disposal problems. Chemical processes provide a solution for waste disposal. Resource recovery of a valuable silica product, together with certain useful associate recoveries (sodium sulphate) is also an added advantage (Ugheoke, Mamat, & Ari-Wahjoedi, 2013).

Residual ash from silica production can be utilized in making good-quality bricks. Sodium silicate in the residue ash acts as a binder and mixing with suitable ingredients can produce high-quality bricks (Ma, et al., 2012). Millions of tonnes of rice husks are generated from rice mills in many developing countries. Disposal methods are usually open burning causing major public health and environmental pollution. Using rice husks as raw materials in various industries would reduce this problem. Silica is highly concentrated in the inner and outermost surfaces of the epidermal. As a result, rice husks are relatively friable, brittle, and abrasive. Silica occurs in nature mainly in three crystalline forms namely; quartz (hexagonal), cristobalite (white), and tridymite (hexagonal). It is an amorphous form like opal. Silica in the biological matter (unicellular and crops) contains biogenic amorphous silica (BAS) (Todkar, Deorukhkar, & Deshmukh, 2016). Silica extraction from rice husk has been reported (Mohamed, Mkhalid, & Barakat, 2015). Residual carbon was simultaneously reacted with superheated steam and converted to gases below 700 ºC. Salavati-Niasari et al. (2013) have also reported the production of high purity silica (99.9%) from rice husk which was used for industrial purposes.

Shen et al. (2014) have demonstrated silica manufacture using rice husk ash as raw material source. The process to extract all silicate content from rice husk involves burning the rice husks under controlled conditions of air and temperature to get the clear white ash.

The basic steps in the production of precipitated silica are:

a) Obtaining silica from rice husk
b) Dissolution of silica in alkali and
c) Preparation of silica from silicate solution

The reaction steps are characterized and shown in **Equations 2.8-2.9:**

$$SiO_2 + 2NaOH \xrightarrow{80\text{-}90^oC} Na_2SiO_3 + H_2O \ldots\ldots\ldots\ldots \text{Equation 2.8}$$

(ash) (caustic Soda) (sodium silicate)

$$Na_2SiO_3 + H_2SO_4 \xrightarrow{85^oC} SiO_2 + Na_2SO_4 + H_2O \ldots..\text{Equation 2.9}$$

(Sodium Silicate) + (Sulphuric acid) (Silica) + (Sodium Sulphate)

The initial step involves the extraction of silica from RHA as sodium silicate using caustic soda. The reaction was at a temperature in the range of 180 -200 ºC and pressure ranging from 6-8 atmospheres (Dey, Ghosh, & Naskar, 2013).

The ash is amorphous silica reactive around 100 ºC with NaOH solution at atmospheric pressure yielding sodium silicate as presented in **Equation 2.10**;

$$SiO_2 + 2NaOH \xrightarrow{80\text{-}90\ ^oC} Na_2SiO_3 + H_2O \ldots\ldots \text{ Equation 2.10}$$

(ash) (caustic Soda) (sodium silicate)

Viscous, transparent, colorless sodium silicate solution (15 % w/w) was obtained after filtration of the residual slurry consisting of residue, digested ash, sodium silicate, water, and free sodium hydroxide. Acidic conditions resulted in a white precipitate of silica in a solution of sodium sulphate (Yuvakkumar, Elango, Rajendran, & Kannan, 2014). The liquid suspension (wet impure silica) obtained was then filtered. The third step of the process was the purification of this silica by the removal of sulphate impurities. Successive demineralized water washings were done in the purification process.

Removal of sodium sulphate causes a decreasing trend in conductivity of the effluent (Soltani et al., 2015). Conductivity measurement can be used as the criteria to decide the number of washings to obtain the desired purity. The final step of the process involves spray drying the silica after the removal of sulphates (wet silica) to obtain

the amorphous powder form. Purification and drying produce silica in a white amorphous powder form.

2.6 Quality standards for silica, silica gel, and activated carbon

Various grades of sodium silicate are available in the industry and are characterized by their SiO_2:Na_2O weight ratio, which can be converted to the molar ratio by multiplication with 1.032. The ratio varies between 2:1 and 3.75:1. Grades below the ratio of 2.85:1 are termed alkaline. Sodium silicates with a higher SiO_2:Na_2O ratio are termed neutral and are colorless glassy or crystalline solids, or white powders (Sharif, 2018). They are readily soluble in water. Silicon-rich ones produce alkaline solutions. Sodium silicates are stable in neutral and alkaline solutions. In acidic solutions, hydrogen ions react with the silicate ions to form silicic acids, which tend to decompose into hydrated silicon dioxide gel. Heating to drive off the water, the hydrated silicon dioxide gel changes to a hard translucent substance called silica gel, widely used as a desiccant. It can withstand temperatures up to 1100 °C (Jantzen, Brown, & Pickett, 2010).

Sodium silicates solutions in the industry are produced by reacting a mixture of silica (usually as quartz sand), caustic soda, and water, with hot steam in a reactor (Sharif, 2018).

Greenwood and Earnshaw (1997) have outlined the reaction in **Equation 2.11**

$$\mathbf{2}x\mathbf{NaOH + SiO_2 \rightarrow (Na_2O)}_x\mathbf{\cdot SiO_2 + }x\ \mathbf{H_2O}\ldots\ldots \textbf{ Equation 2.11}$$

Sodium silicates are also produced by dissolving silica SiO_2 (whose melting point is 1713 °C) in molten sodium carbonate (melting with decomposition at 851 °C) as shown in **Equation 12**.

$$x Na_2CO_3 + SiO_2 \rightarrow (Na_2O)_x \cdot SiO_2 + CO_2 \ldots \textbf{Equation 2.12}$$

Sodium silicates can also be obtained from sodium sulphate (melting point 884

°C) with carbon as a reducing agent as indicated in Equation 13

$$2x\ Na_2SO_4 + C + 2\ SiO_2 \rightarrow 2\ (Na_2O)_x \cdot SiO_2 + 2\ SO_2 + CO_2$$ **Equation 2.13**

India has several standards of sodium silicate dependent on use.

Several specifications for Sodium silicate-based on their use in various industries have been published by the Bureau of Indian Standards. These include

a) IS 381:1995: Sodium silicate (Second Revision).
b) IS 6773:1978: Sodium silicate for use in foundries (First Revision) Re-affirmed 1991.
c) IS 9601:1980: Sodium silicate for cosmetic industries (Amendment No. 1) Re-affirmed 1991
d) IS 14212:1995: Methods of test for sodium silicate and potassium silicates.

2.6.1 Types and grades of sodium silicate

Liquid and solid forms of sodium silicate are in two main grades, neutral and alkaline. Two types of liquid neutral sodium silicates exist:

Type 1: used in pharmaceutical and toilet preparations,

Type 2: used in adhesive and other purposes.

Liquid, alkaline sodium silicates are of three types:

Type 1-used in soap and detergent,

Type 2-used in textile

Type 3: used in welding electrode and cement industries (Nematollahi, Sanjayan, & Shaikh, 2015).

According to sodium silicate Indian Standard (IS 381), the main quality requirements are:

i. Neutral sodium silicate shall be clear, free from dirt and other visible impurities.

ii. Liquid sodium silicate shall also be thick, viscous, translucent mass of water white or slightly grey colour.

IS 381 standards further prescribe solid sodium silicate shall be in the form of glassy lumps of pale grey or green color. Particle size shall be as mutually agreed between the purchaser and the supplier to meet their special requirements. Other quality requirements include parameters like relative density, total soluble silicates, the ratio of total alkalinity to total soluble silica, loss in mass on the ignition, viscosity, and limits for iron, chloride, and sulphate content.

Kenya has also published a similar Standard KS 2350:2012. **Table 2.4** shows the main requirements.

Table 2.4: Standard requirements for sodium silicate KEBs KS2350:2012

	Requirements				**Test**
	Solid neutral	**Solid alkali**	**Liquid neutral**	**Liquid alkali**	
Appearance	Clear to opaque	Clear to opaque	Clear to hazy	Clear to hazy	Visual
Total Alkali content as Na_2O % by mass	20 min	30 min	5-10 %	10.1-20.2 %	Annex A
Density g/mL at 20°C	-	-	1.25-1.45	1.46-1.70	Annex B
The ratio of the mass of SiO_2:Na_2O	1:2.9-1:1:3.6	1:1.65-1:2.85	1:2.9-1:3.6	1:1.65-1:2.85	Annex C
Mass of SiO_2 and Na_2O	>97.5 %	>97.5%	>97.5 %	>97.%	Annex D

Note: the insoluble matter shall be less than 2.5 %

Source: (Kenya Bureau of Standards (KEBS), 2012)

2.6.2 Silica gel

Silica gel is formed from the chemical reactions of sodium silicate and acids (H_2SO_4, HCl). It is stable and reacts only with strong alkali and hydrofluoric acid (HF). Pores are irregular tri-dimensional frameworks with alternating silicon and oxygen atoms. Pore sizes average 2.9 nm with a strong affinity for water (Greenwood & Earnshaw, 1997).

Silica gel is of three main types

i. Type A –pore diameter: 2.5 nm, clear pellets, drying, and moisture-proof properties, used as catalyst carriers, separators, adsorbents, and variable-pressure adsorbents.
ii. Type B –pore diameter: 4.5 – 7.0 nm, translucent white pellets, liquid adsorbents, drier and perfume carriers, also may be used as catalyst carriers.
iii. Type C –micro-pored structure, translucent, forms macro-pored silica gel and used as drier, adsorbent, and catalyst carrier.

Other types include silica-alumina gel and stabilizing silica gel. Silica gel can also be classified specific to the internal content;

i. Aquagel – when the pores are filled with water,
ii. Xerogel - by the process of evaporation, aqueous phase in the pores are removed,
iii. iii) Aerogel - solvent removed by supercritical extraction.

Voids could have either water, other liquids, gases, or even a vacuum. Silica xerogel is the material formed when the voids contain a vacuum.

Silica content in silica gel ranges from 60 % to 96 % and is usually specific to the function they perform. Kenya uses international MSD standards for silica gel.

2.6.3 Activated carbon

Activated carbons are specifically carbons with small, low-volume pores that have increased surface areas available for adsorption or chemical reactions. Carbon sources can be from charcoal or other carbonaceous materials such as bamboo, coconut husk, wood, lignite, and coal. One gram of activated carbon has a surface area of over 3,000 m^2 (32,000 sq. ft.) as determined by gas adsorption measurements (Menya et al., 2017)

In developing countries, where more than 96 % of rice husks are produced globally in rice milling, high volumes of rice husks become waste and end up either being openly dumped or merely burnt in open space, causing environmental pollution. Activated carbon from rice husk is abundantly available (Pode, 2016). The conversion of rice husks into activated carbon adds economic value to a product considered waste. It provides inexpensive alternatives to existing commercial activated carbons for numerous applications including water treatment.

Rice husks are an important source of activated carbon due to their physio and biochemical properties. They have high cellulosic biomass, constituting lignin, cellulose, and hemicellulose (Liou & Wu, 2009; Olupot et al., 2016). Cellulose and hemicellulose are volatile fractions removed during pyrolysis and are associated with low carbon yields since a significant fraction of carbon is lost during pyrolysis (Viswanathan, 2009). Factors affecting rice husk's properties include rice variety, soil properties, climatic variation, and geographical location. The quality of rice husk-derived activated carbon is also affected (Menya et al., 2017).

The main activation processes for activated carbon are mainly:

i. **Physical activation:** Hot gases are introduced through the carbon source material. This creates a graded, screened form of activated carbon. The final process is done by using one or a combination of these processes:

a. Carbonization: Carbon materials like rice husks are heated at temperatures (600–900 °C), usually with inert gases like argon or nitrogen.
b. Oxidation/activation: The carbonized material is oxidized either through oxygen or steam, usually in the temperature range of 600–1200 °C.

ii. **Chemical activation**: The carbon source material is reacted with either acid, strong base, or compound salts such as phosphoric acid 25 %, potassium hydroxide 5 %, sodium hydroxide 5 %, calcium chloride 25 %, and zinc chloride 25 %. The material is heated to 250–600 °C to increase surface area and microscopic pores (Menya et al., 2017).

2.6.4 Classification of activated carbon

Activated carbons can be classified based on their behavior and surface characteristics. Broadly, further classification can be made based on general-purpose, preparation methods, and industrial applications. Activated carbon is usually in particulate form as powders or fine granules (< 1.0 mm) with an average diameter (0.15-0.25 mm). Activated carbon (R 1) is defined as the activated carbon particles retained on a 50-mesh sieve (0.297 mm) (Manocha, 2003).

Powdered activated carbon (PAC) which can pass through an 80-mesh (0.177mm) is classified by the American society for testing materials (ASTM international). The standards are comparable with the International Standards Organization (ISO) standards. The PACs are usually added to other process units, such as raw water intakes, clarifiers, rapid mix basins, and gravity filters to purify (Marsh & Rodríguez-Reinoso., 2006). American Society for Testing and Materials (ASTM., 2009) describes the method to be used in determining the apparent density of activated carbon.

a. Apparent density usually ranges between 2000-2100 kg/m^3 with air spaces among particles making it lower 400-500 kg/ m^3. Higher apparent density (greater volume) indicates better-quality activated carbon.

b. Iodine number - used to indicate porosity of activated carbon is also used to approximate the surface area for some types of activated carbons. Changes in carbon raw material, processing conditions, and pore volume distribution also affect the quality. Soluble salts affect the measured iodine number of activated carbon.
c. Hardness/abrasion number – indicates the physical integrity of activated carbon by measuring AC resistance. Activated carbons have differences in hardness dependent on raw materials and activity levels.
d. Ash content – affects the efficiency of reactivation and is dependent on the carbon source (rice husks, coconut, wood, or coal). The PACs with low soluble ash content are preferable to use for marine, freshwater fish to avoid metallic poisoning and uncontrolled algae/plant growth.

Table 2.5 shows the standard specifications of activated carbon.

Table 2.5: Standard Specification for activated carbon analysis

Quality Requirements	Particle	Powder
Volatile matter 950 °C,%	Max.15	Max. 25
Moisture content, %	Max. 4.5	Max. 15
Ash content, %	Max. 2.5	Max. 10
Parts that are not carbonized	0	0
Iodine Number, mg/g	Min. 750	Min. 750
Pure activated carbon, %	Min. 80	Min. 65
Benzene adsorption capacity, %	Min. 25	-
Methylene blue Number, mg/g	Min. 60	Min. 120
Bulk specific gravity, g/mL	0.45 – 0.55	0.3 – 0.35
Escaped mesh 325, %	-	Min. 90

Source: (Hanum, Bani, & Wirani, 2017).

2.7 Organic and inorganic pollutant removal from wastewater

Lignocellulose crops like rice husks offer several advantages for synthesizing activated carbons due to their wide availability and physicochemical properties. Biomasses of the plum kernel and rice husk are alternative lignocellulose precursors for activated carbon preparation. Treviño-Cordero et al. (2013) report the application of Prunus domestica and Jacaranda mimosifolia biomass for the synthesis of

activated carbons to remove commercial dyes (i.e., methylene blue and AB25) and Pb^{2+} ions from aqueous solutions. Two different methodologies for the preparation of activated carbons were compared, namely, direct carbonization at 800 °C and impregnation of the biomass with a calcium solution extracted from eggshell wastes before carbonization. Results confirmed that both carbonization and activation processes improved the uptake of lead, acid blue 25, and methylene blue up to 10 times with respect to adsorption results.

The use of novel nano-adsorbent for the treatment of wastewater can be confirmed by the continuous increase in research articles on the adsorption of heavy metal ions using organic-inorganic nanocomposites (Pandey & Ramontja, 2016). Jung et al. (2020) reported the relationship between surface functionality and adsorption of cadmium (II) using various mesoporous silica and activated carbons. Jung et al. (2020) found that silica surfaces were principally functionalized by mono-amino- and mercapto-groups and that carboxylic groups could be introduced to the activated carbons by oxidation.

2.7.1 Activated carbons use in wastewater treatment

Environmental pollution refers to the introduction of contaminants into the natural environment that causes public and environmental harm. Pollutants can be either foreign substances/energies or naturally occurring contaminants.

Pollution control means the control of harmful emissions and effluents into the soil, air, and water. Without pollution control, the waste products from overconsumption, heating, agriculture, mining, manufacturing, transportation, and other human activities would accumulate and degrade the environment (Riffat, et al., 2016).

Due to the deteriorating quality of water globally it is imperative to ensure wastewater treatments remove possible toxic threats to humans and the environment. Porous carbon and carbon nanotubes have been used for the advanced treatment of wastewaters. Carbon nanomaterials have become promising adsorbents for water treatment (Gupta & Saleh, 2013).

Micropollutants are found in sewage, surface waters, and groundwater. Discharges of treated effluent from wastewater treatment plants (WWTPs) are a major pathway for the introduction of micropollutants to surface water. The WWTP removal efficiency of selected micropollutants in 14 countries/regions depicts compound-specific variation in removal, ranging from 12.5 to 100 %. Advanced treatment processes like activated carbon adsorption, advanced oxidation processes, nanofiltration, reverse osmosis, and membrane bioreactors can achieve higher and more consistent micropollutant removal (Luo, et al., 2014). Removal of micropollutants is dependent on physio-chemical properties and treatment conditions. Adsorption processes are being widely tested by various researchers for the removal of heavy metals from waste streams and activated carbon has been used as adsorbents. Commercial activated carbon remains expensive to use in water and wastewater treatment industries.

The need for safe and economical methods for the elimination of pollutants from contaminated waters has driven research interest toward the production of low-cost alternatives to commercially available activated carbon. Therefore, there is an urgent need to explore agro-based inexpensive adsorbents' ability to remove pollutants. Water pollution by heavy metal ions has been of great concern globally. Industrial activities and anthropogenic activities are the major sources of heavy metal pollution (Nwidu, Oveh, Okoriye, & Vaikosen, 2008). Various conventional methods have been used to remove chemical pollutants from water. Such includes; chemical precipitation, ion exchange, reverse osmosis, coagulation-floatation, and membrane separation (Gherasim, Cuhorka, & Mikulášek, 2013). However, conventional methods have the demerits of the high cost of buying and maintaining the equipment and formation of chemical sludge. Removal of heavy metal by low-cost sorbents have been preferred due to its low cost and availability of sorbents. Various low-cost sorbents which have been used to remove heavy metal ions from wastewater includes; banana pith (Kakoi et al., 2016), low cost activated carbon (Mishra & Patel, 2009), lepiota hystrix (Kariuki et al., 2017), macadamia nutshell powder (Maremeni et al., 2018), among others.

2.7.2 Removal of priority pollutants (lead, chromium, cadmium) in wastewater

There is a global concern due to heavy metals' presence in the environment due to their non-degradability and bio-magnification. Heavy metals especially chromium compounds are used extensively in industrial processes such as electroplating, leather tanning, and in the manufacture of paints, dyes, paper, explosives, and ceramics. Hexavalent and trivalent chromium possesses carcinogenic properties. Large doses of hexavalent chromium lead to corrosive effects in the intestinal tract and nephritis (Shanmugavalli, et al., 2007). Lead has several applications including, plumbing and manufacture of leads. Exposure to lead through ingestion leads to unhealthy effects on both adults and children. Lead is a known carcinogen pollutant (Lu, et al., 2015). Cadmium is a non-essential element in the human body and high exposure can lead to lung cancerous growth (Menya et al., 2018). Chromium exists in two oxidation states namely Cr (III) and Cr (VI). Cr (III) is an essential micronutrient and is found in plants and rocks while Cr (VI) is found in nature and is toxic (Razmovski & Šćiban, 2008). One objective of this work is to prepare rice husk-activated NaOH and rice husk-activated H_3PO_4 here in Kenya and to compare their efficiency in the removal of Pb (II), Cd (II), and Cr (VI) from wastewater.

Utilization possibilities of less expensive adsorbents like rice husk-derived activated carbon for the elimination of inorganic (Pb (II), Cd (II), and Cr(VI) and organic (phenolic) pollutants from wastewater in Kenya is also part of this study. Agricultural and industrial waste by-products such as rice husk have been used in other parts of the world for the elimination of pollutants from wastewater (Riffat, et al., 2016).

Adsorption technologies processes seem to be the most versatile and effective method for the removal of heavy metals (Rao, Dalinaidu, & Singh, 2017). Activated carbon remains expensive despite its extensive use in the water and wastewater treatment industries. Rice husks can be converted into activated carbons, which can be used in environmental remediation. Sorbents made from rice husk have considerable potential for adsorption of heavy metals of environmental concern.

The need for safe and economical methods for the elimination of heavy metals from contaminated waters has sparked research interest in the production of low-cost alternatives to commercially available activated carbon in recent years. Current environmental and economic conditions encourage us to develop and improve technology to reduce or utilize agricultural waste in the best possible way.

According to Gupta et al. (2015), heavy metals used in the manufacture and processing of textile industries end up discharged in the effluent. The importance of the removal of heavy metal pollutants from the environment has received significant attention from researchers and decision-makers across the globe. Bio-adsorbents have emerged as potential remediation materials, which can be used for the removal of heavy metals and metalloids from the environment vis-à-vis water. The bio-adsorbents have an affinity for heavy metal ions to form metal complexes due to having functional groups including carboxyl, hydroxyl, imidazole, sulfhydryl, sulfate, phenol, amino, phosphate, thioether, carbonyl, and amide among others (Lata & Samadder, 2014).

2.8 Analytical techniques for efficiency and quality testing

Chemical analytical tools commonly used for quality testing include Fein optic polarizing microscope (SEM), X-ray Fluorescence spectroscopy (TXRF), X-ray diffraction (XRD), Atomic absorption spectroscopy (AAs), Fourier Transform Infrared Spectrophotometer (FT-IR), and UV spectrophotometer (Kealey & Haines, 2004). Laboratory analysis methods including sample preparations, treatments, digestion, and dilutions were as described by standard official methods of analysis (AOAC, 2019).

2.8.1 Fein optic polarizing microscope/scanning electron microscopy

Scanning electron microscopes (SEM) produce sample images by scanning a focused beam of electrons on the sample. The sample atoms produce various signals that contain information about the sample's surface topography and composition. Sodium silicate and silica gel produced from rice husk, white ash, and sintered composites

have to be metallographically polished before the examination. Characterization can only be done in etched conditions.

Etching can be accomplished using Keller‘s reagent to get pure sodium silicate (Uhrlandt, 2006). Polarizing microscopes use polarizing light with the incident and transmitted illumination to determine natural minerals in silica gel. Microscopic specimen examination while mounted on a thin section identifies the main minerals of the specimen and features of the specimen along with its composition. Polarizing microscopes are also known as petrographic microscopes. Polarizing microscopes may have transmitted light only or both transmitted and reflected light. Polarizing microscopes are used in the fields of geology, pharmaceuticals, chemistry, medicine, and metallurgy (Allen, 2015).

2.8.2 Total X-ray fluorescence spectroscopy

Total X-ray Fluorescence (TXRF) spectroscopy determines the chemical composition (elemental) of materials in a non-destructive process. The principle of operation is that when sample electrons are displaced from their atomic orbital positions, they release a burst of energy that is characteristic of the sample. The X-ray beam is emitted from the front end of the handheld TXRF analyzer and it excites sample atoms, which thereafter release radiation characteristic of the sample. This enables characterization of the sample and thus a profile of its constituents. TXRF spectroscopy is also used in the determination of sample thickness, composition of layers, and coatings. The advantage of TXRF over other spectroscopy techniques is that it is fast, accurate, and non-destructive. It requires minimal sample preparation and can detect multi-elements (Stosnach, 2006).

2.8.2.1 Principle of total X-ray fluorescence spectroscopy

Total x-ray fluorescence spectroscopy (XRF) works on the principle that when atoms are irradiated with X-rays, they emit secondary X-rays called fluorescence radiation. These fluorescence radiations are characteristic of a particular atom (element) and are of specific energy, which enables qualitative and quantitative analyses. Using

these analytical techniques, elemental content in liquids, solids, and loose powders can be determined (Stosnach, 2006).

The TXRF spectroscopy is highly accurate and precise with simple and fast sample preparation. All elements (sodium-uranium) at all concentration levels (100 %-sub-ppm level) can be analyzed. Sample digestion is not required in TXRF analysis. Samples are placed in trays (acrylic or quartz glass) that reflect X-ray radiation. For liquid samples, 10 mL of sample is pipetted onto a clean quartz carrier for drying in an oven to evaporate the liquid. Samples are then irradiated for 100 seconds and using an S2 Pico fox software, the intensities of the readout are converted directly into concentration. The main advantages of TXRF include trace multi-elemental analysis without external calibration, analysis of small samples, fast in-field analysis, low maintenance, and low operating cost (Brouwer, 2006).

2.8.3 UV spectrophotometry

Ultra violet (UV) spectroscopy works by Beer-Lambert law, which states that: when a beam of monochromatic light passes through a solution of an absorbing substance, the rate of decrease of intensity of radiation with a thickness of the absorbing solution is proportional to the incident radiation as well as the concentration.

The expression of Beer-Lambert law is given in **Equation 2.14**

$$\mathbf{A = \log (I_0/I) = Ecl \quad \ldots\ldots\ldots Equation\ 2.14}$$

Where, A = absorbance, I_0 = intensity of light incident on sample cell,

I = intensity of light leaving sample cell, C = molar concentration of solute,

L = Sample cell length (cm.), E = molar absorptivity

From the law, it follows the greater the number of molecules capable of absorbing light of a given wavelength, the greater the extent of light absorption will be (Kealey & Haines, 2004). Common features of UV spectrometers include

i. Light source- light sources that cover the whole UV region like tungsten filament lamps and hydrogen-deuterium lamps are widely used. Tungsten filament lamps emit 375 nm radiations, while hydrogen-deuterium lamps radiations emit below.
ii. Monochromatic- with inbuilt slits and prisms. A rotating prism disperses radiation emitted from the primary source. Various wavelengths of the light source separated by the prism are then selected by the slits. Rotation of the prism results in a series of continuously increasing wavelengths. The beam selected by the slit is always monochromatic.
iii. Sample and reference cells- two beams pass through the reference and sample solution respectively. The cells are commonly made of silica or quartz.
iv. Detector- two photocells are used in UV spectroscopy as detectors. One receives the beam from the sample cell while the other receives the beam from the reference. The intensity of the two radiations results in the generation of pulsating or alternating currents in the photocells.
v. Amplifier- alternating current (AC) generated in the photocells is amplified and coupled to a servo-meter. The photocells produce a very low-intensity current, which needs to be amplified to get clear and recordable signals.
vi. Recording devices- Computers are used as recording devices and they store all the data generated and produce the spectrum of the desired compound (Kealey & Haines, 2004).

2.8.4 Fourier infrared spectroscopy (FTIR) analysis

Fourier transform infrared spectroscopy analyzes the chemical properties of substances by using infrared light. It is an analytical technique commonly used to identify organic, polymeric, and inorganic materials. The FTIR analysis method works on the fact that molecules have a unique vibrational spectrum when interacting with infrared radiation (Kealey & Haines, 2004). The infrared spectrum is characteristic of the molecule and can be used as a fingerprint for identification. This is done by comparing the spectrum from an ‘‘unidentified sample’’ with a reference spectrum. FTIR spectra of pure silica typically exhibit peaks in two distinct regions

(Fidalgo & Ilharco, 2001); Patwardhan et al., (2006): peaks at >2500 cm^{-1} and <1300 cm^{-1}.

The first region corresponds to hydroxyl (-OH) stretching from absorbed or molecular water, while the second region occurs due to several silica modes. While containing several peaks, the silica region can be separated into three peaks: a broad peak at ~ 1100 cm^{-1} and ~ 450 cm^{-1}, ~ 800 cm^{-1}. The absorption at ~ 450 cm^{-1} is assigned to the rocking motion of oxygen atoms. Symmetric vibrations of silicon atoms in a siloxane bond occur at ~ 800 cm^{-1}. Silica infrared spectrum has its highest peak at ~ 1100 cm^{-1}. FTIR instruments have a working range of between 4000- 400 cm^{-1} depending on optics. Some individual functional groups may fall outside the quoted ranges due to several reasons like (Ibrahem & Ibrahem, 2014):

i. Influences of other functional groups within a molecule.
ii. Impact of preferred spatial orientations.
iii. Environmental effects (chemical and physical interactions) on the molecule.

The preferred format for presenting spectral data for qualitative analysis is the percentage transmittance format. Having a logarithmic relation with linear concentration (absorbance) provides a good dynamic range for both weak and intense bands. Peak maximum becomes minimum and represents a point of lowest transmittance for a particular band. Functional groups found in the nitrogen-oxy (NOx), phosphorus-oxy (POx), silicon-oxy (SiOx), and sulfur-oxy (SOx) compounds are not easily identifiable from first principles. Their spectra are characteristic with many of the oxy absorptions occurring within 1350 - 950 cm^{-1}. This region of the spectrum is also crowded and is highly overlapped (Coates, 2000).

Table 2.6 shows the frequencies associated with different functional groups. Silicate is associated with frequency 1100-900 cm^{-1}.

Table 2.6: Example of group frequencies for common inorganic ions

Group frequency (cm^{-1})	**Functional group/assignment**
1490–1410/880–860[a]	Carbonate ion
1130–1080/680–610[a]	Sulfate ion
1380–1350/840–815[a]	Nitrate ion
1100–1000	Phosphate ion
1100–900	Silicate ion
3300–3030/1430–1390[a]	Ammonium ion
2200–2000	Cyanide ion, thiocyanate ion, and related ions

Source: Coates (2000)

Table 2.6 shows typically, the first absorption (a) is intense and broad, and the second has weak to medium intensity and is narrow. Both often exist as multiple band structures, and this is used to characterize individual compounds.

FTIR spectrophotometer have three major components (Kealey & Haines, 2004);

a. Infrared source- For the mid-IR region, 2-25 µm (5000–400 cm^{-1}), a silicon carbide element heated to about 1200 K is normally used. The output is similar to a blackbody. Tungsten-halogen lamps are used for shorter wavelengths of the near-IR, 1-2.5 µm (10000–4000 cm^{-1}) because of higher temperature requirements.
b. Beam splitter—ideal beam-splitter transmitting and reflecting 50% incident radiation. Several beam-splitters may be used together to cover a wide spectral range due to range limitations of optical transmittance. In the mid-IR region, the beam splitter is usually made of KBr (with germanium-based coating) that is semi-reflective. KBr absorbs effectively at wavelengths beyond 25 µm (400 cm^{-1}). Bands related to inorganic compounds and organometallic complexes are typically observed in the infrared region to 240 cm^{-1}. The FTIR spectrophotometer has a Csl beam splitter that can be mounted on the IRTracer-100 for measuring spectra in this region. Since absorption due to water is greater in the 400 - 240 cm^{-1}, the instrument

requires to be purged with desiccated air before performing measurements. The csl beam splitter is also normally stored in a desiccator when not in use since it is highly sensitive to moisture.

c. Detectors-Deuterated triglycine sulfate (DTGS) or lithium tantalate ($LiTaO_3$) are used as they respond to changes in temperature as the intensity of IR radiation falling on them varies. Operating at ambient temperatures, they provide adequate sensitivity routine applications. To achieve the best sensitivity, scan time is typically a few seconds (Dutta, 2017).

2.9 Fabrication of rice husk gasifier

Rice husk biomass is considered waste and is found in all rice-growing areas. Rice husks gasifier can produce rice husk ash. RHA can be used as raw material in the production of industrial chemicals. This would reduce rice husk disposal issues, which contribute to environmental pollution. **Figure 2.4** shows the principle of operation of a rice husk reactor.

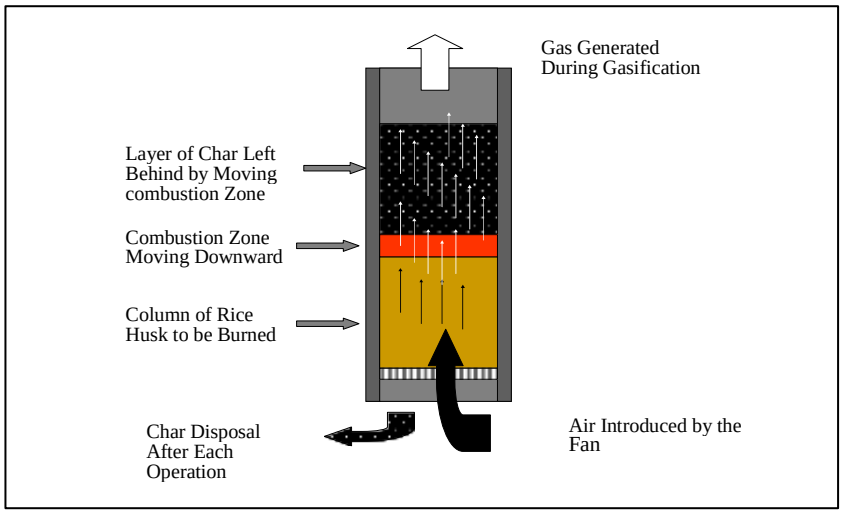

Figure 2.4: Principle of operation of the rice husk gasifier reactor.

Source: (Belonio, 2005)

Figure 2.4 shows how rice husks are burnt in limited air-producing char, which reacts further with oxygen in the air to produce carbon monoxide (CO), hydrogen

(H_2), and methane (CH_4). By increasing the air supply later, the residual char completely burns to white rice husk ash. The movement of rice husks layers is downward depending on the amount of air supplied by the fan. To burn 1 kg rice husks, an excess of 4.7 kg of air is needed, after gasification the percentage of char leaving the reactor is about 32% of the total volume of rice husks previously landed (Belonio et al., 2013). Burning with 30-40% of air produces a flammable bluish gas. With an air density of 1.25 kg/m^3 (International Standard Atmosphere), the combustion air needed is 3.76 m^3/kg of rice husks (Kaupp, 2013).

The reactions of gases during the process are shown in **Equations 2.15-2.20** (Kaupp 2013);

Combustion $C + O_2 \longrightarrow CO_2$ …… **Equation 2.15**

Water gas $C + H_2O \longrightarrow CO + H_2$…….. **Equation 2.16**

Water shift reaction $CO + H_2O \longrightarrow CO_2 + H_2$…….. **Equation 2.17**

Boudouard reaction $C + CO_2 \longrightarrow 2\ CO$…… **Equation 2.18**

Methane reaction $C + 2\ H_2 \longrightarrow CH_4$…… **Equation 2.19**

When all rice husks have been burnt to black char, continuous stoichiometric air supply will result in white RHA used to make industrial chemicals.

Char (C) + O_2 ⟶ White rice husk ash… Equation 2.20

There are generally two main types of gasifiers used for rice husks. There are the fixed bed type gasifier and the fluidized-bed gasifiers. The fixed bed type gasifier has been found more suitable (Belonio, 2005). Fixed bed gasifiers have several designs. Downdraft-type Gasifier has the gas flowing downwards with top reloading allowing for continuous operation. The top-lit Updraft has the combustion zone descending downwards. The rice husk fuel is ignited on top of the reactor. In the Up-Draft type gasifier, the combustion and pyrolysis zones start at the bottom, with the high temperatures gases moving upwards with lateral exit. The rice husk fuel moves

downwards to fill the space created thus allowing for continuous operation (Kaupp, 2013).

2.9.1 Rice husk oxidation reactor design

Basic factors to consider when fabricating a oxidation reactor to burn rice husks to produce rice husk ash include (Belonio, 2005).

1. Reactor Type- The up-draft type would fit our purposes to produce rice husk ash. The up-draft type also allows top loading thus enabling continuous operation.
2. The cross-sectional area of the reactor- a large area of the reactor means the stove will burn more rice husks and thus produce more usable ash. Better uniform burning is achieved when the reactor is circular (Belonio, 2005).
3. Height of the reactor- The reactor height determines the pressure draft and is a major design factor when choosing the blower. The size of the blower and its air supply requirement is calculated using the reactor height.
4. Fan airflow and Pressure- The stoichiometric air requirement is about 4.7 kg/kg rice husks for complete combustion. Initially for gas production, 30-40 % of the air will be required which can then be increased gradually to ensure the char is completely converted to ash.
5. Insulation of the reactor- Proper insulation results in better rice husk conversion to RHA and gas production.
6. Size of the char chamber- Bigger chamber size means less emptying of RHA and better aeration resulting in more residual char conversion to RHA.

2.10 Green chemistry strategies

Green chemistry came about due to a shift in environmental problem-solving strategies. The shift was from environmental legislation (legislated mandated reduction of industrial emissions) to active prevention of pollution through changes in the innovative design of production technologies. The new concepts now called green chemistry expanded the broader meaning of the term sustainable and clean chemistry (Anastas & Warner, 1998).

Twelve (12) principles were published to guide the practice of green chemistry. The principles addressed ways of reducing the environmental and health impacts of chemical production. The principles covered concepts such as the design of processes, use of renewable material and energy, design of energy-efficient systems, and avoidance of waste production (Anastas & Warner, 1998).

Principles of green chemistry applicable to this study include

i. **Prevention of waste**. Preventing waste is better than treating or cleaning up waste.
ii. **Use of less hazardous chemical syntheses** to avoid using or generating substances toxic to humans and/or the environment.
iii. **Designing safer chemicals** to achieve their desired function while being as non-toxic as possible.
iv. **Safer solvents and auxiliaries**. Auxiliary substances should be avoided wherever possible, and safer solvents like water, Supercritical water, Supercritical CO_2 should be used.
v. **Design for energy efficiency**. Energy requirements for chemical conversions should be minimal, and processes should preferably be undertaken at ambient temperature and pressure.
vi. **Use of renewable feedstocks**. Renewable feedstocks or raw materials are preferable to non-renewable ones.
vii. **Design for degradation**. Chemical products should be designed to not pollute the environment.

2.11 Previous works relevant to study

Jang research group and Chareonpanich research group synthesized SBA-15 (Santa Barbara Amorphous type) mesoporous silica using RHA derived from non-treated RH (Chareonpanich, Nanta-Ngern, & Limtrakul, 2007).

Hegazi (2013) tested the use of rice husks as adsorbent material, metal solutions of (Cu, Ni, Fe) were prepared by dissolving copper sulfate ($CuSO_4 \cdot 5H_2O$), nickel nitrate $(NiNO_3)_2 \cdot 6H_2O$ and iron sulfate ($FeSO_4 \cdot 7H_2O$) separately in double-distilled

water to result in known concentrations of the metal ions required and to make synthetic wastewater.

Grisdanurak et al. (2007) used HBr solution on RHA to get high-purity silica. Posted treated RHA was treated with base to form sodium silicate. By using cetrimonium bromide (CTAB) as a templating agent, the authors produced MCM-41 with a surface area of approximately 750-1100 m^2/g and an average pore diameter of 2.95 nm. Results also indicated surface hydrophobicity of MCM-41 obtained from rice husks could be enhanced by the silylation with silane.

Liu et al. (2019) successfully shortened the porous silica preparation time (within 10 hours) without compromising the specific surface area. The aging step was skipped and a microwave oven was used for drying to save time. During synthesis, by using a much lower pH, the amount of PEG incorporated into the silica-PEG composites increased. This resulted in higher surface area porous silica (792 m^2/g at pH 5.7 and 1018 m^2/g at pH 3.2) (Li, Chen, & Zhu, 2011).

Adam and Iqbal (2010) produced sodium silicate by reacting rice husk ash (RHA) and aqueous sodium hydroxide in open and closed reaction systems.

Gu et al. (2013) have studied temperature effect on morphology and phase transformation of nano-crystalline rice husk extracted silica. Pyrolysis of rice husk (RH), an agricultural by-product, was studied at different temperatures (700–1100 ^oC) in presence of air.

CHAPTER THREE

MATERIALS AND METHODS

3.1 Introduction

This chapter outlines in detail how research activities were conducted. It describes how the research objectives, synthesizing and characterizing green industrial chemicals from rice husks and testing their technological application in wastewater treatment was carried out. The specific objective steps included,

a) To determine the ash content, volatile organic compounds, particle size distribution, and moisture content of sampled rice husks.
b) To design and fabricate a small-scale silica extraction oxidation reactor for agro-wastes (rice husks) for local industrial use.
c) To develop and optimize a chemical conversion process for RHA to sodium silicate (Na_2SiO_3), silica gel, and activated carbon using green chemistry.
d) To compare the synthesized Silica gel (SG) and Activated Carbon (AC) chemical products with reference KEBs standard (KS 2350: 2012) and other international characterization standards.
e) To conduct laboratory-scale technological application studies of the rice husk derived activated carbons for wastewater treatment by
    i. Studying the removal efficiency of Phenolic organic load pollutants in tea factory wastewater using rice husk derived activated carbons
    ii. Studying the removal efficiency and kinetics of removal of Priority Pollutants (Pb, Cd, and Cr) from water using rice husk-derived activated carbons.

3.2 Sample collection and treatment

The samples were collected from millers in Kirinyaga County, Kenya, specifically

a. Mwea rice millers (Kirinyaga County),
b. Euro rice millers (Kirinyaga County)
c. Nice rice millers (Kirinyaga County)

Figure 3.1 shows the sampling area of rice husks in Mwea, Kirinyaga County

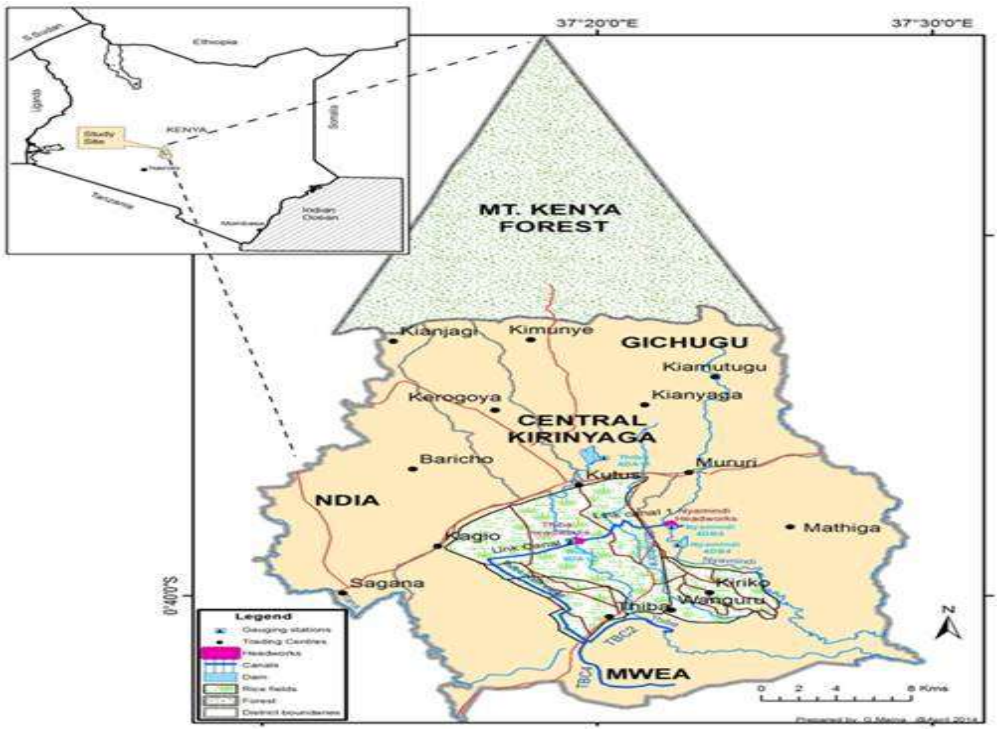

Figure 3.1: Rice husk sampling area

Source: (Wanja, et al., 2019)

Sample collection was carried out between March 2017 and June 2017. 20kg of rice husks were collected from each miller. Samples were collected from different points in the milling areas in each factory to ensure representation. They were labeled and transported to the Food Science laboratory, Jomo Kenyatta University of Agriculture and Technology. In the laboratory, the rice husks were washed with sodium dodecyl sulfate solution at constant stirring for 10 min to remove dirt and water-soluble impurities and dried in the sunlight for 24 hr. Sample drying was finally done in an air oven (Memmert model UF110) at 110°C overnight and stored in glass containers.

3.2.1 Sampling of wastewater

Wastewater samples from the Theta tea factory in Kiambu county, Kenya were collected in March 2018. Sampling was done from wastewater collection pods within the factory premises. The major source of factory wastewater was from cleaning

processes. Major cleaning is done weekly generated about 47- 30 m^3 while minor cleaning is done daily generated about 10-7 m^3 of wastewater. A total of 30 samples of 1litre wastewater were collected from lagoons and collection pods and were mixed to ensure a representative sample.

3.2 Reagents and solvents

Analytical grade reagents - (Nitric acid, hydrochloric acid, sulphuric acid) used in the trials were procured from Rankem, India. Standard solutions used in Analytical Equipment (Atomic Adsorption spectrophotometer, UV spectrophotometer) were from the equipment manufacturers. All other chemical reagents were purchased from Sigma-Aldrich, Germany.

3.3 Cleaning of glassware

Glassware of 50 mL, 100 mL, and 300 mL used in this work was cleaned by soaking in warm water containing a non-ionic liquid detergent. Distilled water was used in rinsing the glassware. Volumetric flasks of 100 mL, 50 mL, and 10 mL capacity used in standard solutions preparation were cleaned, by soaking in warm water, rinsing them in distilled water, and drying them in the oven. Final drying was done in an Electronic oven (Memmert model UF110) at a temperature of 105 °C.

3.4 Experimental design

The research design chosen for this study was mainly an experimental research design where one or more subjects or dependent variables are assigned to different treatments (i.e. independent variables) and the results are observed to conclude. The most common type of research design for researchers in laboratory work is experimental research. Related to a laboratory test procedure, experimental research designs include the collection of quantitative data and its statistical analysis during research. Thus, making it an example of a quantitative research method. True experimental research design relies on statistical analysis to approve or disprove a hypothesis. Considered the most accurate experimental design it can proceed with or without a pretest on a minimum of two (2) randomLy assigned dependent subjects.

Research conducted under scientifically acceptable conditions uses experimental methods. The success of experimental studies is dependent on confirmation that the change of a variable is based solely on the manipulation of the constant variable. The research needs to establish a notable cause and effect (Campbell & Stanley, 2015).

Characteristics of Experimental Research include

i. Variables- They can be dependent, independent, and extraneous variables. The dependent variables are the variables being treated or manipulated and are sometimes called the subject of the research. Independent variables are the experimental treatments being exerted on the dependent variables. Extraneous variables, on the other hand, are other factors affecting the experiment that may also contribute to the change.
ii. Setting- location of the experiment (laboratory) where control can be exerted on the extraneous variables, thereby eliminating them.
iii. Multivariable- suitable for research whose aim is to examine cause-effect relationships, e.g. explanatory research.

3.5 Physicochemical properties of rice husks

3.5.1 Moisture content determination

Three grams (3.0 g) of rice husk sample was weighed in triplicate into numbered moisture dishes in an analytical electronic balance (model: LibrorAEG-220, NO: D400402854, capacity: 220 g, readability: 0.1 g). The moisture dishes had previously been cleaned, dried in a hot air oven, and cooled in a desiccator.

The weighed samples were then dried in an oven (model: Memmert UF 110) at 105 °C for 30 min. The samples were thereafter cooled in a desiccator and weighed again. This was repeated every 30 min until the weight was constant.

3.5.2 Particle size determination of sampled rice husks

Using a vibratory feeder Test Sieve BS410/1986, 10.8 g of sample was weighed and shaken for 20 minutes. The vibratory feed is a high-speed assembly machine

designed and manufactured by VSI Automation Company. It is a stainless steel mesh test Sieve. Various fractions separating were individually recorded.

3.5.3 Determination of ash content of sampled rice husks

A sample mass of 18.0 g was weighed in triplicate and put in numbered crucibles.

Weighed samples were heated on a hot plate in the fume cupboard until no visible smoke was present. The charred samples were placed in a heat-resistant mat and transferred to an electronic muffle furnace (Advantec KL-420). They were then heated at 600 °C for 3 hours until they turned greyish white.

Cooling of the crucibles was done in a desiccator to prevent them from absorbing moisture from the atmosphere. The thermally treated samples were weighed after cooling and the results recorded.

3.6 Design and fabrication of small-scale silica extraction oxidation

The oxidation reactor will convert rice husks to rice husk ash (RHA) which will be used to produce green chemicals for local industrial use. The silica extraction is a rice husks oxidation reactor, which converts rice husks to produce white RHA. RHA can be converted to sodium silica solution by a chemical process. The resultant solution will then be used to produce silica gel by an acidification process. After a review of several designs of rice husk oxidation reactors a design was adapted and customized for fabrication based on Gas Stove design (Belonio, 2005).

3.6.1 Design parameters

The size and functionality of the oxidation reactor were determined by considering the following parameters adapted from the Gas Stove design (Belonio, 2005).

The design parameters considered were**,**

i. **Reactor diameter –** diameter of the inner core (reactor) where the burning of rice husks occurs. The reactor diameter determines the cross-sectional area. A wider cross-sectional area results in more rice husks consumption by the

oxidation reactor and more RHA production. Uniform burning is best achieved when the reactor is designed in a circular shape (Belonio, 2005).

ii. **The height of the reactor** – is the total distance from the top and bottom end of the reactor. The height of the reactor determines the operational time of the oxidation reactor (Belonio, 2005).

iii. **Time to consume rice husks–** is the total time required to completely combust the rice husks inside the reactor. Burnt layers of rice husks move down the reactor dependent on supplied air from the fan. The downward movement is faster when more air is introduced. Burnt rice husks are left in the reactor as char or carbon when the combustion zone moves downward (Suvarnakuta & Suwannakuta, 2006).

iv. **The amount of air needed for Combustion –** is a measure of the rate of flow of air needed to combust rice husks. The size of the fan will determine the rate of flow of air.

v. **Superficial air Velocity-** is the speed of the airflow in the fuel bed, dependent on reactor diameter D and airflow rate (AFR). The air velocity in the reactor with rice husks will cause channel formation, which could affect combustion adversely (Belonio, 2005).

vi. **Resistance to Airflow –** is resistance exerted by fuel and char inside the reactor during combustion. It is a function of the thickness of the fuel column and the specific resistance (Sr) of rice husk. Oxidation reactor design can be adjusted when fabricating to accommodate more rice husk processing according to particular needs. Rice milling industries can fabricate it as per their needs. If the production of rice results in 100kg of rice husk waste, modification to process all the rice husk waste can be made to produce Silica for the production of sodium silicate solution.

The design parameters are linked by **Equations 3.1-3.5** (Belonio, 2005); Rice husk consumption rate is calculated from **Equation 3.1** as,

$$FCR = Qn/HVf\,\xi g \quad \text{…….. Equation 3.1}$$

Where: **FCR** – Rice husk consumption rate, kg/hr.

Qn – heat energy requirement, kJ/hr.

HVf – the heating value of rice husks, kJ/kg,

ξg – Rice husk oxidation reactor efficiency, %

D (Reactor diameter) for the desired rice husks consumption rate of **20 kg per hour** would be as shown in **Equation 3.2**

$D = [1.27 \times FCR / SAR]^{0.5}$……. Equation 3.2

D= [$1.27 \times 20 / 100]^{0.5}$ = **0.22m**

Height of the reactor can be calculated from **Equation 3.3** as shown

H= SAR × T/ ρrh……. Equation 3.3

H = 100kg/m^2-hr × 0.3 hr. / 100kg/m^3 = **0.30m**

Where: **H** – Height of the reactor, m., **SAR** – Stoichiometric air of husks, kg/m^2-hr, **ρrh** - density of rice husks, Kg/m^3 (Belonio, 2005).

Time taken to consume the rice husks can be calculated from **Equation 3.4**

T = ρrh × Vr / FCR……. Equation 3.4

T = (100× π $(0.22m)^2$0.3m/4)/0.21**= 5.4 hrs.**

Where: **T** – Time to consume the rice husks, hr., **Vr** – Volume of the reactor, m^3., **ρrh** – Rice husks density, Kg/m^3., **FCR** – Rate of consumption of rice husk, kg/hr.

This means the designed 30cm diameter RH- oxidation reactor with a 0.30cm height will be operated at a fuel consumption rate of 20kg/hr.

The airflow rate of the RH-combuster can be calculated from **Equation 3.5** as shown,

$$\mathbf{AFR = FCR \times SA/ \rho a \ldots\ldots Equation\ 3.5}$$

$$\mathbf{AFR} = [0.3(2.5\ kg/hr.)\ (4.5\ kga/kg\ rh)/\ (1.25\ kga/m^3)] = \mathbf{2.7\ m^3/hr.}$$

Where: **AFR** – Airflow rate, m^3/hr., **FCR** – Rice husk consumption rate, Kg/hr., **ρa** – Air density, 1.25 kg/m^3., **SA** – Stoichiometric air of rice husks, 4.5 kg of air per kg rice husks.

3.6.2 Fabrication method

One stainless steel (SS) sheet (203*102*2 mm) was used for the construction of the inner cylinder of the reactor, outer cylinder, and char chamber. The burner assembly started with the fabrication of the outer cylinder (30 cm) and the inner cylinder (22 cm). They were made with the same MS sheet material of a similar gauge as that of the reactor. The reactor was designed with a strong material as it was in direct contact with flammable gases. The SS sheet offered good resistance to heat.

The pot support and handle of the burner assembly including the frame for the char grate and the lever are also made of stainless steel material for better durability. Insulation of the oxidation reactor was made of high-temperature refractory cement (Hi-Castable cement) to form a good insulating material due to its high silica content. A direct current fan operated with a 6v battery was used to provide the air needed for combustion. The ash box attached to the reactor was enlarged to ensure a continuous collection of white ash. Detailed structural drawings of the fabrication process are attached in **Appendix 2**.

3.6.3 Testing performance of the oxidation reactor

Efficiency in the generation of RHA by the fabricated RH-oxidation reactor was evaluated using the following procedures adapted from two sources.

a. Determination of Ash in Biomass, (Sluiter, et al., 2008).
b. Rice gas stove handbook (Belonio, 2005)

1kg portion of dry rice husks was loaded into the reactor by first removing the burner seated on top of the fabricated oxidation reactor. Loading was done by directly pouring the rice husks from a plastic storage container. Small pieces of paper were placed on top of the rice husks. The papers were lit, and the fan attached to the oxidation reactor switched on to provide stoichiometric air needed for complete combustion. The reactor was closed by replacing the burner top after three-quarters of the entire reactor area was observed to be burning. After all the rice husks were burnt, the fan was shut off to stop smoke from coming from the oxidation reactor. The burned rice husks were allowed to stay inside the reactor for 6 hours to produce white RH ash. The ash was then removed using a scoop and placed in the weighed can. The ash weight was measured and the percentage RHA produced was calculated.

Ash conversion efficiency of the RH-oxidation reactor was observed by following parameters adapted from the Rice gas stove handbook (Belonio, 2005)

a. Total operating time –the time from rice husks ignition to complete rice husk char.
b. Rice husk consumption rate – the amount of rice husk utilized divided by operating time.
c. Combustion zone rate – Time taken for the combustion zone to move down the reactor.
d. Percentage RHA produced – the ratio of the weight of ash produced to rice husks used. The Water Boiling Test (WBT) stove performance test protocol used was developed by the University of California-Berkeley (Bailis, et al., 2007).

3.7 Conversion of RHA to novel chemicals

Preliminary trials were for determining the best conditions for producing sodium silicate, silica gel, and activated carbon. After obtaining laboratory use permissions, the following trials were conducted in the food science laboratory using rice husks from the Mwea area, Kirinyaga County.

3.7.1 Pre-leaching rice husks with acid

Samples were divided into two portions and separately leached with acid reagents (0.5M HCL, 0.5M H_2SO_4). Rice husk samples were mixed with acid at 60 ºC for 30 minutes with constant stirring. Samples were washed with distilled water to remove acidity. Leached samples were filtered and air-dried for 24 hrs at room temperature. Final drying was done for 2 hrs at 110 °C in an oven (Memmert UF110). Removal of carbonaceous matter and subsequent thermal treatment at 500 °C, 600 °C, and 700 °C for 30 minutes was carried out in a muffle furnace (Advantec KL-420). Samples were analyzed using XRF spectroscopy. Standard analytical methods for sample preparation and treatment were followed (AOAC, 2019).

3.7.2 Leaching rice husk ash with acid/water

Rice husks were converted to RHA at three furnace temperatures (400, 500, and 600 °C). Openly burnt RHA samples were also prepared by burning rice husks in the open. Oxidation reactor also was fed with rice husks and allowed to burn and smolder slowly for 3 days. RHA was then collected and used in the leaching trials.

Rice husk ash was leached with 0.5M HCL, 0.5M H_2SO_4, and water separately, by mixing sample and acid or water at 60 °C for 30 minutes with constant stirring. Acid leached RHA samples were also washed with distilled water until free from acidity. A pH meter was used to ensure samples were acid-free. Drying was done in an oven at 105 °C. Leached rice husk ash samples were analyzed for elemental content using TXRF spectroscopy (Bogert, 2015).

3.7.3 Conversion of rice husks to sodium silicate solution

Rice husk samples were burnt in the open while some were thermally treated at 400, 500, and 600 °C to produce Silica. Each sample was reacted with a different concentration (1 M, 2 M, 3 M) of sodium hydroxide (NaOH) to find the optimum conditions for producing the best quality sodium silicate solution. Three openly burnt rice husk samples (OPB1, OPB2, and OPB3) were also reacted with different concentrations of NaOH for comparison purposes. Resultant liquid suspensions were decanted, stored into sample bottles, and analyzed for elemental content using a TXRF spectrophotometer (Bogert, 2015).

3.7.4 Conversion of the sodium silicate solution to silica gel

Sodium silicate solution samples obtained from earlier trials were mixed with 3 M HCL for 3 hr. Suspensions were filtered, washed repeatedly with water until the filtrate was non-acidic. Excess water was decanted and the suspension dried at 110 °C in an oven (Memmert UF110) for 2 hr. Dried solid samples (silica gel) were characterized using X-ray fluorescence (XRF), SEM (Fein optic polarizing), X-ray diffraction spectroscopy (XRD DS PHASER), and Fourier transformation infrared spectroscopy (FTIR).

3.7.5 Preparation of activated carbon from rice husks

Rice husks were carbonized and the residual char was activated with sodium hydroxide (NaOH) or phosphoric acid (H_3PO_4). The following procedures were used: The raw rice husks were washed with water to remove dirt and other contaminants, and then oven-dried at 110 ºC for 12 hours. They were then ground, sieved to fractions with an average particle size of 1.0 mm. 200 g of rice husks were reacted with 300 mL of 3 M NaOH (3:2). The mixture was digested for 4 hrs at 80 ºC and dried in an oven at 105 ºC for 5 hrs. The prepared husks were carbonized at 550 ºC for 30 minutes. Finally, the activated product was grounded, neutralized with 0.1 M HCl solution, and washed several times with hot distilled water to a constant pH (6.6– 7.0). The washed activated carbon samples were then dried under vacuum at 120 ºC for 24 h and stored in a desiccator. The process was repeated with 300 mL of

3 M Phosphoric acid. The two activated carbons were tested for efficiency in the absorbance of phenolic compounds in tea wastewater using a UV spectrophotometer. Sodium hydroxide (NaOH) and phosphoric acid (H_3PO_4) activated rice-derived carbons were also characterized using an SEM (Fein optic polarizing) instrument.

3.8 Characterization of the synthesized silica, sodium silicate, silica gel, and rice husk activated carbons (RHACs)

3.8.1 Analysis of silica, sodium silicate, and sodium gel elemental content from different treatments using TXRF spectroscopy

Silica (SO_2) samples produced from different experimental treatments were analyzed for mineral content to assess the optimum conditions for the best yield. TXRF (XRF SI Titan 800) Spectrophotometer) instrumental analysis was used to analyze the samples using the following procedures:

i. Samples were dried in an oven (110 °C for 24 hrs).
ii. 2. 5 g of each sample was weighed into a sample carrier
iii. Each sample carrier was then irradiated for 1000 seconds using an XRF SI Titan 800 spectrophotometer. The instrument was operated at 50 kV and a current of 1000 µA. and used a molybdenum anode.
iv. Measured spectra were evaluated using S2 Pico fox software based on chosen elements. Using the same software (S2 Pico fox), concentrations were correlated with the net intensities of the element.

Silica samples produced from different experimental trials were reacted with varying amounts of sodium hydroxide (NaOH) to find the optimum amount needed to produce the best quality sodium silicate solution. Samples were analyzed using a TXRF spectroscopy instrument. Procedural steps were different because the sodium silicate produced was in liquid form.

i. 10 mL of each sample was pipetted to a clean vial

ii. 20 µL of 1000 mg/L Gallium stock solution was added into each sample (internal Standard) resulting in a concentration of 20 mg/kg Gallium in each sample.
iii. Each sample was shaken for a minute for homogenization.
iv. Aliquots of 10 µL of each sample were pipetted using a micropipette onto a clean quartz carrier.
v. The carriers were dried in an oven to evaporate the liquid.
vi. The sample carriers were then irradiated and the mineral content determined.
vii. Liquid sodium silicate was tested for conformity to Standard KS 2350:2012. Rice husk-derived sodium silicate was analyzed using test methods as described in the Kenya Standard for Liquid Sodium silicate solution KS 2350:2012 (Kenya Bureau of Standards (KEBS), 2012). The quality parameters tested are as described in the standard,
    a. Appearance of product
    b. Total alkali content as Na_2O % by mass
    c. Density g/mL at 20 °C
    d. The ratio of mass SiO_2/ Na_2O
    e. The combined mass of SiO_2 and Na_2O

3.8.2 Characterization of novel chemicals using SEM

The following procedure was followed,

i. Silica gel, sodium hydroxide (NaOH), and phosphoric acid (H_3PO_4) rice husk-derived activated carbons were initially subjected to a bonding process using a resin (Petropoxy 154) before viewing under the Scanning electronic microscope (SEM).
ii. Effective bonding took 8 days, producing a good viewable slide of 30µm.
iii. Under the microscope, primary crystals constituting each sample were identified in both planes-polarized and closed polarized light.

3.8.3 Characterization of novel chemicals using FTIR

Analysis of leached silica samples and activated carbon samples from different treatments were carried using a Fourier Transform Infrared Spectrophotometer IR Tracer-100 (Shimadzu C103-E091A). The following procedure was followed,

i. 10 g of the solid sample was put in a micro spatula,
ii. 0.25-0.50 mg teaspoons of KBr was added,
iii. The mixture was thoroughly ground in a mortar with the pestle; the Sample was pressed at 5000-10000 psi.
iv. The sample was removed from the die and placed in the FTIR sample holder for scanning.

3.8.4 Characterization of SG using XRD

Silica gel prepared from rice husks was characterized using an XRD D2 PHASER. The concentration of an unknown silica phase was determined from calibration, using the DIFFRAC.DQUANT software. It has holders for small sample amounts, low-absorbing and weakly diffracting samples, for filters, for environment-sensitive samples. 1.0 g of solid sample was placed in the sample holders and scanned.

3.9 Technological application of AC in WW treatment

3.9.1 Removal efficiency of phenolic organic load pollutants in tea factory wastewater using rice husk derived activated carbons

Evaluation of the removal efficiency of prepared rice husk-derived activated carbons was carried out by mixing aliquots of 15 mL of wastewater; 0.5 g of the adsorbent (activated RH carbon) and shaking for 2 hours. The suspension was centrifuged for 10 min at 4500 rpm using a Centurion Model C2004. Portions of 2 mL of the supernatant were mixed with 2 mL of 20 % sodium carbonate solution and 2 mL Folin reagent and vortexed for 2 min, the resultant mixture was incubated for 20 min until a dark blue color was formed.

Phenolic compounds are responsible for the color of wastewater from tea factories. The ability of the phenolic ring to absorb UV light and the fact that some of the phenolic substances are colored compounds that is show absorption features in the visible region, make UV-visible spectroscopy a suitable technique to investigate and quantify phenolic compounds (Aleixandre-Tudo & Du Toit, 2018).

Control samples were prepared by centrifuging without adding activated RH carbon and following the previous procedures. Samples were tested for adsorption using UV-1800 Shimadzu UV spectrophotometer at 765 nm. For reliability samples were processed in the same way. The removal efficiency was determined by calculating phenol removed as a percentage of total phenols. The phenol standard was Quarcetin (CAS no.6151-25-3, EC no.204-187-1) from Sigma-Aldrich. The phenol standard specification is

a. Synonym: 2-(3,4-dihydroxyphenyl)-3,5,7-trihydroxy-4*H*-1-benzopyran-4-onedihydrate, 3,3′,4′,5,7-pentahydroxyflavone dehydrate.
b. Empirical Formula (Hill Notation): **$C_{15}H_{10}O_7 \cdot 2H_2O$**
c. Molecular weight: **338.27**

3.9.2 Removal efficiency and kinetics of removal of priority pollutants (Pb(II), Cd(II), and Cr(VI)) from water using RHACs

3.9.2.1 Effect of pH on Pd(II), Cd(II), and Cr(VI) removal

To determine the effect of pH on Pb(II), Cd(II) and Cr(VI) removal by NaOH activated and H_3PO_4 activated carbons, 2.0 g of the adsorbent was mixed with 10 mg/L of metal ions solution. Solutions were adjusted to pHs 2, 4, 6, and 8. Adjustment of pH was done using solutions of 0.5 M NaOH and 0.5 M HNO_3. The pH-adjusted solutions were centrifuged in a mechanical shaker (Centurion Model C2004) at 130 RPS (revolutions per second). The temperature was maintained at 25 °C for 120 minutes. Sample mixtures were left to stand for 30 minutes after removal from the mechanical shaker. The number of metal ions remaining at equilibrium was determined using a flame atomic absorption spectrophotometer (AA7000-Shimadzu

Japan). The equilibrium point was the point where there was no change in metal ion concentration at each pH level. Analysis of Pb (II), Cd (II), and Cr(VI) at various pH values was done in triplicate to reduce random errors.

3.9.2.2 Effect of sorbent mass on Pb (II), Cd (II), and Cr (VI) removal

Effect of sorbent mass on Pb (II), Cd (II), and Cr (VI) removal from aqueous solution was determined at optimum pH identified earlier. 10 mg/l of Pb (II), Cd (II), and Cr (VI) solutions were mixed with a range of dosages (0.5-2.0 g) of adsorbent. Resultant suspensions were centrifuged in a shaker (Centurion Model C2004) at 130 revolutions per minute. The temperature was maintained at 25°C. Samples were then removed from the shaker and allowed to settle for 30 minutes and filtered (Whatman number 42). The number of metal ions remaining was determined using a Flame atomic absorption spectrophotometer (AA7000-Shimadzu Japan). Analysis at various values of adsorbent dosages was done in triplicate to reduce random errors.

3.9.2.3 Effect of contact time and initial concentration on Pb (II) and Cd (II) and Cr (VI) removal using NaOH and H_3PO_4 activated rice husks

Optimum contact time determination was carried out by mixing 10 mg/l of Pb (II), Cd (II) and Cr (VI) solution at optimum pH and dosage identified earlier. Sample mixtures were centrifuged in a mechanical shaker (Centurion Model C2004) at 130 RPS and a temperature of 25°C. Removal of treated samples was done at regular time intervals of 30, 60, 90, to 200 minutes. Samples were allowed to settle for 30 minutes and then filtered (Whatman number 42). Amounts of Pb(II) and Cd(II) remaining in equilibrium after the various set time intervals were determined using Flame atomic absorption spectrophotometer (AA7000-Shimadzu Japan). Samples were prepared in triplicate to reduce random errors.

Initial Pb (II), Cd (II), and Cr (VI) concentrations ranging from 5, 10, 15, and 20 mg/L were also mixed at optimum pH, dosage, and contact time. Samples were centrifuged at 130 RPS in a mechanical shaker (Centurion Model C2004) at 25 °C, then allowed to settle for 30 minutes, and then filtered (Whatman number 42). Equilibrium concentration remaining for various initial concentrations was then

determined using flame atomic absorption spectrophotometer (AA7000-Shimadzu Japan). All the analyses at various time intervals were done in triplicate to reduce random errors.

3.9.2.5 Kinetic studies

The rate and the mechanism for Pb(II, Cd(II), and Cr (VI) adsorption onto the surface of the activated carbon were done as follows; Optimum initial concentration was mixed with optimum dosage and set at optimum pH. Samples were put in a mechanical shaker which at 130 revolutions per second and a temperature of 25 °C. Sample mixtures were then withdrawn at regular time intervals ranging from 15- 120 minutes. Samples were then allowed to settle for 30 minutes and filtered using Whatman number 42 filter paper. The equilibrium concentration of Pb(II), Cr(VI), and Cd(II) solution at regular time intervals was determined using a flame atomic absorption spectrophotometer. Sampling was done in triplicate to reduce errors.

3.10 Data analysis

Quantitative data were presented in either table format, charts, or other graphics. This enabled a quick understanding of data. Data presentation indicated numerical scores and percentages according to related categories. The visual presentation of data (tables, charts, and graphics) in numbers and percentages enabled an analytical description and interpretation of data using descriptive statistical procedures (Creswell, 2014).

COMPARISON OF THE VARIANCE OF TWO DIFFERENT DATA SETS TO DETERMINE IF THERE IS A STATISTICALLY SIGNIFICANT DIFFERENCE WAS DONE USING F-TESTS AND ANOVA TESTS. DATA COLLECTED WAS PROCESSED USING SOFTWARE SUCH AS MICROSOFT EXCEL. THE ANALYSIS INCLUDED CALCULATIONS OF AVERAGE VALUES, ANOVA SINGLE FACTOR TESTS, T-TESTS, AND F-TESTS (KEALEY & HAINES, 2004). COMPARATIVE GRAPHS WERE DRAWN TO ILLUSTRATE THE DIFFERENCES BETWEEN THE DIFFERENT TREATMENTS. THIS ENABLED CLEAR VISUALIZATIONS OF THE EFFECTS OF THE DIFFERENT TREATMENTS. INFORMATION ON YIELDS AND BEST PRODUCTION METHODS FOR SILICA, SODIUM SILICATE, SILICA GEL, AND ACTIVATED CARBONS WAS OBTAINED FROM EXPERIMENTAL DATA IN THIS MANNER. INFORMATION ON THE EFFECTIVE USE OF RICE HUSK-DERIVED CARBONS IN ENVIRONMENTAL POLLUTION INCLUDING OPTIMUM ADSORPTION PH, CONTACT TIME; INITIAL CONCENTRATIONS (METALLIC PRIORITY POLLUTANTS) WERE ALSO OBTAINED SIMILARLY.

CHAPTER FOUR

RESULTS AND DISCUSSION

4.1 Introduction

This chapter presents the results and analysis of the quantitative findings of the study. Discussions of results are in light of previous research findings and available literature, where applicable, to identify similarities and differences between this study and previous studies and literature. Laboratory experimental results are presented in tables and graphs. The main method for data analysis was by calculations of proportion and average values for both the laboratory and field-related results. Data were presented as means ± standard deviation (SD) and were analyzed by ANOVA. Experimental data were tested using statistical tools (Microsoft-Excel) for significance. F-tests were used to test significant variance in treatments. Data were presented and discussed in the same order as the research objectives.

4.2 Physicochemical properties of RH

4.2.1 % Moisture content of rice husks.

The moisture content of the rice husks sampled from Mwea, Euro, and Nice milling factories are shown in **Table 4.1**

Table 4.1: Moisture content of rice husks

Sample Description	**Weight Dish+Sample**	**Weight Dish+Sample** (3.5 hrs.Drying)	**Moisture weight**	**% Moisture**
Mwea Milling	9.3786	9.1665	0.2121±0.0057	7.07± 0.63
Euro Milling	7.5596	7.3476	0.2120±0.0056	7.06± 0.62
Nice Milling	7.6612	7.4662	0.1950±0.0113	5.17± 1.26

± Standard deviation.

From **Table 4.1,** rice husks had average moisture of 7.07 % after 3½ hours of drying at 105 ℃. Doorvasan et al. (2014) have reported a moisture range of 8.0-9.0%. Ephantus et al. (2016) have also analyzed moisture content levels of maize cobs and rice husks using multiple regression analyses and found they range from 8.21± 0.18%. No significant difference in moisture content was found between the millers and the other researchers.

4.1.2 Particle size distribution of RH

The distribution of the different-sized rice husks was determined. **Table 4.2** shows the results.

Table: 4.2: Rice husk samples diameter distribution

Aperture size(mm)	Mass(g)	% Rice husks
2.0	7.9563±0.0435	73.65
1.0	2.5639±0.0495	23.73
0.71	0.1877±0.0044	1.74
0.50	0.0323±0.0014	0.30
0.25	0.0080±0.0010	0.07

As can be seen in **Table 4.2**, 73.65 % of the sampled rice husks had diameters ranging from 2.00-1.00 mm. Only about 1.74 % of rice husk had a diameter within a range of 0.710 mm. Hadipramana et al. (2016) determined pore sizes of rice husk compared to cement and found most were over 3.0 mm.

4.1.3 Ash content of Mwea, Euro, and Nice Millers rice husk samples

Ash content in sampled rice husks from Mwea, Euro, and Nice millers was determined and results are shown in **Table 4.3**

Table 4.3: Percentage ash content of RH

Sample Description	Sample Weight (g)	Ash Weight (g)	% Ash Content
Mwea Milling	3.0043	0.7040±0.0239	23.43±0.77
Euro Milling	3.0005	0.6712±0.0089	22.36±0.29
Nice Milling	3.0000	0.6652±0.0149	22.17±0.48

From **Table 4.3**, sampled rice husk had an average ash content of 22.65 %. Major components of rice husk include 75-90 % organic materials such as hemicellulose, cellulose, and lignin. Ash content was about 17-20 % was reported (Bakar, Yahya, & Gan, 2016). Good quality silica can be obtained with the controlled combustion of rice husks. Metallic impurities like iron (Fe), manganese (Mn), calcium (Ca), sodium (Na), potassium (K), and magnesium influence the purity and color of the silica. Elimination by pre-treatments with hydrochloric acid, sulfuric acid, or nitric acid before combustion is preferred (Yalcin & Sevinc, 2001). Strong acid digestion is effective in breaking down rice husks into small fragments thus exposing more organic components. Surface area increase can accelerate pyrolysis.

Umeda and Kondoh (2010) reported the function of acid pretreatment in rice husk contains two aspects. One is to accelerate the hydrolysis and dehydration of lignocellulose to monosaccharides by removing hydrogen bonds or extractives. When polysaccharides are converted to monosaccharides, metallic impurities bound in organic matters are exposed. Exposure leads to reactions with acid leaching solutions. Metallic impurities in rice husks may be classified into three main categories: the water-soluble, the acid-leachable, and residual fraction. Ashes are black with gray particles due to different stages in carbon combustion during burning. Rice husk burning will result in the formation of silica ash. The ash color varies from gray to black depending on inorganic impurities amounts. The burning of rice husks results in the formation of silica ash, which varies from gray to black depending on inorganic impurities

4.2 Design and fabrication of small-scale silica extraction oxidation

The oxidation reactor burns rice husks to produce white RHA (Silica) which was chemically processed into sodium silicate solution. Sodium silicate solution was further processed to silica gel through an acidification process. After a review of several designs, a modifiable design shown in **Figure 4.1** was selected. The top-view diagram shows the inner core reactor.

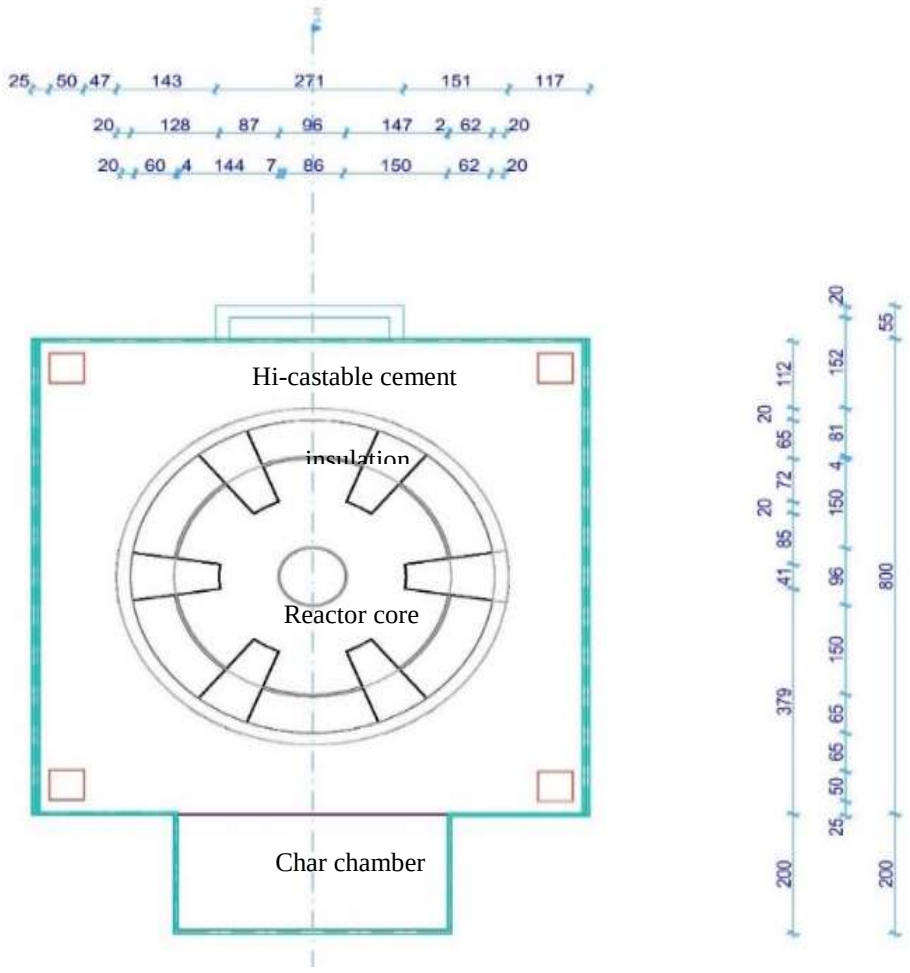

Figure 4.1: Dimensions of the silica extraction oxidation reactor

The cross-section of the oxidation reactor with measurements is shown in **Figure 4.2**.

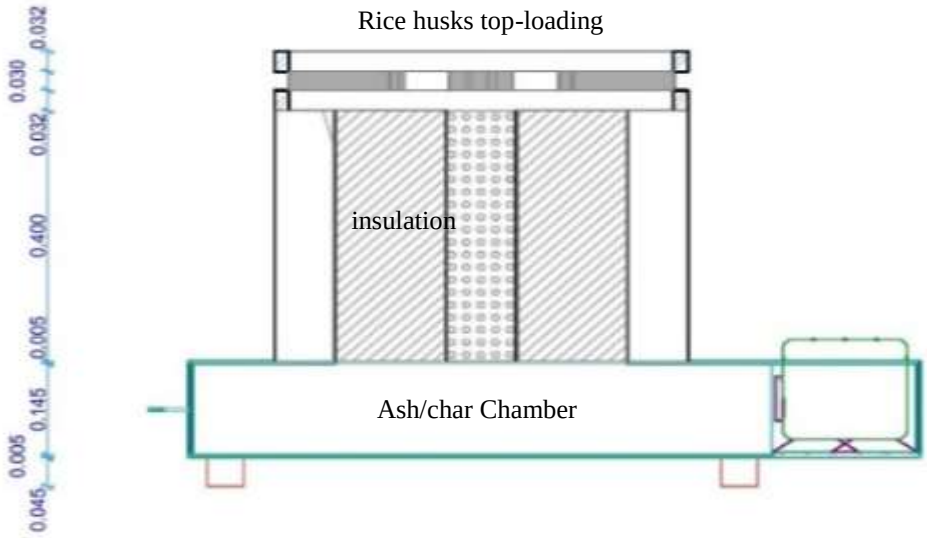

Figure 4.2: Cross-sectional view of the oxidation reactor

Figure 4.1 and **Figure 4.2** show the dimensions of the oxidation reactor used which complied with the proposed design equations (Belonio, 2005). The design parameters were used in the fabrication process. **Table 4.4** shows the properties of the oxidation reactor.

Table 4.4: Properties of the designed Silica oxidation reactor

Parameter	Specifications
Reactor Inner diameter	0.22 metres
Reactor Outer diameter	0.30 metres
Height	0.30 metres
Cross-sectional area	0.038m^2
Insulation material	H-Castable
Inner cylinder material	S/S*Gauge 16
:er cylinder material	
Fan	M/S* Mild Steel 16 12V DC
Air needed	5.4 hr. 9. 0 m^3/hr

Table 4.5 shows the cost and materials used in the fabrication process

Table 4.5: Fabrication materials/cost

ITEM	Cost/Kshs
1 black sheet 203*102*2mm	6000
1 Flat bar 600m*3mm	650
1 Round tube 19mm*3m	800
1 Round tube 50mm*400mm	200
1 kg welding rods	250
1 Sieve 250*250*3mm	3000
1 Sieve 250*500*1.5mm	3000
1 holed pipe 30mm*25mm	200
½ litre Paint	500
Total material cost plus 10 %	**16,000**
Labour charge 30% of cost	4380
Total Fabrication Cost	**20,380**

As shown in **Table 4.5** the total cost for the materials in producing the oxidation reactor was kshs.14,600. This includes the costs of metal sheets, bars, and other basic parts. With the additional 10% contingency, the material cost was kshs16000 at the time of fabrication.

Plate 4.1 shows a view of the oxidation reactor in the engineering workshop, Jomo Kenyatta Unversity.

Plate 4.1: Photo of oxidation reactor in the workshop (2019)

Plate 4.1 shows the position of the reactor. Rice husks are ignited in the reactor, with a stoichiometric air supply the residual char turns to white rice husk ash (WRHA). The temperature of the RH is increased under an air atmosphere or with stoichiometric amounts of air, to decompose organic components during

thermochemical processes. Combustion is normally applied to produce biogenic silica in general (Chen, Lv, Zhang, Zhang, & Ye, 2011).

Plate 4.2 and **4.3** show the testing process and RHA produced in the combustion process.

Plate 4.2: Silica extraction oxidation reactor (Testing)

Plate 4.3: Silica extraction oxidation reactor with RHA

Plate 4.2 shows the ignition point during the combustion of rice husks. **Plate 4.3** shows the RHA after the combustion process. Residence time and temperature are the two main influential factors for silica purity in the reactor. Silica purity increases with increasing conversion temperature and residence time (Bie, Song, Liu, Ji, & Chen, 2015). The risk of crystallization of the obtained biogenic silica is enhanced with increased conversion temperature and residence time (Shen, Liu, Zhu, Zhang, & Tan, 2011).

4.2.1 Performance of oxidation reactor

4.2.1.1 Oxidation efficiency of reactor

Rice husk ash generation was monitored after three trial runs, and the results tabulated in **Table 4.6**

Table 4.6: Ash conversion efficiency test of oxidation reactor

Items	Run#1	Run#2	Run#3	Average (±std)
Starting time (min)	1.38	1.40	1.43	**1.40±0.020**
Operating time (min)	15.00	12.00	13.25	**13.40±1.230**
Fuel rate (FCR;kg/h)	5.0	5.7	5.4	**5.4±0.286**
% Ash produced	17.83	20.50	16.66	**18.33±1.607**

The maximum temperature attained at the reactor cylinder was 432 °C as measured by AssTech PF ST 677 laser instrument. The oxidation reactor had an efficiency value of 18 % as shown in **Table 4.6**. The starting time was 2 minutes, the fuel consumption rate was 2.26 kg/h, and the time required to boiling of 2 kg of water was 7-8 minutes. Suvarnakuta and Suwannakuta (2006) reported a rice husk oxidation reactor with an average efficiency of about 21.77 %. By increasing the conversion temperature, carbon content and silica purity remain around the same until silica crystallization takes place, On the other hand, higher conversion temperature and residence time reduce specific surface area (SSA) and total pore volume of RHA (Blissett, Sommerville, Rowson, Jones, & Laughlin, 2017). Chen et al (2015) have found the optimum conversion temperature for combustion of untreated RH is around 600 °C, with the quality of the resulting biogenic silica also dependent on the combustion technology. A sufficient air flow rate is required for complete combustion to produce pure biogenic silica; otherwise, the resulting ash will contain unburned carbon (Umeda & Kondoh, 2008).

4.2.1.2 Water heating test

Water (1L) was brought to boil with time and temperature changes tracking to produce the profile in **Figure 4.3**.

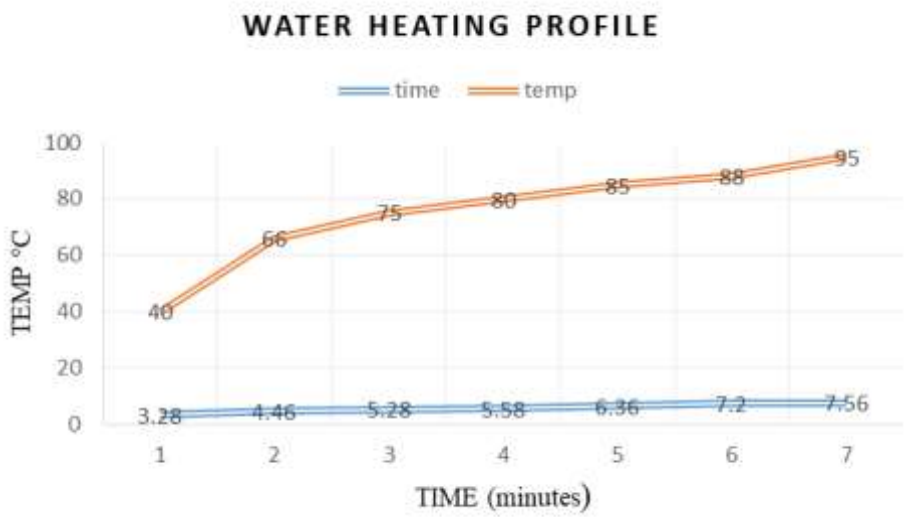

Figure 4.3: Oxidation reactor water boiling profile test.

The starting temperature was 34.1 °C. The time required to boil 2 kg of water measured from putting the pot on the burner to boiling point is 7.50 minutes from **Figure 4.3**. Ismail et al. (2016) have reported rice husks from Mwea mills have suitable moisture content thus requiring no further drying before use. Higher density rice husks were found to have more starting times compared to lower density ones.

4.3 Conversion of RHA to novel chemicals using green chemistry strategies

4.3.1 Silica yield after acid leaching effects at different temperatures

Collected rice husk samples were divided into three portions; two leached separately with 0.5 M HCL and 0.5 M H_2SO_4 acids and one portion used as a control. Each leached portion was subjected to three different thermal treatments (500, 600,700 °C). The results are shown in **Tables 4.7-4.10**

Table 4.7: Elemental composition of leached and un-leached RHA at 500 °C

%Element	Un-leached	HCl-leached	H_2SO_4-leached
SiO_2	97.372 ±1.489	99.173 ± 1.325	99.020 ± 1.348
MgO	*	*	*
Al_2O_3	0.172 ± 0.431	0.117 ± 0.382	*
P_2O_5	0.430 ± 0.070	0.204 ± 0.049	0.247 ± 0.052
K_2O	1.177 ± 0.034	0.141 ± 0.015	0.161 ± 0.015
CaO	0.582 ± 0.025	0.235 ± 0.016	0.290 ± 0.017
Mn	0.088 ± 0.013	0.030 ± 0.007	0.037 ± 0.008
Fe	0.125 ± 0.011	0.082 ± 0.008	0.095 ± 0.009
Zn	0.011 ± 0.003	0.004 ± 0.002	0.006 ± 0.002
Cl	0.027 ± 0.027	*	*
Na_2O	*	*	*
S	0.045 ± 0.024	0.027 ± 0.020	0.113 0.025

*Not detectable

Table 4.8: Elemental composition of leached and un-leached RHA at 600 °C

% Element	Un-leached	HCl-leached	H_2SO_4-leached
SiO_2	95.933 ± 1.464	98.899 ± 1.330	98.237 ± 1.332
MgO	*	*	*
Al_2O_3	*	0.402 ± 0.390	0.506 ± 0.388
P_2O_5	0.622 ± 0.085	0.252 ± 0.052	0.256 ± 0.054
K_2O	2.172 ± 0.052	0.107 ± 0.015	0.185 ± 0.015
CaO	0.817 ± 0.029	0.245 ± 0.016	0.418 ± 0.019
Mn	0.138 ± 0.016	0.027 ± 0.007	0.059 ± 0.008
Fe	0.093 ± 0.010	0.133 ± 0.012	0.127 ± 0.009
Zn	0.016 ± 0.004	0.005 ± 0.002	0.006 ± 0.002
Cl	0.048 ± 0.039	*	*
Na_2O	*	*	*
S	95.933 ± 1.464	98.899 ± 1.330	98.237 ± 1.332

* Not detectable

Table 4.9: Elemental composition of leached and un-leached RHA at 700 °C

% Element	Un-leached	HCl-leached	H_2SO_4-leached
SiO_2	96.266 ±1.40	98.999 ± 1.358	98.647 ±1.332
MgO	*	*	*
Al_2O_3	*	0.243 ± 0.387	0.073 ± 0.389
P_2O_5	0.563± 0.075	0.242 ± 0.051	0.295 ± 0.056
K_2O	1.936± 0.042	0.142 ± 0.015	0.227 ± 0.017
CaO	0.773± 0.027	0.251 ± 0.017	0.477 ± 0.020
Mn	0.130± 0.015	0.086 ± 0.008	0.058 ± 0.010
Fe	0.119± 0.012	0.120 ± 0.009	0.108 ± 0.009
Zn	0.014± 0.003	0.005 ± 0.002	0.008 ± 0.002
Cl	0.024± 0.033	*	0.002 ± 0.032
Na_2O	*	*	*
S	*	*	*

* Not detectable

Table 4.10 and **Figure 4.4** summarize the mean % silica content after the treatments.

Table 4.10: Silica content after treatment (Rice husks)

Thermal Treatment	500 °C	600°C	700°C
Un-leached	97.372 ± 1.489	95.933 ± 1.464	96.266 ± 1.400
HCL-leached	99.173 ± 1.325	98.899 ± 1.330	98.999 ± 1.358
H_2SO_4-leached	99.020 ± 1.348	98.237 ± 1.332	98.647 ± 1.332

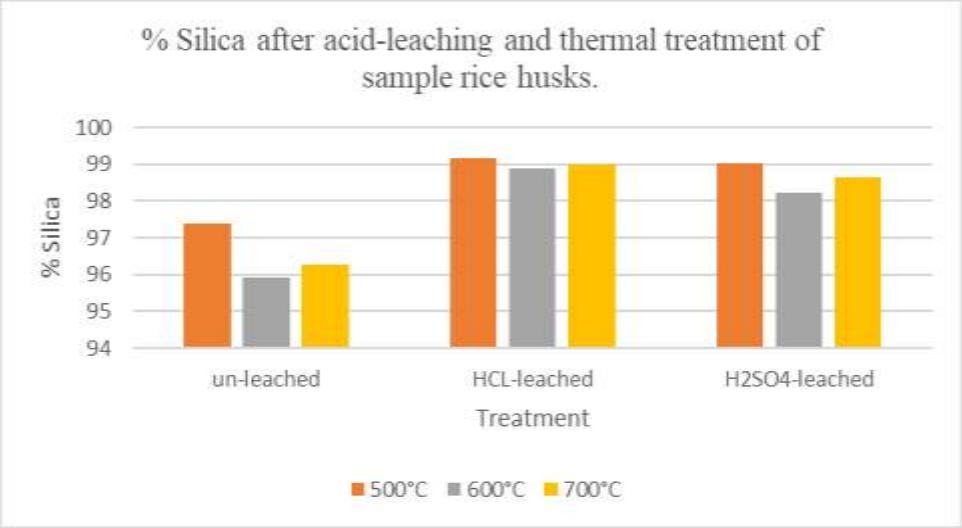

Figure 4.4: Silica content after RH- acid leaching (0.5 M HCL, 0.5 M H_2SO_4)

Table 4.10 shows the mean % silica yield (SiO_2) of rice husks leached with HCL at 500 °C temperature was the highest at 99.2 %. Overall, these conditions were the best in producing silicate. **Figure 4.4** also summarizes the results showing the effects of acid leaching with different thermal treatments. Statistical analysis of the three data sets (**Tables 4.7, 4.8, 4.9**) of the three different treatments found F=0.0286278 less F critical (5.143253) implying there is a significant difference in values at a 95 % confidence level. This implies acid-leaching causes a significant difference to the % Silica (SiO_2) content with the three treatments.

Yalçin and Sevinç (2001) demonstrated that rice husk incineration between 600 °C and 800 °C preceded by chemical and thermal pretreatment produces high purity silica. The authors used different chemical and thermal treatment approaches but reported that acid leaching pretreatment followed by oxygen-rich incineration and combustion of rice husk produced the highest silica content. One of the reasons why it is more difficult to obtain silica with purity above 97 % from rice husk by direct incineration is the presence of metallic contaminants, especially potassium and sodium oxides (Ugheoke & Mamat, 2012). These compounds affect the surface of silica particles, increasing their surface area and reactivity, and thereby increasing silica crystallization rate. Acid leaching followed by thermal treatment induced the production of silica with the lowest carbon level (Krishnarao, Subrahmanyam, & Kumar, 2001). The fact is that acid leaching prevents the formation of black particles

since it removes potassium, the main agent responsible for the presence of unburnt carbon in ash.

Figure 4.4 shows sampled rice husks HCL- leached produced more Silica (SiO_2), 99.173 % at 500 ºC, 98.899 % at 600 ºC, and 98.999 % at 700 ºC respectively. Acid leaching removes metallic impurities more efficiently before combustion and incineration of rice husks. Results indicate that the yield of silica is high when acid-washed RHA is used instead of un-leached RHA (Selvakumar, et al., 2014). This implies acid-leaching has statistical significance on the Silica (SiO_2) yield from rice husks. Fernandes et al. (2017) found that a pretreatment strategy to remove metallic contaminants using acid leaching results in high purity silica with particles of larger specific surface area. The methods tested by the authors resulted in silica with purity above 98 %, especially acid leaching followed by thermal treatment. Acid leaching followed by thermal treatment induced the production of silica with the lowest carbon level (0.09 %). Krishnarao et al. (2012) found acid leaching prevents the formation of black particles by removing potassium. Potassium works as a catalyst in the crystallization of silica. When reaction temperature rises above the dissociation temperature of K_2O (approximately 347 ºC), the surface of ash particles begins to melt, blocking the transportation of oxygen and CO_2 and increasing the amount of unburnt carbon. Bakar et al. (2016) have found that rice husks leached with hydrochloric acid (HCl) can even produce 99.58 % silica content at 600 °C.

According to **Tables 4.7-4.9**, the degree of removal of each metal is different due to its chemical form in rice husk. The percentage removal of potassium (K) is significant. Mohamed et al. (2015) have reported how the thermal decomposition of raw rice husks starts at about 230 °C compared to acid-treated rice husks (200° C) and how acid-treated rice husk undergoes greater mass loss. Commencement of thermal decomposition at the lower temperature of acid-treated rice husks can be ascribed to two factors: (i) acid leaching of partially oxidized carbohydrates and (ii) activated amide groups in rice husk such as NH_2 and CN.

Authors like Krishnaroa et al. (2001), and Della et al. (2002) have shown preliminary acid leaching of rice husks before thermal treatment is highly effective in the

removal of most metallic impurities. Silica ash with a high specific surface area (>250 m^2/g) is produced in the process. Several acidic leaching agents like HCl, H_2S0_4, and HNO_4 can be used in the extraction of inorganic impurities from rice husks. Using H_2SO_4 leads to the formation of metallic sulphates ($CaSO_4$), some of which are not easily soluble in water. Silica content in husk can be increased from 88.03 % to 99.70 % with HCl acid treatment before the calcination process. HCl is cheaper and more effective (Kurama & Kurama, 2003).

Chemical pretreatment of RH with acid leaching is an effective method of removing metallic impurities. Acids include mineral acids such as HCl, H_2SO_4, H_3PO_4, and HNO_3, and organic acids such as acetic, citric, and oxalic acid (Mahmud, Megat-Yusoff, Ahmad, & Farezzuan, 2016). As shown in **Table 4.7-4.9**, pretreatment of RH with acid leaching resulted in the production of RHA/silica with less amount of metal contaminants such as K_2O. Among all acids studied, HCl seems to be the most effective. Umeda and coworkers obtained very high purity of silica ashes of 99.14 % to 99.3 % when using 5 % citric acid and 1% to 5 % H_2SO_4, respectively (Umeda & Kondoh, 2008).

Bakar et al. (2016) reported the decomposition of rice husks in stages, the first stage being the removal of moisture, which takes place at a temperature range of 50–150 °C. The loss of water is 1% to 2 % irrespective of acid leaching. The second stage is the release of volatile matter by thermal decomposition of hemicellulose and cellulose at 240–360 °C. RH with acid-leaching showed lower thermal stability compared to unleached RH. The third stage is the combustion of combustible materials due to lignin, and the weight loss is 26 % to 31 %. The results suggest that acid treatment of RH could decrease the combustion temperature.

Kurama et al. (2003) found that the silica percent yield of rice husk does not have a linear relationship with the molarities of acid used. However, yield increased from 88.02% to 99.50 % with 0.5 M to 2.0 M HCl increased concentration. Based on temperature range and duration of combustion of rice husk, crystalline and amorphous forms of silica are obtained (Asavapisit & Ruengrit, 2005). Amorphous silica is formed below 800 °C, whereas crystalline silica occurs above 900 °C

(Chandrasekhar & Pramada, 2006). The crystalline and amorphous forms of silica have different properties, and it is significant to produce ash with correct specifications for specific end-use.

Elemental content removed after acid treatments at different thermal temperatures was calculated from **Table 4.7-4.9** and results were tabulated in **Table 4.11**.

Table 4.11: Elemental content change (%) after 0.5 M HCL and 0.5 M H_2SO_4 leaching at the three different temperatures.

Temp. / Element	500 °C		600 °C		700 °C	
	HCl	**H_2SO_4**	**HCl**	**H_2SO_4**	**HCl**	**H_2SO_4**
SiO_2	1.801(1.85%)	1.648 (1.69%)	2.966 (3.06%)	2.304 (2.40%)	2.733(2.84%)	2.381(2.47%)
Al_2O_3	-0.055 (-32%)	*	*	*	*	*
P_2O_5	-0.226 (-52%)	-0.183 (-42%)	-0.370 (-59%)	-0.366 (-59%)	-0.321 (-57%)	-0.268 (-47%)
K_2O	-1.036 (-88%)	-1.016 (-86%)	-2.065 (-95%)	-1.987 (-91%)	-1.794 (-92%)	-1.709 (-88%)
CaO	-0.347 (-60%)	-0.292 (-50%)	-0.572 (-70%)	-0.399 (-49%)	-0.522 (-67%)	-0.296 (-38%)
Mn	-0.058 (-66%)	-0.051 (-58%)	-0.111 (80%)	-0.079 (-57%)	-0.044 (-34%)	-0.072 (-55%)
Fe	-0.043 (-34%)	-0.030 (-24%)	-0.04 (-43%)	0.034 (36%)	0.001 (0.8%)	-0.011 (-9%)
Zn	-0.007 (-63%)	-0.005 (-45%)	-0.011 (-68%)	-0.01 (-62%)	-0.009 (-64%)	-0.006 (-42%)

*not detectable acid leached - water leached (% silica content change)

Table 4.11 show 0.5M HCL leaching combined with thermal treatment at 600°C yielded the most % silicon dioxide and removed the most metallic impurities (P_2O_5, K_2O, CaO, Mn, Zn). Temperature increase from 600°C slightly reduced the % silicon dioxide yield.

Table 4.11 shows 0.5 M HCI concentration used produced 99.17 % silica yield. SiO_2 yield with water-leached RH was 97.37 % compared with 99.17 % (HCl-leached) and 99.02 % (H_2SO_4 -leached). Chemical reactions occur when RHA dissolves in water as shown in **Equations 4.1-4.6** (Greenwood & Earnshaw, 1984):

SiO_2 and Al_2O_3 do not react with water however, some reactions occur as shown below

$$P_2O_5 + H_2O \longrightarrow 4H_3PO_3 \quad \textbf{Equation 4.1}$$

$$P_4O_{10} + 6H_2O \longrightarrow 4H_3PO_4 \quad \textbf{Equation 4.2}$$

$$Na_2O + H_2O \longrightarrow 2NaOH \quad \textbf{Equation 4.3}$$

$$CaO + 2H_2O \longrightarrow Ca(OH)_2 \quad \textbf{Equation 4.4}$$

$$K_2O + H_2O \longrightarrow 2KOH \quad \textbf{Equation 4.5}$$

$$MgO + H2O \longrightarrow Mg(OH)_2 \quad \textbf{Equation 4.6}$$

Sodium oxide is strongly basic. It is basic due to the oxide ion, O^{2-}, which has a high affinity for hydrogen ions. RH-sodium oxide reacts exothermically in water producing sodium hydroxide solution. RH-Magnesium oxide reacts in water to produce magnesium hydroxide (insoluble), an alkaline solution. Magnesium oxide is also basic due to oxide ions. However, it is not as strongly basic as sodium oxide because the oxide ions are not so free. Aluminum oxide exists in several different forms. One of those forms is very unreactive. It is known chemically as alpha-Al_2O_3 and it's the form found in RHA. Aluminum oxide is amphoteric. It has reactions as both a base and an acid. Aluminum oxide is not soluble in water like sodium oxide and magnesium oxide.

When RHA is leached with conc. hydrochloric acid (HCl), the following reactions occur as shown in **Equations 4.7- 4.12** (Greenwood & Earnshaw, 1984; Housecroft & Constable, 2018);

$$MnO_2 + 4HCL\ (aq) \longrightarrow Mncl\ (aq) + 2H_2O + Cl_2\ (g) \quad \textbf{Equation 4.7}$$

$$ZnO + 2HCL \longrightarrow ZnCl_2 + 2H_2O \quad \textbf{Equation 4.8}$$

$$Al_2O_3 + 6HCL \longrightarrow AlCl_3 + 3H_2O \quad \textbf{Equation 4.9}$$

$$FeO + 3HCL \longrightarrow FeCl_3 + H_2O \quad \textbf{Equation 4.10}$$

$$MgO + HCL \longrightarrow MgCl_2 + H_2O \quad \textbf{Equation 4.11}$$

$$Na_2O + 2HCL \longrightarrow 2NaCL + H_2O \quad \textbf{Equation 4.12}$$

When RHA is leached with conc. sulfuric acid (H_2SO_4), the following reactions shown in **Equations 4.13-15** occur (Greenwood & Earnshaw, 1984; Housecroft & Constable, 2018)**;**

$$S\ (s) + 2H_2SO_4 \longrightarrow 3SO_3 + 2H_2O \quad \textbf{Equation 4.13}$$

$$Al_2O_3 + 2H_2SO_4 \longrightarrow AlSO_4 + H_2O \quad \textbf{Equation 4.14}$$

$$MgO + H_2O \longrightarrow Mg(OH)_2 \quad \textbf{Equation 4.15}$$

Sodium oxide (a strong base) reacts with acids in RHA. Reactions with hydrochloric acid and sulphuric acid produce sodium chloride and sodium sulphate solutions respectively. Magnesium oxide in rice husk reacts with acids to produce salts. Its reaction with hydrochloric acid produces magnesium chloride solution.

Aluminum oxide contains oxide ions and reacts with acids in the same way as sodium or magnesium oxides. Aluminum oxide in rice husk will react with

hydrochloric acid to give an aluminum chloride solution. Silicon dioxide is not basic, does not contain oxide ions, and does not react with acids. It is a very weak acid, reacting with strong bases.

RH-Silicon dioxide does not react with water, due to its giant covalent structure. RH-Sulphur reacts with leaching acids to produce SO_3 and SO_2 gases in solutions. Sulphur dioxide is soluble in water, reacting with it to give a solution known as sulphurous acid, and traditionally given the formula H_2SO_3. However, the main species in the solution is simply hydrated sulphur dioxide - SO_2, xH_2O. Sulphur dioxide also reacts directly with bases like sodium hydroxide solution produced in situ as shown in **Equations 4.16-4.19** (Greenwood & Earnshaw, 1984; Housecroft & Constable, 2018)**;**

$$\mathbf{SO_2 + NaOH \longrightarrow Na_2SO_3 + H_2O} \quad \textbf{Equation 4.16}$$

$$\mathbf{Na_2SO_3 + H_2O + SO_2 \longrightarrow 2NaHSO_3} \quad \textbf{Equation 4.17}$$

$$\mathbf{CaO + SO_2 \longrightarrow CaSO_3} \quad \textbf{Equation 4.18}$$

$$\mathbf{SO_3 + H_2O \longrightarrow H_2SO_4} \quad \textbf{Equation 4.19}$$

Sulphuric acid is a strong acid, it reacts with water to produce a hydroxonium and a hydrogen sulphate ion. This reaction is shown in **Equations 4.20-4.21** is virtually 100% complete.

$$\mathbf{H_2SO_4(aq) + H_2O(l) \Longleftrightarrow H_3O^+(aq) + HSO_4^{2-}(aq)} \quad \textbf{Equation 4.20}$$

The remaining hydrogen removal requires more energy. The hydrogen sulphate ion is a relatively weak acid. The equilibrium:

$$\mathbf{H_2SO_4(aq) + H_2O(l) \Longleftrightarrow H_3O^+(aq) + SO_4^{2-}(aq)} \quad \textbf{Equation 4.21}$$

Sulphur trioxide will react directly with bases to form sulphates. **Equation 4.22** shows the reaction with calcium oxide to form calcium sulphate. This is similar to the reaction with sulphur dioxide described above.

Equation 4.22

4.3.2 Leaching rice husk ash (RHA) with acid/water

Sampled rice husks were converted to rice husk ash (RHA) at temperatures 600 °C, 500 °C, and 400 °C then leached with water or acids. Percentage elemental contents are tabulated in **Tables 4.12- 4.14**.

Table 4.12 indicates that at 600 °C leachings of RHA with H_2SO_4 produced slightly more % SiO_2 when compared with water leaching.

Table 4.12: Chemical composition of acid leached and water-leached RHA at 600 °C

%Element	water-leached	HCL-leached	H_2SO_4-leached
SiO_2	98.191 ± 1.168	96.926 ± 1.215	99.089±0.896
MgO	*	2.040 ± 1.954	*
Al_2O_3	*	0.016 ± 0.343	*
P_2O_5	0.286 ± 0.050	0.148 ± 0.038	0.113 ± 0.028
K_2O	1.617 ± 0.022	0.444 ± 0.020	0.423 ± 0.014
CaO	0.532 ± 0.020	0.134 ± 0.013	0.127 ± 0.010
Mn	0.103 ± 0.012	0.061 ± 0.010	0.051 ± 0.009
Fe	0.158 ± 0.011	0.178 ± 0.011	0.151 ± 0.010
Zn	0.010 ± 0.002	0.007 ± 0.002	0.005 ± 0.002
Cl	*	*	*
Na_2O	*	*	*
S			

*not detectable

Table 4.13 below indicates that at 500 °C leachings with HCL caused a slight decrease (2%) while H_2SO_4 leaching caused a decrease. At this temperature % silica (SiO_2) was reduced with acid leaching.

Table 4.13: Chemical composition of acid leached and water-leached RHA at 500 °C

%Element	water-leached	HCL-leached	H_2SO_4-leached
SiO_2	98.041 ± 1.406	95.862± 1.126	97.099±1.175
MgO	*	*	*
Al_2O_3	*	0.243 ± 0.387	*
P_2O_5	0.277 ± 0.049	0.104 ± 0.387	*
K_2O	0.592 ± 0.022	0.142 ± 0.015	0.437 ± 0.019
CaO	0.692 ± 0.022	0.251 ± 0.017	0.088 ± 0.012
Mn	0.123 ± 0.013	0.086 ± 0.008	0.044 ± 0.008
Fe	0.188 ± 0.012	0.120 ± 0.009	0.204 ± 0.012
Zn	0.013 ± 0.002	0.007 ± 0.002	0.006 ± 0.002
Cl	0.028 ± 0.027	0.028 ± 0.026	0.029 ± 0.027
Na_2O	*	*	*
S	*	*	*

*not detectable

Table 4.14 below indicates that at 400 °C, leaching with HCl decreases percentage silica (SiO_2) while leaching with H_2SO_4 increased silica content.

Table 4.14: Chemical composition of acid leached and water-leached RHA at 400 °C.

% Element	water-leached	HCL-leached	H_2SO_4-leached
SiO_2	98.486 ± 1.149	97.845 ± 1.148	99.409 ± 1.143
MgO	*	*	*
Al_2O_3	*	0.243 ± 0.387	*
P_2O_5	0.222 ± 0.045	0.118 ± 0.027	*
K_2O	0.402 ± 0.019	0.188 ± 0.015	0.193 ± 0.015
CaO	0.485 ± 0.019	0.018 ± 0.011	0.029 ± 0.011
Mn	0.094 ± 0.011	0.086 ± 0.008	0.044 ± 0.008
Fe	0.198 ± 0.012	0.137 ± 0.010	0.173 ± 0.011
Zn	0.008 ± 0.002	0.003 ± 0.001	0.005 ± 0.002
Cl	0.037 ± 0.026	*	*
Na_2O	*	*	*
S	*	*	*

*not detectable

Statistical analysis of **Table 4.12-4.14** implies the temperature at which the rice husk waste is burnt has no significant relation with the availability of silica. Availability of Silica at 600 °C is not very significantly different for both water/acid leached RHA. At 500°C leaching with water or acid yields similar silica content. **Table 4.15** shows

a summary of the yields at the three thermal treatments. Statistical analysis of the effect of treatments had F critical (5.143253) more than F-value (2.695752) implying the different leaching of prepared rice husk ash (RHA) with water, HCl and H_2SO_4 had no significant effect on percentage silica yield. This indicates to produce silica from rice husks we can use water as a leaching agent thus ensuring synthesized industrial chemicals are green products.

Table 4.15: Silica of RHA with varying temperatures and leaching conditions

Thermal Treatment	**400 °C**	**500°C**	**600°C**
Water-leached	98.486 ± 1.149	98.041 ± 1.406	98.191 ± 1.168
HCL-leached	97.845 ± 1.148	95.862± 1.126	96.926 ± 1.215
H_2SO_4-leached	99.409 ± 1.143	97.099±1.175	99.089±0.896

Metallic impurities in RHA can adversely affect the properties of silica and its applications, so it is important to reduce the impurities to improve their characteristics. Silica or silicon dioxide (SiO_2) usually exists in two forms, amorphous and crystalline (Holleman & Wiberg, 2001). Processing of silica of specific quality results in several types of specialty silica. Among them, silica in its amorphous form has been widely used in industry and is more reactive than crystalline silica (Chandrasekhar et al., 2003). The crystal forms of silica in RHA are usually determined by X-ray diffraction (Kim et al., 2008).

Increasing the temperature up to 900°C leads to crystallization of the ash from amorphous form into cristobalite or tridymite. Furthermore, the formation of the crystalline phase is accelerated by the presence of metallic impurities such as potassium oxide in the rice husks (Haslinawati et al., 2009). The properties of RHA such as color, activity, content of impurities, and SiO_2 are influenced by various factors such as incinerating conditions (temperature and duration), geographical location and origin, rate of heating, burning equipment, pretreatment (acid leaching or not), crop variety, and fertilizer used (Menya et al., 2018).

Rice husk ash consists of SiO_2, C, K_2O, P_2O_5, CaO, and minor amounts of Mg, Fe, and Na. Silica is the most abundant element in RHA, and no other plant except RH has such a huge proportion of silica. Trace elements most commonly found in RHA are Na, K, Ca, Mg, Fe, Cu, Mn, and Zn, and differences in the composition may be due to geographical factors, year of harvest, sample preparation, and analysis methods (Della et al., 2002). The levels of impurities such as K_2O and Na_2O were reported to be related to soil type and the amount of fertilizer used during the process of paddy growth (Moraes, et al., 2014).

4.4 Conversion of silica to sodium silicate solution

Silica samples were reacted with different concentrations of sodium hydroxide (NaOH) to find the optimum conditions for producing the best quality sodium silicate solution.

Openly burnt rice husk samples 1, 2, and 3 (OPB1, OPB2, and OPB3) were also reacted with different concentrations (300 mL of 1,2 and 3 M) of NaOH for comparison purposes. **Table 4.16** shows the experimental results.

Table 4.16: Sample composition using TXRF spectral analysis on NaOH treated RHA

Sample ID	% SiO_2	% Cl	% K_2O	% CaO	% P_2O_5
INC 400 (1 M)	88.319±1.089	1.868±0.102	0.157±0.102	0.050±0.013	0.523±0.064
INC 400 (2 M)	92.293±0.440	0.000±0.008	1.530±0.017	0.265±0.012	0.330±0.035
INC 400 (3 M)	96.436±0.537	0.000±0.010	1.701±0.023	0.928±0.020	0.407±0.049
INC 500 (1 M)	79.465±0.392	0.000±0.005	1.877±0.021	1.721± 0.021	0.519±0.037
INC 500 (2 M)	96.717±0.486	0.000±0.007	1.717±0.021	0.687±0.018	0.585±0.045
INC 500 (3 M)	89.498±0.555	0.000±0.010	1.619±0.023	0.747±0.019	0.355±0.047
INC 600 (1 M)	86.313±0.448	0.000±0.007	1.593±0.020	0.208±0.015	0.486±0.044
INC 600 (2 M)	91.731±0.539	0.000±0.009	1.152±0.020	0.156±0.016	0.415±0.043
INC 600 (3 M)	97.391±0.591	0.000±0.010	1.528±0.023	0.376±0.017	0.407±0.038
OPB1 (1 M)	97.448±0.574	0.000±0.010	1.757±0.023	0.169±0.016	0.435±0.045
OPB1 (2 M)	97.299±0.534	0.000±0.008	1.793±0.022	0.125±0.016	0.504±0.035
OPB1 (3 M)	96.739±0.593	0.000±0.010	1.592±0.023	0.891±0.020	0.382±0.038
OPB2 (1 M)	82.875±0.440	0.000±0.007	1.830±0.021	0.351±00.017	0.485±0.035
OPB2 (2 M)	89.355±0.504	0.000±0.008	1.670±0.021	0.264±0.016	0.445±0.044
OPB2 (3 M)	96.490±0.517	0.000±0.008	1.656±0.022	0.954±0.019	0.504±0.046
OPB3 (1 M)	96.644±0.439	0.000±0.006	1.790±0.020	0.354±0.017	0.738±0.036
OPB3 (2 M)	97.242±0.483	0.000±0.007	1.726±0.021	0.090±0.016	0.620±0.035

INC 400 (1 M) -Incineration at temperature 400 ℃ and reacted with 1M Sodium hydroxide

OPB1 (1 M) -Openly burnt sample 1 reacted with 3M Sodium hydroxide

Table 4.16 shows silica samples reacted with 300 mL of 3M NaOH have better yields 96.4 % to 96.7 % except for sample ID INC 500 (3 M) with 89.5 %. There is an indication from that NaOH concentration (>3M) increases sodium silicate availability. Openly burnt rice husks did not show a significant decrease in SiO_2 availability. **Table 4.16** also indicates treatments at relatively lower temperatures and lower NaOH have less % K_2O content.

Table 4.16 shows incineration at 600 ℃ followed by the 3 M NaOH treatment yielded relatively more sodium silicate as compared with the other treatments. Differences in yield between incinerated samples and openly burnt samples were minimal. Andreola et al (2020) have synthesized sodium silicate solutions by treating RHA with sodium hydroxide solutions at low molar concentrations (1–4 M). The findings of the study confirm that the extraction of SiO_2 increases by increasing NaOH concentration. Alkaline concentrations (NaOH solution) of 1.5 and 2 M show the best results for SiO_2/Na_2O ratio close to 2, this ratio is widely used as deflocculating agents (Andreola, Barbieri, & Lancellotti, 2020). Foletto et al (2006) studied process variables time, the temperature of the reaction, and composition of the reaction mixture (expressed in terms of molar ratios $NaOH/SiO_2$ and H_2O/SiO_2) and found about 90% silica conversion contained in the RHA into sodium silicate was achieved in a closed system at 200 °C. The results showed that sodium silicate production from RHA can generate aggregate value to rice husks.

Sodium silicate solution samples were analyzed using specified analytical methods outlined in KEBS Standard KS 2350:2012 and results are shown in **Table 4.17.**

Table 4.17: Comparison of sodium silicate with KS 2350:2012

Sodium Silicate ID	Density g/mL at 20C	%Na_2O	% SiO_2 XRF analysis	SiO_2/Na_2O
OPB1 1M	1.197793	14.4666	97.448	6.736035
OPB2 1M	1.116947	8.26666	82.875	10.0252
OPB3 1M	1.158828	8.26666	96.644	11.69081
OPB1 2M	1.200078	11.3666	97.299	8.560027
OPB2 2M	1.179000	13.4333	89.355	6.651739
OPB3 2M	1.177936	13.4333	97.242	7.23886
OPB1 3M	1.333048	26.8666	96.739	3.600707
OPB2 3M	1.252281	20.6666	96.490	4.66887
OPB3 3M	1.245307	23.7666	84.930	3.573492
INC400 (1 M)	1.122620	9.3000	88.319	9.496667
INC500 (1 M)	1.154139	10.3333	79.465	7.690164
INC600 (1 M)	1.105797	7.23333	86.313	11.93267
INC400 (2 M)	1.262367	15.5000	92.293	5.954387
INC500 (2 M)	-0.86421	27.9000	96.717	3.466559
INC600 (2 M)	1.202599	10.3333	91.731	8.877196
INC400 (3 M)	1.280451	22.7333	96.436	4.242053
INC500 (3 M)	1.275723	19.6333	89.498	4.558473
INC600 (3 M)	1.27986	23.7666	97.391	\4.097797
KEBS KS 2350:2012	**1.25-1.45**	**5-10**	-	**1:2.9-1:3.6**

*OPB1, OPB2, and OPB3 - Sodium silicate solution from (3) Openly burnt rice husks samples treated with 1 M, 2 M, 3 M NaOH

*INC (400 °C, 500 °C, 600 °C) – Sodium Silicate solution from rice husk samples incinerated at indicated temperature

It can be concluded from **Table 4.17** that sodium silicate samples prepared from openly burnt RH samples and reacted with 3 M NaOH all complied with the density requirement of KEB KS 2350:2012 liquid neutral sodium silicate standard. Incinerated RH samples at a temperature of 400 ℃ and reacted with 3 M NaOH also complied. The standard requirements are listed in the last row for comparison. Foletto et al. (2006) had varied conditions in their study in an open and closed system: time of reaction (varying of 0 to 80 minutes), molar ratio $NaOH/SiO_2$ (1, 2, 3 and 4), molar ratio H_2O/SiO_2 (11 and 22) and reaction temperature (100, 110, 120, 150 and 200 °C). For the attainment of sodium silicate with molar ratio

H_2O/SiO_2 = 22 and $NaOH/SiO_2$ = 2, for example, they used 70 g of RHA, 80 g of NaOH, and 396 g of distilled water.

Table 4.18 shows experimental data of a sodium silicate (Liquid neutral) sample taken to the Kenya Bureau of Standards (KEBS) for chemical analysis. Results of the sample analyzed as per KEBS KS2350:2012 methods are listed in the first column while the standard requirements are listed in the third column.

Table 4.18: SS conformity with KEBS Standard KS 2350: 2012 (Liquid neutral)

Characteristics	**KEBs sample composition**	**KS 2350:2012 specifications**	**Test method**
1. Appearance	Clear to hazy	Clear to hazy	Visual
2. Total alkali content as Na_2O % by mass	6.35 %	5-20.2%	Annex A
3. Density g/mL at 20 °C	1.53	1.25-1.70	Annex B
4. Ratio of mass of SiO_2:Na_2O	1:4.3	1:1.2.9 – 1:3.6	Annex C
5. Combined mass of SiO_2 & Na_2O	>97.5%	>97.5%	Annex D
6.Insoluble matter	<2.5%	<2.5%	

Table 4.18 comparisons of the 2nd and 3rd columns indicate that the sample complied with KS 2350:2012 specifications**.** The implications are that marketable sodium silicate can be produced in rice-growing areas in Kenya where RHs are available.

4.5 Conversion of the sodium silicate solution to silica gel

Silica gel was prepared by reacting 15 mL of 37 % HCL acid to 25 mL of the alkali sodium silicate solution in a 500 mL beaker. FTIR Tracer-100 (C103-E091A) was used to analyze chemical content in the prepared silica gel. **Table 4.19** shows the results.

Table 4.19: Chemical composition of silica gel after sodium silicate treatment using HCl using TXRF

Silica gel ID.	% SiO_2	% Cl	% K_2O	% CaO	% P_2O_5
INC 400 (1 M)	88.319± 1.089	10.868± 0.102	0.157± 0.016	0.050± 0.013	0.523 ± 0.064
INC 400 (2 M)	96.771± 1.088	1.437 ± 0.039	0.073± 0.013	0.027± 0.011	0.139 ± 0.035
INC 400 (3 M)	96.072± 1210	2.006 ± 0.055	0.064± 0.013	0.017± 0011	0.119 ± 0.049
INC 500 (1 M)	91.022± 0.974	8.224 ± 0.067	0.147± 0.015	0.072± 0.013	0.392 ± 0.055
INC 500 (2 M)	91.354± 0.849	7.712 ± 0.057	0.262± 0.014	0.092± 0.011	0.430 ± 0.047
INC 500 (3 M)	94.048± 1.104	5.345 ± 0.070	0.174± 0.016	0.071± 0.013	0.290 ± 0.053
INC 600 (1 M)	94.784± 0.952	2.149 ± 0.035	0.095± 0.013	0.021± 0.011	0.162 ± 0.043
INC 600 (3 M)	84.368± 0.924	14.625± 0.086	0.186± 0.016	0.033± 0.012	0.720 ± 0.064
OPB1 (1M)	95.916 ± 1.091	3.810 ± 0.057	0.030 ± 0.012	0.030 ± 0.011	0.138 ± 0.048
OPB1 (2 M)	88.941 ± 0.882	10.286 ± 0.061	0.071 ± 0.013	0.053 ± 0.012	0.540 ± 0.054
OPB1 (3 M)	82.210 ± 0.847	16.551 ± 0.077	0.141 ± 0.015	0.093 ± 0.013	0.089 ± 0.062
OPB2 (3 M)	96.804 ± 1.048	1.147 ± 0.035	0.030 ± 0.012	0.037 ± 0.011	0.146 ± 0.033
OPB3 (1 M)	96.903 ± 0.918	2.738 ± 0.034	0.095 ± 0.012	0.023 ± 0.010	0.183 ± 0.035
OPB3 (2 M)	88.695 ± 0.970	10.448 ± 0.078	0.129 ± 0.015	0.016 ± 0.012	0.558 ± 0.059
OPB3 (3 M)	93.512 ± 1.056	5.952 ± 0.067	0.090 ± 0.014	0.061 ± 0.012	0.291 ± 0.054
OPB3 2:3	93.400 ± 1.163	6.192 ± 0.084	0.042 ± 0.013	0.004 ± 0.011	0.285 ± 0.053
OPB3 2 M 2:2	94.131 ± 1.184	5.268 ± 0.080	0.151 ± 0.016	0.013 ± 0.012	0.247 ± 0.055

*OPB1, OPB2, and OPB3 - Sodium silicate solution from (3) Openly burnt rice husks samples treated with 1 M, 2 M, 3 M NaOH

* OPB3 2:3 Sodium silicate (2) : HCl (3) ratio

*INC (400 °C, 500 °C, 600 °C) – Sodium Silicate solution from rice husk samples incinerated at indicated temperatures.

Table 4.19 indicates that the 3M NaOH treated RH had the highest % Cl while the open burn samples had the least. This is probably the result of salt formation (NaCl) by the strong NaOH alkali solution. Openly burnt rice husks lost the most % potassium during the silica gel formation process. Rice husk ash formed from open burning had residual % K (reactive form) leached out by NaOH. Acid leaching of rice husks removes most metallic impurities in the rice husks (Liou & Wu, 2009). The removal mechanism is through the dissolution of metals in acid, which is later removed by rinsing the treated rice husk samples with distilled water (Muniandy et al., 2014).

Incineration samples at 500 °C had the most available % CaO while the open burn samples had the least. According to **Table 4.19** incineration of rice husks at 600 °C resulted in the most available % P_2O_5 content. Thirty (30) % silica gel samples had silica (SiO_2) content of over 95%. Openly burnt rice husks produced good yields of silica gel after treatment with (1-3 M HCL). The open burn treatments produced equal or better SiO_2 yields of silica gel compared with incineration samples. According to Lima et al. (2011) amorphous silica contained in rice husk ash is solubilized when treated with a sodium hydroxide solution that has a pH value greater than 10. When solubilized, the silica is in the monomeric form of silicic acid. When sodium silicate is acidified, a supersaturated solution of Si $(OH)_4$ monomers is formed. Thereafter silica gel is formed during the gelation of a silicic acid solution through a polymerization process, which is divided into three phases: monomer polymerization to form particles; particle growth; and particle union in chains that extend throughout the solution, which increases the viscosity and forms a gel (Lima, et al., 2011). When amorphous silica contained in the RHA is dissolved in an alkaline solution, a silicate solution forms that has a solubility of 876 mg/L in water at 25°C. After the sodium silicate is acidified, a supersaturated solution of silica gel is produced utilizing a polymerization process, which is divided into three phases: monomer polymerization to form particles; particle growth; and particle union in ramified chains that extend throughout the solution (Lima et al., 2011).

Table 4.20 shows the quality requirements of silica gel in the market compared with the produced silica gels in this study.

Table 4.20: Silica gel MSD data versus experimental data (silica gel)

SAMPLE	% $Si0_2$	% Cl	% K_20	% CaO	% P_2O_5
SG MSD Standard	**99.6**	**N/A**	**N/A**	**0.04**	**N/A**
INC 400 (2M)	96.771±1.088	1.437±0.039	0.073±0.013	0.027±0.011	0.139±0.035
INC 400 (3M)	96.072±1210	2.006±0.055	0.064±0.013	0.017±0011	0.119±0.049
OPB2 (3M)	96.804±1.048	1.147±0.035	0.030±0.012	0.037±0.011	0.146±0.033
OPB3 (1M)	96.903±0.918	2.738±0.034	0.095±0.012	0.023±0.010	0.183±0.035

Table 4.20 indicates that INC 400 (2M), INC 400 (3M), OPB2 (3M), and OPB3 (1M) silica gels have 96.9 -96.0 % silica content. MSD sheets state a 99.6 % Silica (SiO_2) requirement in silica gel as indicated in **Table 4.20**. Silica gels have many grades dependent on use with different chemical content requirements. Percentage SiO_2 content is the most important. Silica gels produced are good candidates for further purification to meet the various needs of the industry.

4.6 Characterization of leached silica samples, silica gel, and rice husk derived activated Carbons using FTIR spectroscopy

Synthesized silica, silica gel, and rice husk-derived activated carbons (RHAC) samples were pressed in a hydraulic press between smooth stainless steel die (at 1544×10^5 Pa pressure for 2 min) to give a clear potassium bromide (KBr) disk and scanned with an FTIR spectroscopy instrument IRTracer-100. **Figure 4.5** shows the FTIR spectra acquired of silica from RH leached with H_2SO_4.

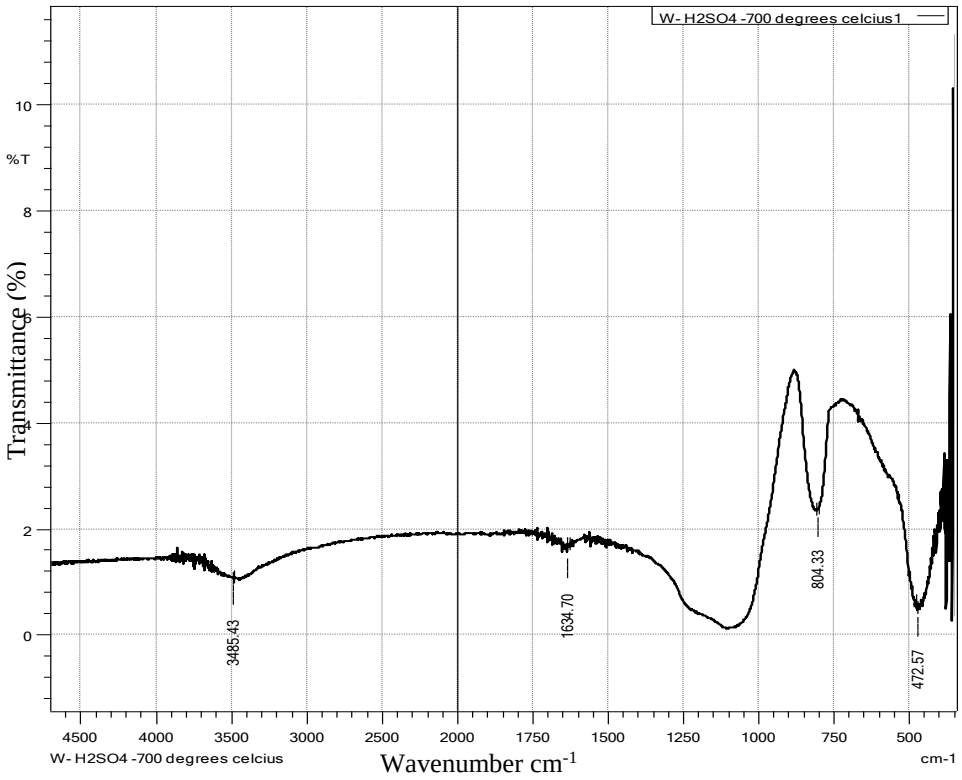

Figure 4.5: FTIR spectra of silica from RH leached with H_2SO_4

Fourier Transform infrared software scan revealed the presence of silicon dioxide (SiO_2), Mol. weight: 60.085, Purity: Food grade. **Figure 4.6** shows the spectra acquired. The reference red silicon dioxide (SiO_2) is from the FTIR spectral library while the green is from the silica RH sample leached with H_2SO_4.

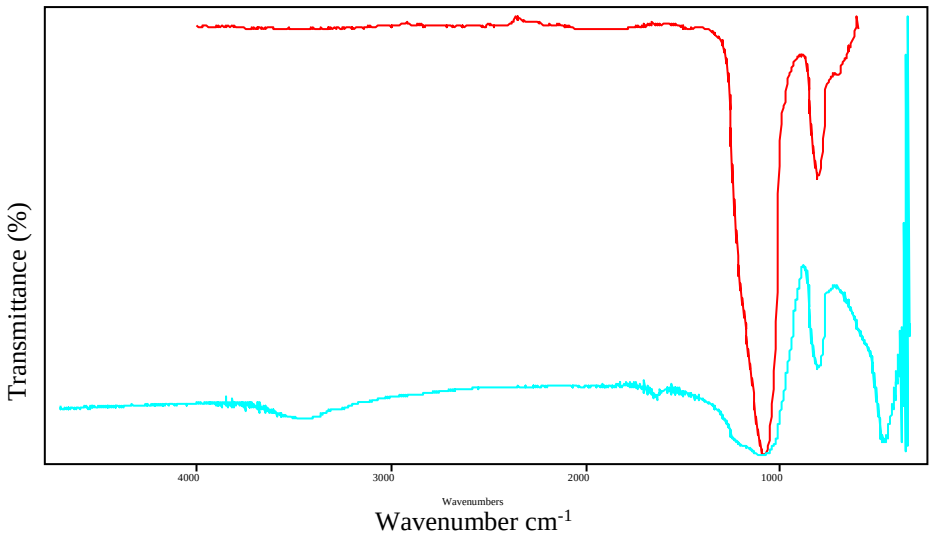

Figure 4.6: Spectral graph from FTIR Instrument – silica-H_2SO_4 - leached -700 ℃ (green) vis reference red - silicon dioxide (SiO_2)

Rice husks leached with HCl and thermally treated at 700 ℃ were scanned with an FTIR spectroscopy instrument. **Figure 4.7** shows the FTIR spectra acquired.

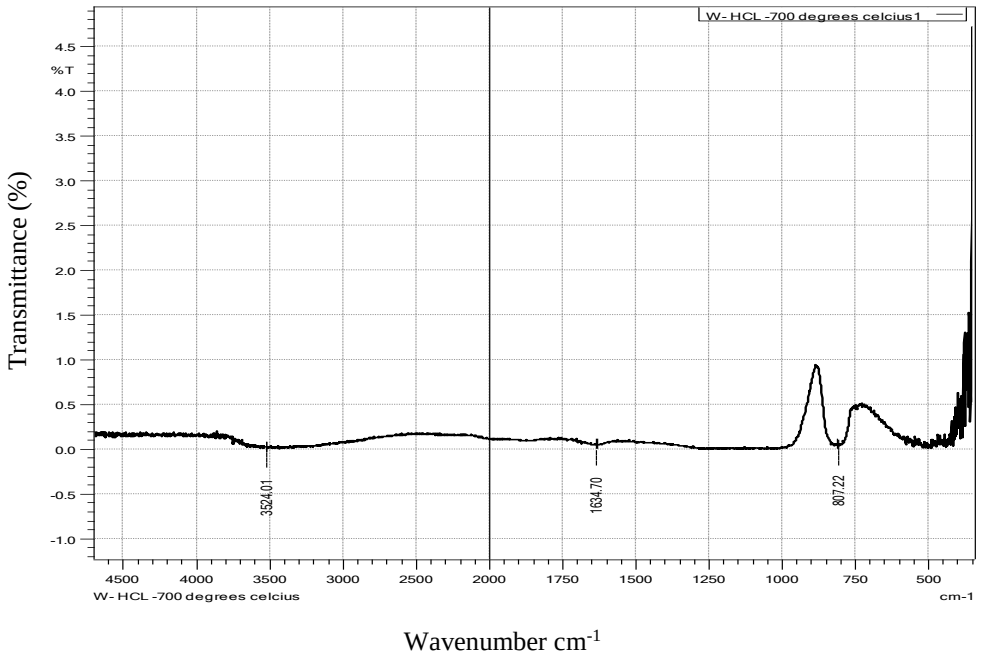

Figure 4.7: FTIR spectra of silica from RH leached with HCL

Fourier Transform infrared software scan revealed the presence of silicon dioxide (SiO_2), Mol. Weight: 60.085, Purity: Food grade. **Figure 4.8** shows the spectra acquired. The reference red silicon dioxide (SiO_2) is from the FTIR spectral library while the green is from the silica RH sample leached with HCl

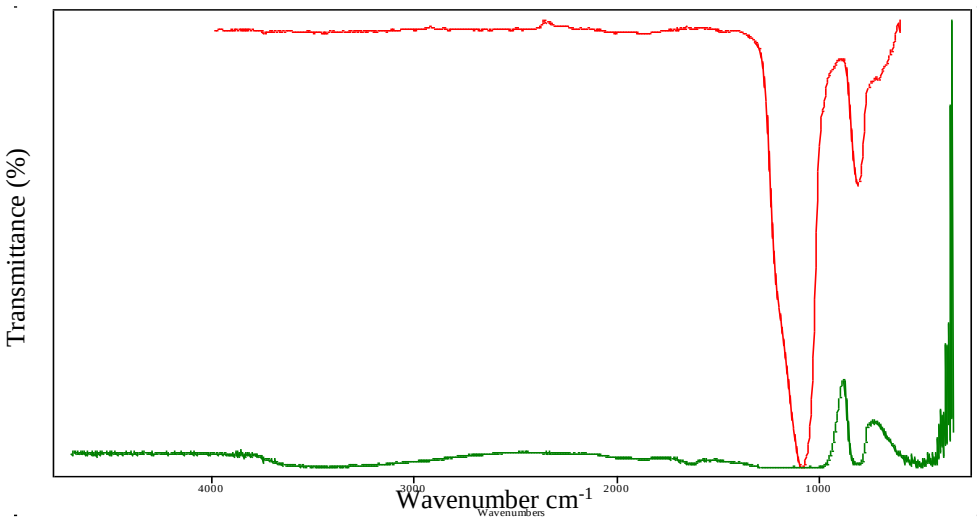

Figure 4.8: Spectral graph from FTIR Instrument – silica-HCl - leached 700 ℃ (green) vis reference red - silicon dioxide (SiO_2)

Unleached rice husks thermally treated at 700 ℃ were also scanned with an FTIR spectroscopy instrument. **Figure 4.9** shows the FTIR spectra acquired.

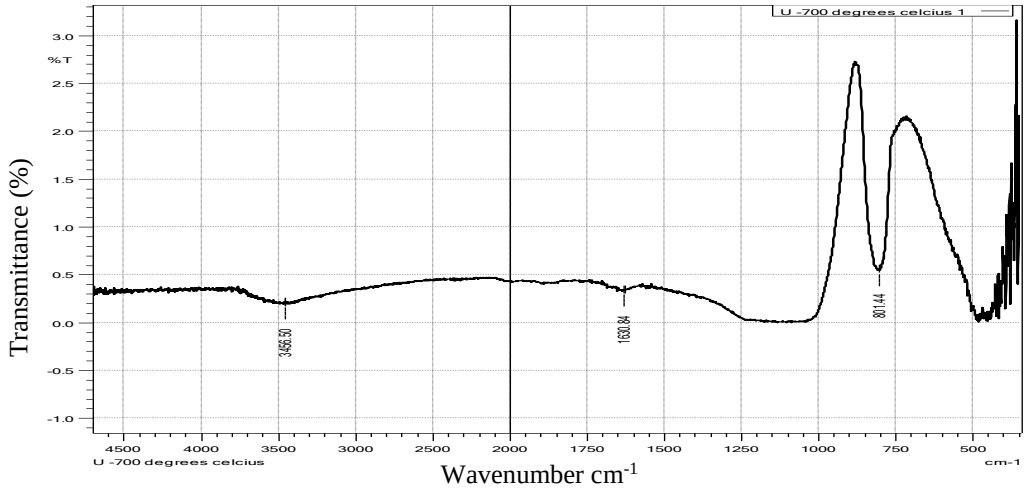

Figure 4.9: FTIR spectra of Silica from un-leached RH

Figure 4.9 shows absorption intensity at 1100-900 cm^{-1} is relatively lower without acid leaching. The Fourier Transform infrared (e-FTIR) software scan report is shown in **Figure 4.10**.

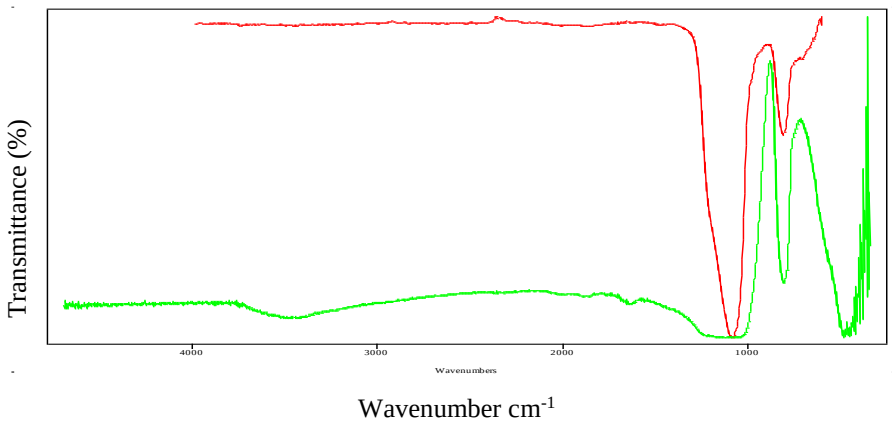

Figure 4.10: Spectral graph from FTIR instrument – silica-unleached -700 °C (green) vis reference red - silicon dioxide (SiO_2)

Figure 4.5, Figure 4.7, and Figure 4.9 show four main characteristic absorption bands indicating the presence of an inorganic compound. Intense to moderate bands at 1600-1300, 1200-1000, and 800-600 cm^{-1} also indicate the presence of a hydroxyl compound. The relatively narrow absorption at 1626 cm^{-1} indicates olefin unsaturation and aromatic compound. The multiple bands between 1000-880 cm^{-1} indicate C-H out-of-plane bending. Absorption at 1100-900 cm^{-1} is a presence marker for silicate ions. Pure silica FTIR spectra typically exhibit peaks in two distinct regions (Fidalgo and Ilharco, 2001; Patwardhan et al., 2006): peaks at > 2500 cm^{-1} and < 1300 cm^{-1}. The first region corresponds to hydroxyl (−OH) stretching from absorbed or molecular water, while the second region occurs due to several silica modes. While containing several peaks, the silica region can be primarily separated into three peaks at a broad peak at ~ 1100 $cm^{-1}$and ~ 450 cm^{-1}, ~ 800 cm^{-1}. Absorption at ~ 450 cm^{-1} is due to the rocking motion of oxygen atoms. Symmetric vibrations of silicon atoms in siloxane bonds occur at ~ 800 cm^{-1}. The largest peak observed in a silica spectrum is present at ~ 1100 cm^{-1}. The average FTIR instrument records spectra from an upper limit of around 4000 cm^{-1} down to 400 cm^{-1} defined by optics of the instrument (commonly based on potassium bromide (KBr).

FTIR spectra indicate hydrochloric acid (HCL) leaching avails more Silica content than Sulphuric acid (H_2SO_4) leaching from rice husks. **Figures 4.6, 4.8, and 4.10** show FTIR) software scan revealing the presence of silicon dioxide (SiO_2), Mol.Weight: 60.085, of food-grade quality for the acid-leached rice husks. **Figure**

4.10 spectra are of the silica from un-leached rice husks. **Figure 4.11** shows the spectra acquired after acid leaching and thermal treatment.

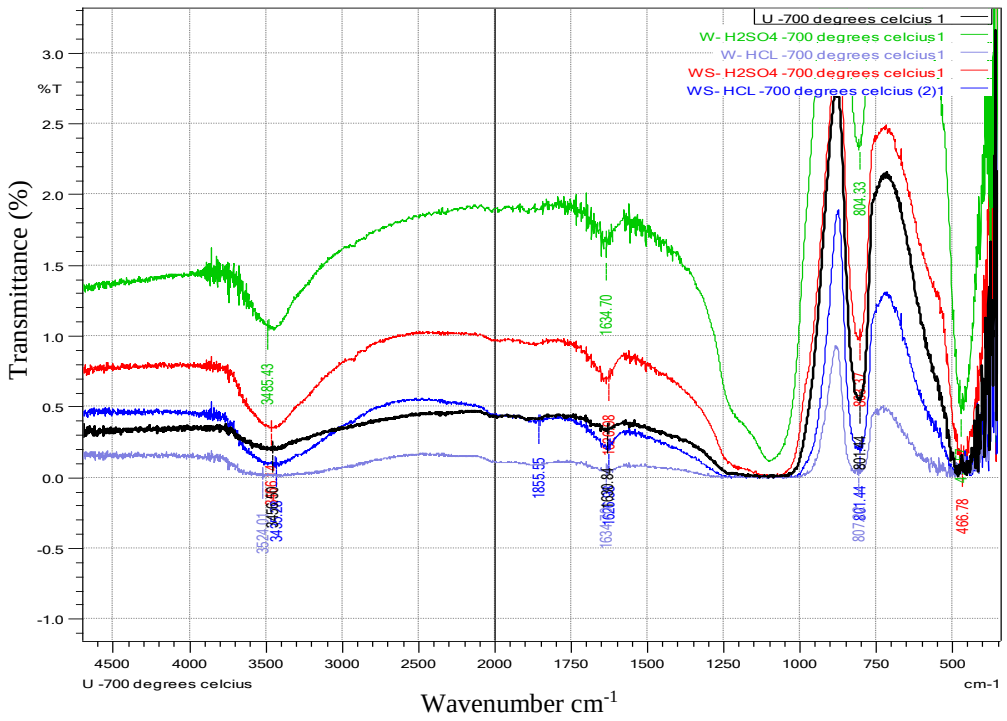

Figure 4.11: FTIR spectra of silica from all treatments.

Figure 4.11 shows acid leaching with HCl (blue) avails more silica than H_2SO_4 (red and green). There is less transmittance with HCl-leaching of rice husks. Strong acid leaching treatment has been carried out on rice husks to remove metallic impurities and organics before (Umeda & Kondoh, 2010). Researchers have found that preliminary leaching of rice husk with a solution of HCl, HNO_3, H_2SO_4, NaOH, and NH_4OH, boiled before thermal treatment with temperatures ranging from 500 °C to 14000 °C for various time intervals, is effective in substantially removing most of the metallic impurities and producing ash-silica completely white in colour with a high specific area (Della et al., 2002). Yalcin and Sevinc (2001) have also acid leached rice husks by reflux boiling in 3 % (v/v) HCl and 10% (v/v) H_2SO_4.

4.6.1 FTIR characterization of the RH derived activated carbons (RHAC)

Prepared NaOH-RHAC and H_3PO_4-RHAC samples were scanned using a Shimadzu Fourier Transform Infrared Spectrophotometer IRTracer-100. **Figure 4.12** shows the acquired FTIR scan of H_3PO_4 – RHAC.

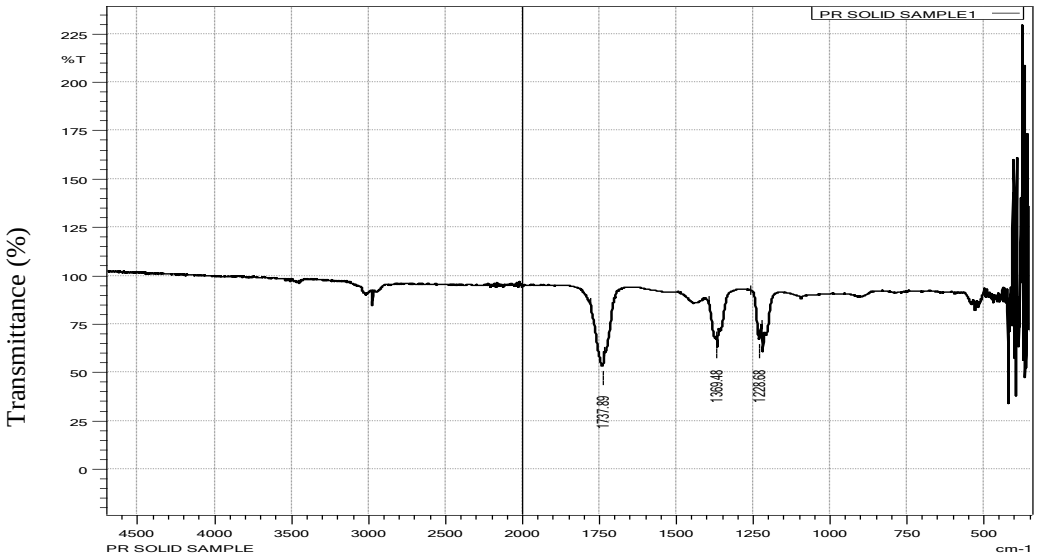

Wavenumber cm^{-1}

Figure 4.12: FTIR scan of Phosphoric acid-activated - RHAC

Figure 4.12 had three clear peaks at 1737, 1369, and 1226 cm^{-1} associated with Esters, Carboxylate, and Aromatic C-H plane bonds sites. The phosphoric acid used to activate the carbon also acts as an acid causing the formation of the esters and carboxylate reaction sites. In studies, H_3PO_4 acting as an activation agent reacted with phenolic and carbonyl groups of activated carbon, forming P-containing carbonaceous species, which further promoted the development of micropores of the activated carbon and then increased the surface area, H_3PO_4 also acted as a catalyst to adjust and control the texture properties and structures of activated carbon (Luo, et al., 2014).

Figure 4.13 shows the acquired FTIR scan of NaOH – RHAC.

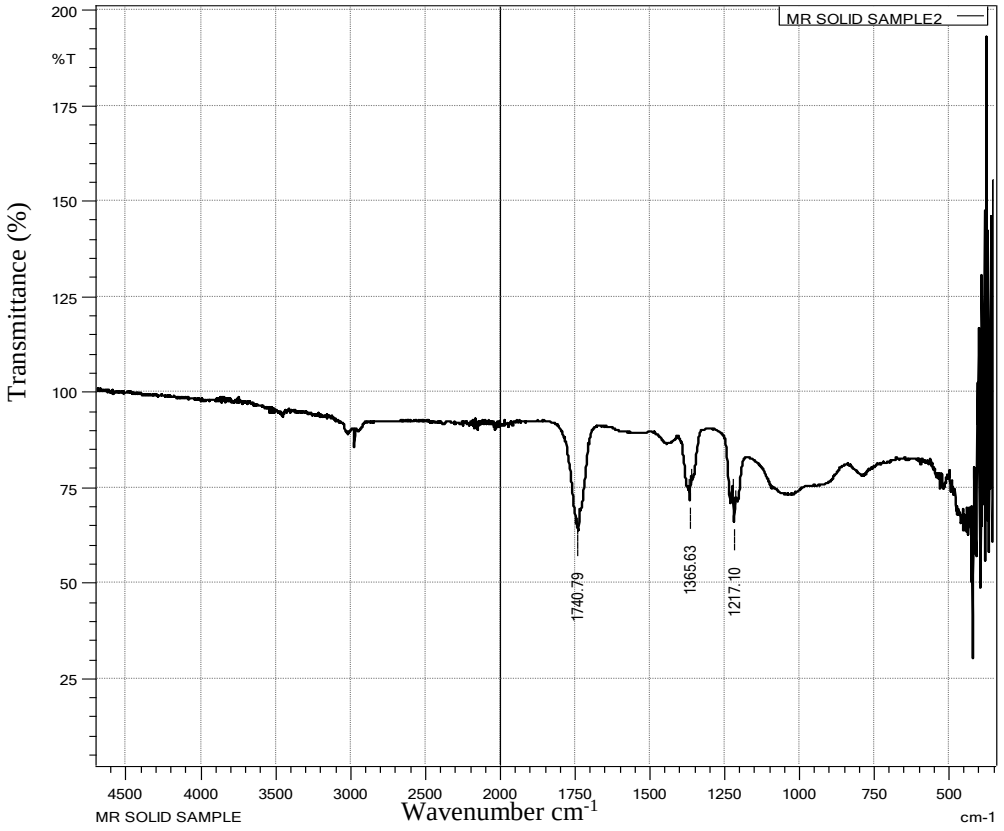

Figure 4.13: FTIR scan of sodium hydroxide activated- RHAC

Figure 4.13 shows the NaOH activated-RHAC had similar FTIR scan peaks (1740, 1365, 1217cm^{-1}) as the H_3PO_4 activated-RHAC. The activation process seems to produce similar structural compounds. Bands at 2924 and 1365 cm^{-1} are attributed to the C–H stretching of aliphatic carbon or due to CH_2 of CH_3 deformation. Band appearing at 1627 cm^{-1} corresponds to C=O vibration of lactonic, carboxyl or anhydride groups (Le Van & Thi, 2014). Bands around 1545 and 1096 cm^{-1} are assigned to ring vibration in large aromatic skeletons generally found in carbonaceous material, such as activated carbon according to the same authors. The band in regions 700 and 1200 cm^{-1} reflect aromatic, out of plane C–H bending with different degrees of substitution. Since there are no SiO_2 absorption peaks at 1101, 944, 789, and 470 cm^{-1} we can conclude that FTIR analysis confirms that the AC samples are activated carbons without silica.

Sodium hydroxide (NaOH) used to activate the RHAC also predominantly removes SiO_2 when it reacts with NaOH to form sodium silicate (Na_2SiO_3) according to **Equation 4.22** shown below (Liou & Wu, 2009).

$$2NaOH + SiO_2 \longrightarrow Na_2SiO_3 + H_2O \qquad \textbf{Equation 4.22}$$

Because Na_2SiO_3 is soluble in water, it is easily removed by water-washing (Liou & Wu, 2009). A study by Li et al (2011) found water-washing effectively removed ash from RHAC via H_3PO_4 activation. Silicon phosphate (SiP_2O_7) formed has good solubility in water. The removal of metallic impurities in rice husks via acid leaching is due to the dissolution of metals in acid, which are later removed by rinsing the treated rice husk samples with distilled water (Muniandy et al., 2014).

4.6.2 FTIR Characterization of the RH derived silica gel

Rice husk-derived silica gel sample was pressed in a hydraulic press between smooth stainless steel die (at 1544×10^5 Pa pressure for 2 min) to give a clear potassium bromide (KBr) disk and scanned with an FTIR spectroscopy instrument IRTracer-100. **Figure 4.14** shows the FTIR scan acquired.

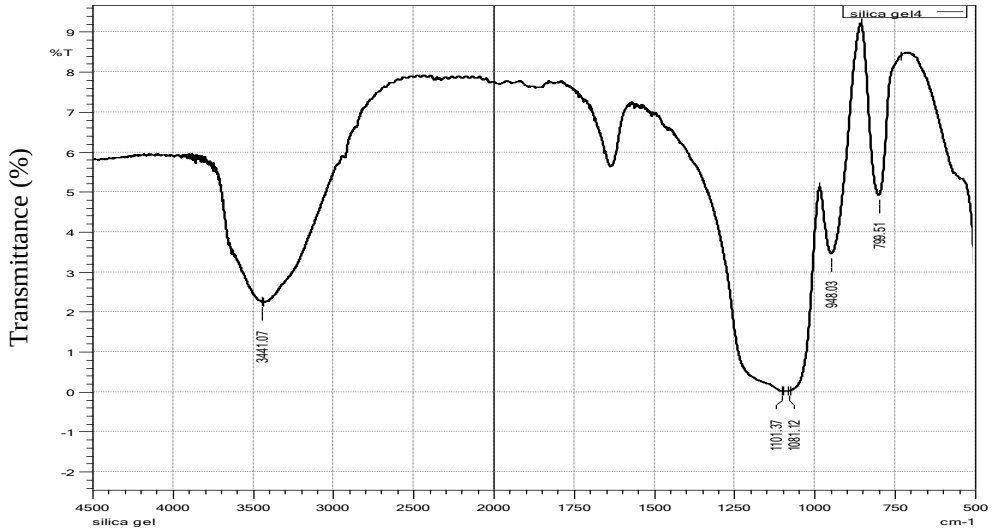

Wavenumber cm^{-1}

Figure 4.14: FTIR of RH-derived silica gel sample.

Figure 4.14 shows absorption peaks 1101.37cm^{-1}, 1081.12cm^{-1}, 948cm^{-1} and 799.51cm^{-1}, which are considered presence markers for silica gel (Radi, Basbas, Tighadouini, & Bacquet, 2014). The peaks at 3441, 1101, 1081, 948, and 799.5cm^{-1}, are similar to silica gels in literature as shown in **Figure 4.15** (Radi et al., 2014). The peaks are associated with 3441(O-H Hydroxyl group, H-bonded, OH stretch), 1101(Si-O-C), 1081(Si-O-Si), and 799 (Silicate ion) (Coates, 2000).

Figure 4.15 shows a silica gel FTIR scan obtained by Radi et al 2014 from rice husk-derived activated carbons.

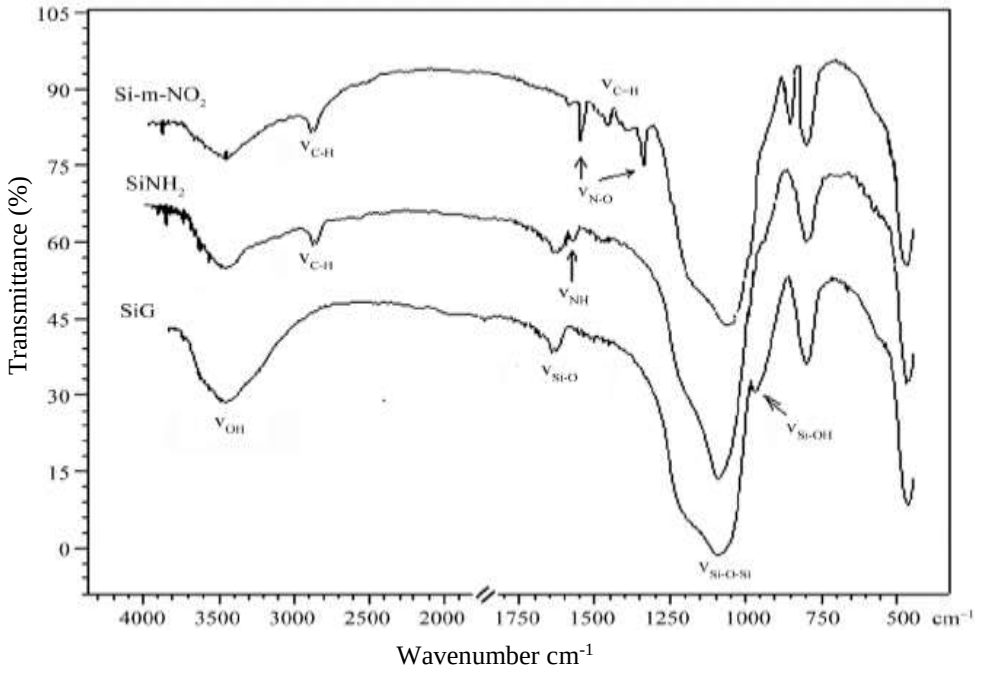

Figure 4.15: FTIR scan of RH-derived silica gel

Source: (Radi, Basbas, Tighadouini, & Bacquet, 2014)

Figure 4.15 shows an FTIR spectra scan of silica gel (SiG), modified samples ($SiNH_2$), and (Si-m-NO_2). **Figure 4.14** silica gel peaks compare well with reference (**Figure 4.15**). Both have 1101 cm^{-1}, 1081 cm^{-1}, 948 cm^{-1} and 799 cm^{-1} peaks indicating the produced silica gel is characteristically the same.

4.6.3 XRD analysis of RH-derived silica gel

Silica gel samples were examined using an XRD D2 PHASER. It offers a non-destructive characterization of crystalline samples, enabling qualitative and quantitative phase analysis, and structural investigation. It has holders for small sample amounts, low-absorbing and weakly diffracting samples, for filters, for environment-sensitive samples, and for examining materials that tend to show a preferred orientation. **Figure 4.16** and **Figure 4.18** show the X-ray diffraction (XRD) pattern scan acquired for silica gels.

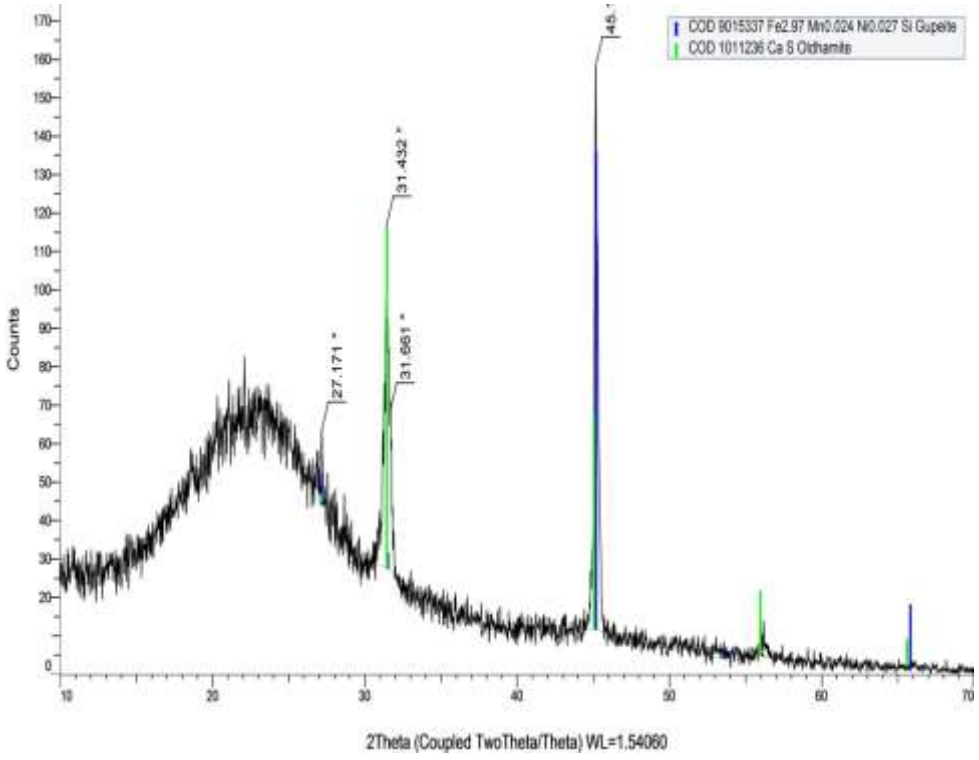

Figure 4.16: XRD pattern of RH-derived silica gel (1)

Figure 4.17 shows the mineral list from the XRD D2 PHASER library associated with the spectral scan from **Figure 4.16**.

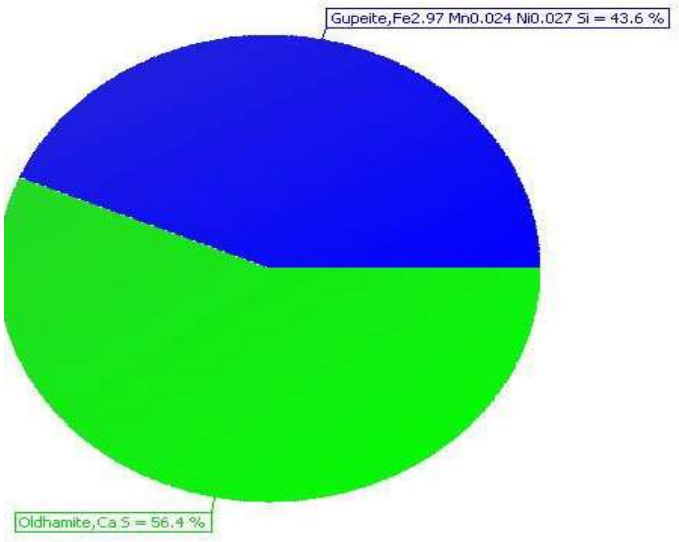

Figure 4.17: XRD mineral list of RH-derived silica gel (1)

Figure 4.17 shows the main minerals in the silica gel (1) samples were Gupeite (Fe 2.97, Mn 0.024, Ni 0.027 and Si 43.6%) and Oldhamite (CaS 56.4%) as obtained from the XRD D2 PHASER mineral list library. **Figure 4.17 and Figure 4.19** show the main minerals in the silica gel produced. The mineral list data is from the XRD D2 PHASER mineral library. The composition and/or structure of unknown material can be found from a library of XRD spectra containing a broad array of materials. Efforts have been made to map phase diagrams of a particular material or investigate species variations in crystalline materials (Macchiarola, et al., 2007).

Figure 4.18 shows the X-ray diffraction (XRD) pattern scan acquired for the silica gel (2) sample.

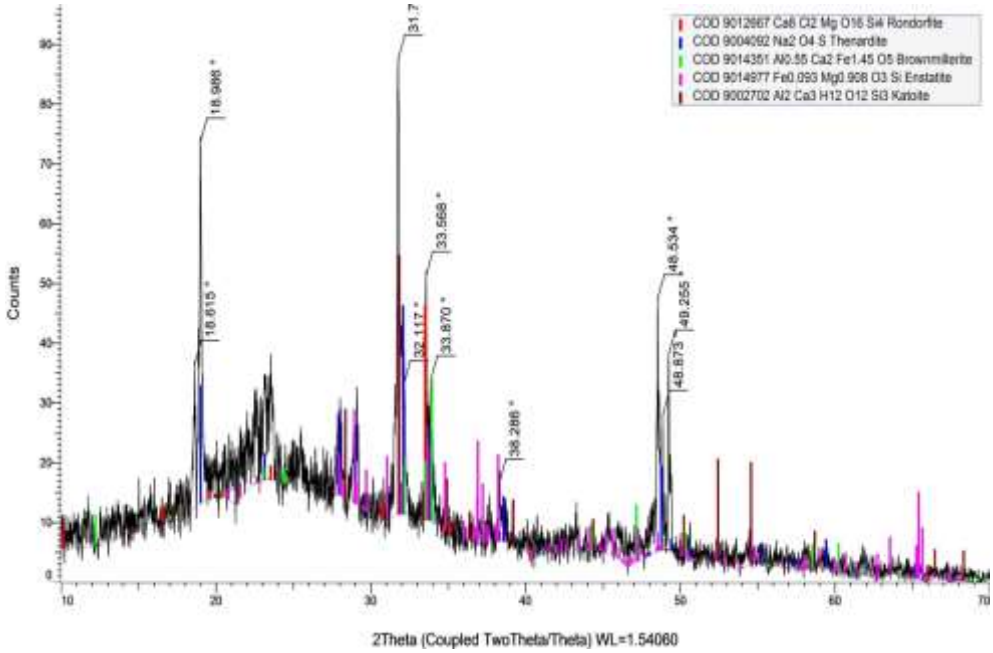

Figure 4.18: XRD pattern of RH-derived silica gel (2)

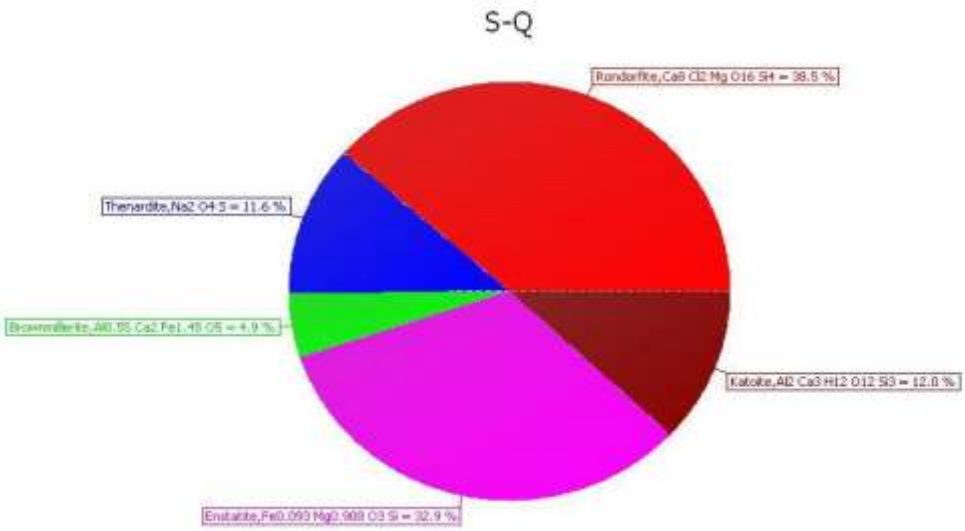

Figure 4.19: XRD mineral list of silica gel (2) from RHA.

Figures 4.16 and **4.18** XRD patterns obtained from RH-derived silica gels were consistent with other XRD patterns (**Figure 4.20**) of silica gel published by other researchers.

Figure 4.20 shows the typical XRD pattern scan of silica gel (Rivera-Muñoz, 2011).

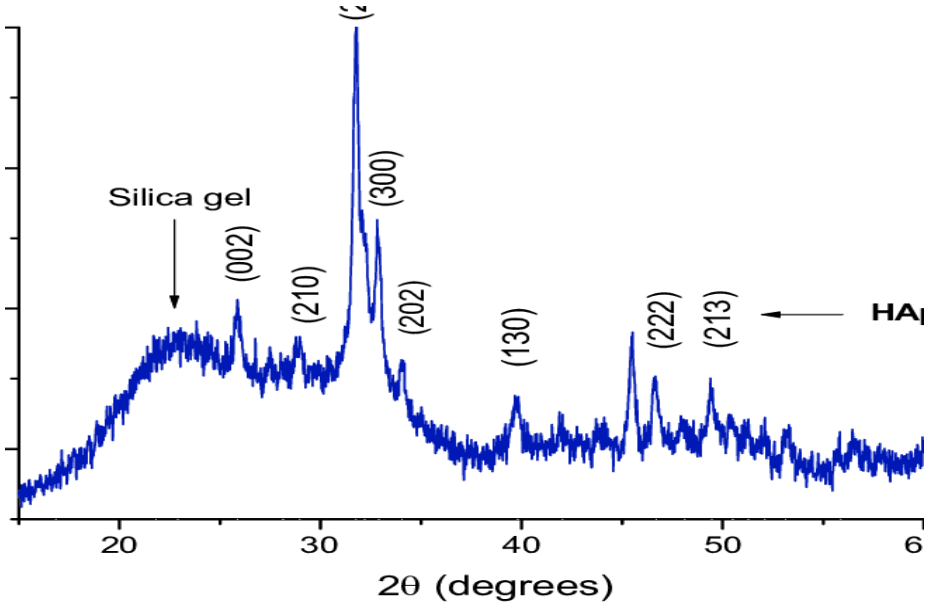

Figure 4.20: X-ray diffraction pattern of silica gel

Source: (Rivera-Muñoz, 2011).

4.6.4 Properties of SG and RHACs using SEM

RH-derived Silica gel and activated carbon samples were subjected to a bonding process using a resin (Petropoxy 154) before viewing under the Fein optic polarizing electronic microscope. **Plates 4.4-4.5** show cross and plane-polarized views of phosphoric activated rice husk-derived carbon (H_3PO_4-RHAC).

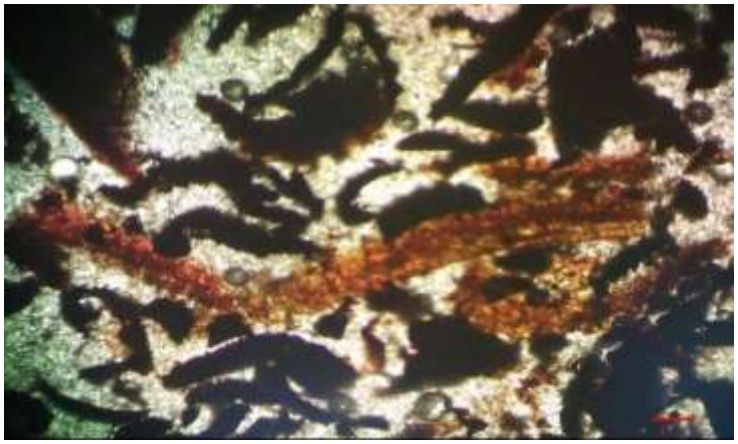

Plate 4.4: Close polar view XPL (400× cross-polarized light) of H_3PO_4-RHAC

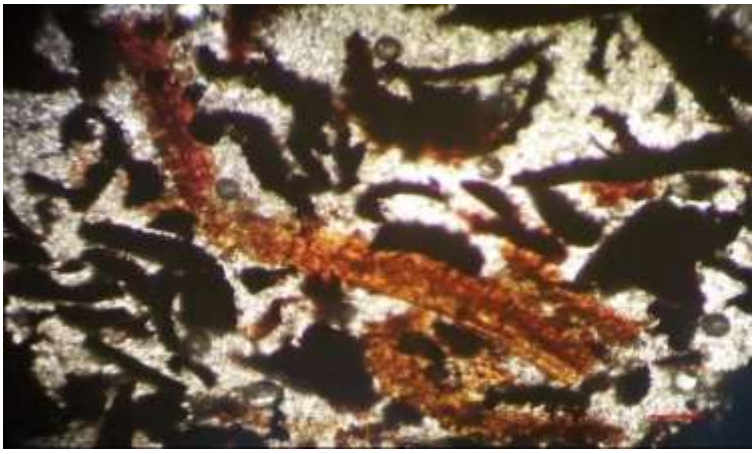

Plate 4.5: Close polar view PPL (400× plane-polarized light) of H_3PO_4- RHAC

Plates 4.4 and 4.5 show fractal-like shapes of the activated carbon. During H_3PO_4 - activation, molecules diffuse into the carbon structure developing more pores. At higher activation temperatures, the removal of volatile matters becomes more extensive, resulting in a lower solid yield (Kumar & Jena, 2016). After the activation process, the volatile matter content decreases significantly whereas the fixed carbon content increased in activated samples.

Carbon content can increase up to 73.8% for RHAC due to the pyrolytic effect at high temperatures where organic substances are degraded and discharged both as gas and liquid tars leaving a material with high carbon purity (Menya et al., 2018).

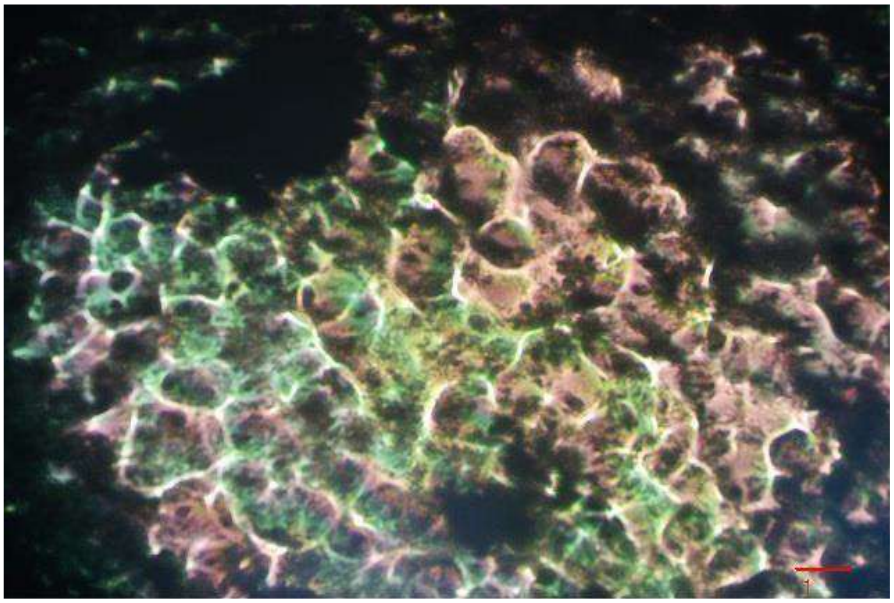

Plate 4.6: Close polar view (400×) XPL of silica gel

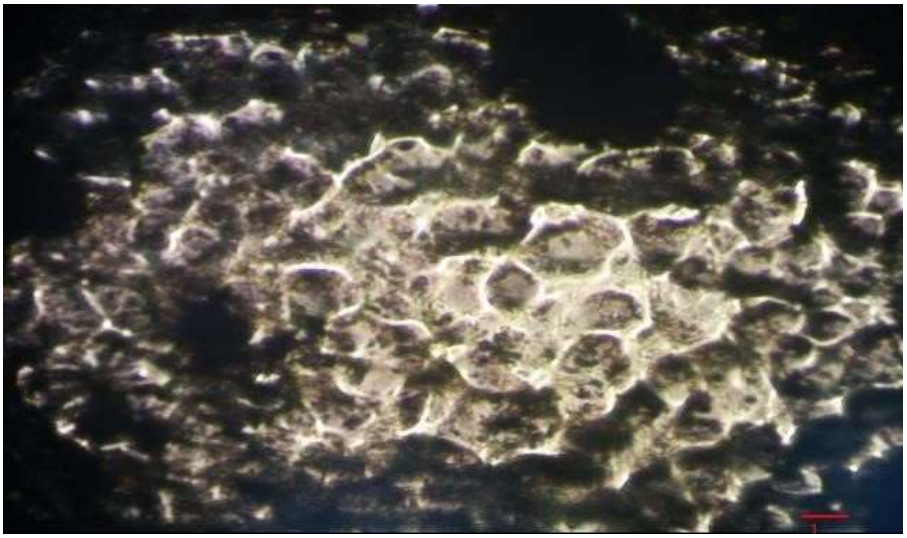

Plate 4.7: Close polar view (400×) PPL of silica gel

Plates 4.6 and 4.7 indicate the silica gels have enormous surface area. Definition of mineral composition and geometrical arrangement is possible at a microscopic level. The dark spaces indicate the degree of porosity of the activated carbons.

Plate 4.8 shows (a) Scanning Electron Microscope and (b) Transmission Electron Microscope picture of silica aero-gels showing its pore characteristics.

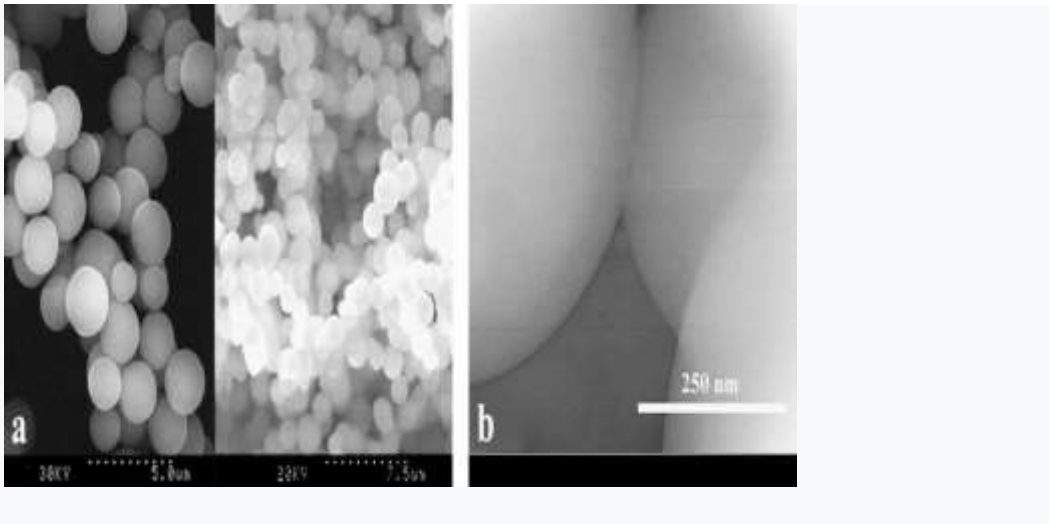

Plate 4.8: (a) SEM (b) TEM image, showing the pore characteristics of silica aero-gels. (Reichenauer & Scherer, 2001).

Plate 4.8 shows the pore characteristics of silica aerogels. Traditionally Silica gel is synthesized from Tetraethylorthosilicate (TEOS). Silica gel made from TEOS is more expensive compared with RHA, and additionally, TEOS is a hazardous chemical (Prasad & Pandey, 2012). RHA gives a yield of 73.10% Silica gel meaning 10 g of it can produce 7.31 g of silica gel (Pijarn, Jaroenworaluck, Sunsaneeyametha, & Stevens, 2010).

Plate 4.9 shows a micrograph of rice husk-derived activated carbon.

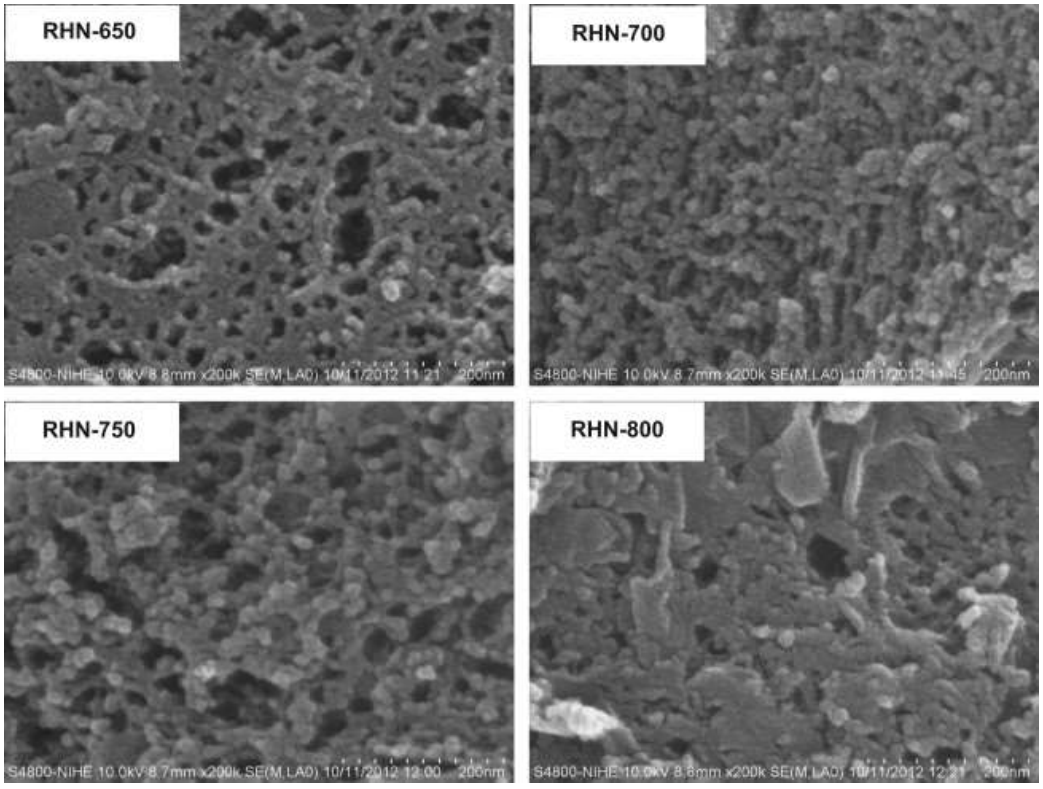

Plate 4.9: Rice husk derived NaOH-activated carbon at different temperatures (Le Van & Thi, 2014)

Plate 4.9 shows the micrograph of RHACs activated using sodium hydroxide at four (4) temperatures 650 ℃, 700 ℃, 750 ℃, and 800 ℃. The RHAC micrographs are similar to micrographs in **Plate 4.4-4.7**.

4.7 Technological application studies of RHAC

4.7.1 Removal efficiency of phenolic organic load pollutants in tea factory wastewater

Phenol standards of different concentrations were scanned using a UV-1800 Shimadzu UV spectrophotometer for absorbance. The phenol standards relationship with the UV peaks was a linear regression line ($y = 0.06499 x + 0.00741$). **Figure 4.29** shows the linear relation between the standard phenol solutions concentration and UV absorbance.

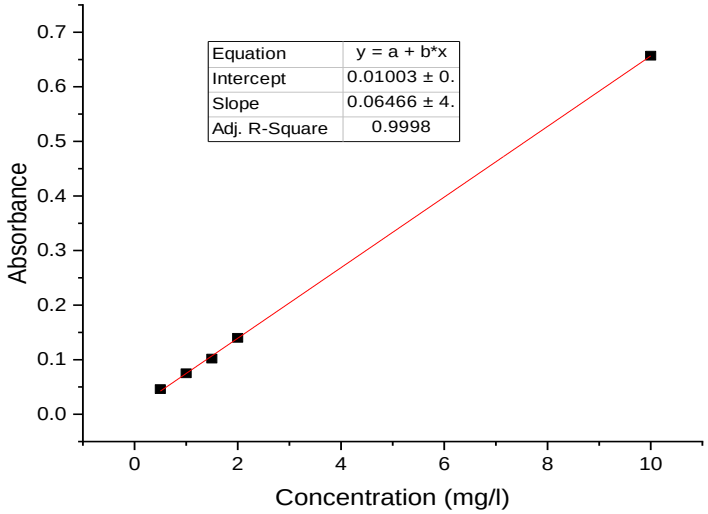

Figure 4.21: Standard curve (y = 0.064966 x + 0.01003)

Table 4.21 shows the UV absorbance peaks associated with the different RHACs and the phenol concentrations after treatments. The phenol concentrations associated with the UV absorbance peaks were calculated from the **Figure 4.29** calibration curve.

Table 4.21: UV-readings of effluent with RH-derived carbons

RHAC Sample ID	Conc. (mg/L)	UV(Absorbance) 765.0 nm
NaOH-RHAC 1	12.517	0.821
NaOH-RHAC1 (X10)	0.406	0.034
NaOH-RHAC2 (X10)	0.330	0.029
H_3PO_4- RHAC1(X20)	1 054	0.076
H_3PO_4- RHAC2(X20)	0.728	0.055
Untreated 1 (X20)	0.741	0.056
Untreated 2 (X20)	0.747	0.056
CONTROL	0.161	0.018

*NaOH-RHAC1**(**X10)- NaOH activated RH derived carbon sample 1 diluted X 10

*H_3PO_4- RHAC2(X20)- H_3PO_4 activated RH derived carbon sample 2 diluted X 20

Table 4.21 shows RH-derived activated carbons (RHACs) used removed colored organic compounds from the tea factory wastewater. NaOH-RHACs had better poly-phenolic removal. Shen (2018) has reported using RHACs to remove phenol, with an adsorption capacity of 201 mg/g within a few minutes of adsorption, confirming that silica has a great influence on phenolic compound removal. H_3PO_4- RHACs have also been utilized for the removal of p-nitrophenol, where a maximum adsorption capacity of 39.21 mg/g was reported (Ahmaruzzaman & Sharma, 2005).

Commercial activated carbons are utilized for the removal of phenolic compounds. However, their adsorption capacity was not significant as that of RH-derived carbons. For instance, the adsorption capacity of 2, 4-dichlorophenol by H_3PO_4-modified commercial activated carbons were found to be 48.18 mg/g (Anisuzzaman, Joseph, Taufiq-Yap, Krishnaiah, & Tay, 2015). Therefore, RHACs have great potential in the removal of phenolic compounds as compared to commercial activated carbons.

Using **Table 4.21** Percentage removal efficiency of NaOH-activated carbon and H_3PO_4-activated carbon was tabulated in **Table 4.22.**

Table 4.22: Total polyphenols % Removal efficiency by RHACs

Wastewater sample	Conc. (mg/L) (total phenols)	Removal(R-S)	% Removal Efficiency
NaOH-RHAC-1	0.203± 0.314	0.544	72
NaOH-RHAC-2	0.165± 0.285	0.585	77
H_3PO_4-RHAC	0.728± 0.256	0.019	2.6

R- un-treated with RHAC sample phenol concentration

S- treated RHAC sample concentration

Table 4.22 indicates NaOH-RHAC had 35 times more efficiency in total phenols removal. The removal efficiency was between 72-77 % as compared with 2.6 % H_3PO_4-RHAC. The NaOH-RHAC is a better absorbent, due to the higher percentage of ash content (Abdo, 2002). The authors also found that acidic H_3PO_4-RHAC has a basic surface while (NaOH) RH-activated carbon has an acidic one. This implies that basic NaOH-RHAC reacts more with Phenolic OH-groups thus increasing its efficiency in color removal and organic content removal.

Rice husk-derived carbons are valuable as low-cost alternatives to commercial activated carbons in wastewater treatment for the removal of organic content. Being a bio-based adsorbent material, of low cost and a renewable resource are important factors for its use in pollutant removal (Nayak & Bhushan, 2019).

4.7.2 Organic phenolic removal from tea factory wastewater by RHAC using FTIR analysis

Untreated tea factory wastewater samples (R1, R2) were scanned with an FTIR spectroscopy instrument IRTracer-100. **Figure 4.30** shows the FTIR scan acquired.

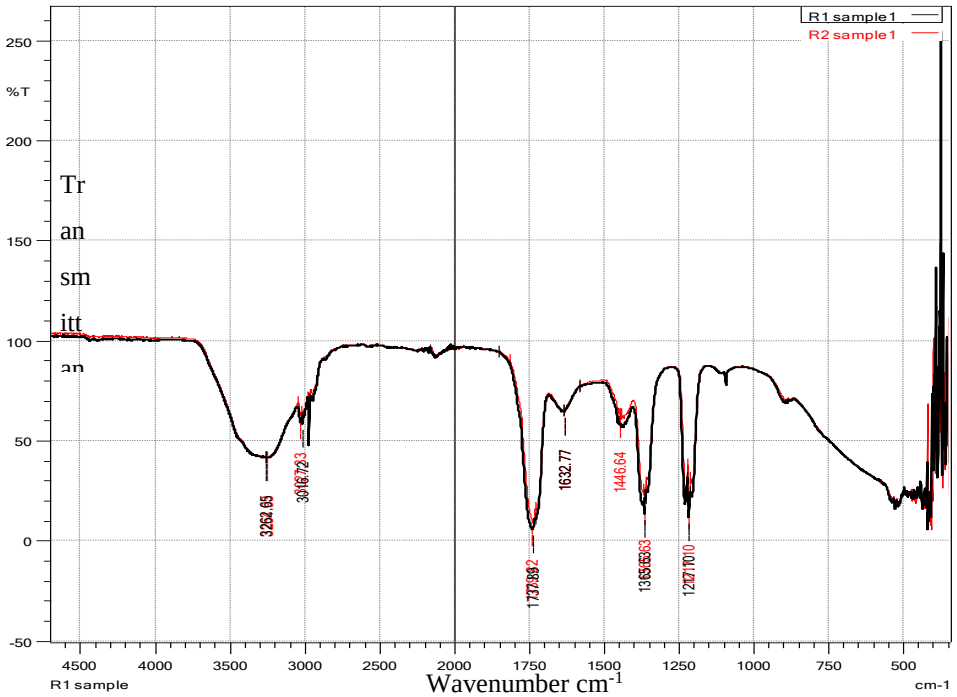

Figure 4.22: Percentage transmittance of untreated wastewater samples (R1, R2) from tea factory

Figure 4.30 shows the hydroxyl (O-H) function existing in the band (3200-3570 cm-1) as the most visible and characteristic of all of the infrared group frequencies. Polyphenols are the most characteristic organic compounds in tea factory wastewater. The main organic group in polyphenols is the hydroxyl (OH) group (Coates, 2000). In most chemical environments, the hydroxyl group exists with a high degree of association resulting from extensive hydrogen bonding with other hydroxyl groups. These hydroxyl groups form hydrogen bonds and are intramolecular. Bands 1670-1500 cm^{-1} are associated with aromatic compound unsaturation and esters (Coates, 2000).

Figure 4.31 shows an FTIR scan acquired of untreated tea factory wastewater (R1, R2) samples, and a NaOH- RHAC (S2) treated wastewater sample scanned with an FTIR spectroscopy instrument IRTracer-100.

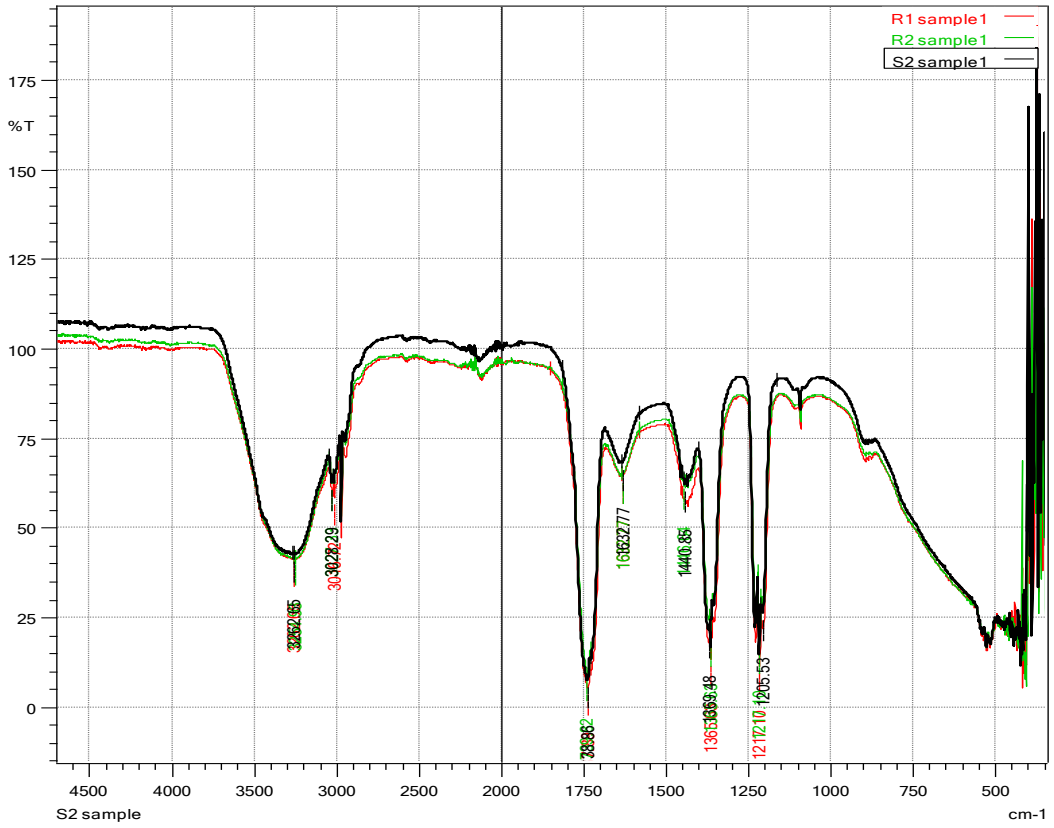

Figure 4.23: Untreated (R1, R2) wastewater samples compared with treated NaOH-RHAC (S2)

Figure 4.31 overlay graph indicates the removal of phenolic organic content by the NaOH-RHAC (S2). The bandwidth between the black, green, and red lines indicates differences in phenol organic content among the samples. Effluents in wastewater from tea factories are reddish-orange, and have substantial amounts of organic and inorganic pollutants, and suspended solids. The reddish-orange colour of the effluent discharged from tea factories is caused by phenolic compounds, theaflavins (TFs), and thearubigins (TRs), formed during the fermentation stage of tea processing (Otieno et al., 2014)..

Figure 4.23 and **Figure 4.33** show the chemical structures of Theaflavins and Thearubigins.

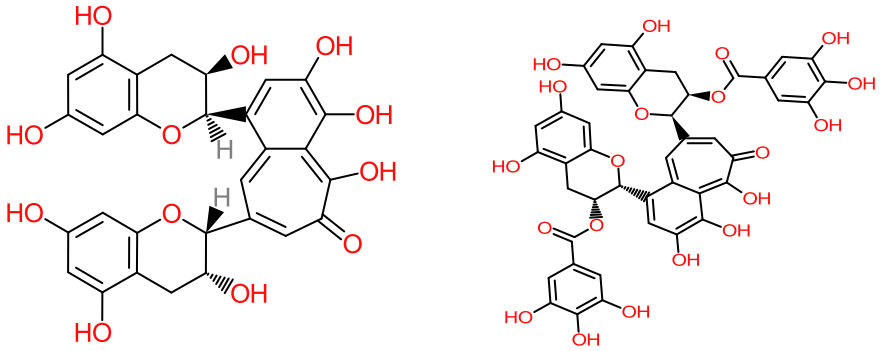

Figure 4.24: Chemical structure of theaflavins

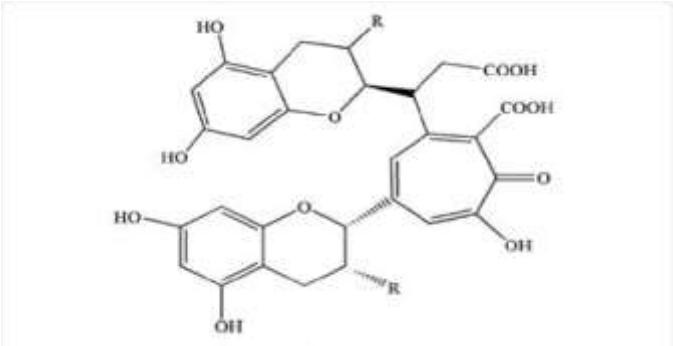

Figure 4.25: Chemical structure of thearubigins

The main characteristic of theaflavins and Thearubigins are the many -OH groups as shown in structures **Figure 4.32** and **Figure 4.33**. These compounds generally referred to as polyphenols are responsible for the dark color in tea factory wastewater. They are responsible for the bandwidth difference between the treated and untreated sample's FTIR lines in **Figure 4.31** because of removal by the NaOH-RHAC. Thearubigins are the most abundant group of phenolic pigments found in tea factory wastewater and account for an estimated 60 % of the solids in a typical black tea infusion (Debnath, Haldar, & Purkait, 2021)**.**

4.8 Removal efficiency of (Pb (II), Cd (II), and Cr (VI)) from water using RHACs.

Metal ions before and after adsorption were determined using a flame atomic absorption spectroscopy AA-7000 Shimadzu model, while pH determination was done using the HI-2211 HANNA pH meter. **Figure 4.26** shows the effects of

variation of pH 2-8 to percentage removal of Pb (II), Cd (II), and Cr (VI) using NaOH-RHAC.

4.8.1 Effect of pH on Pb (II), Cd (II), and Cr (VI) removal from solution

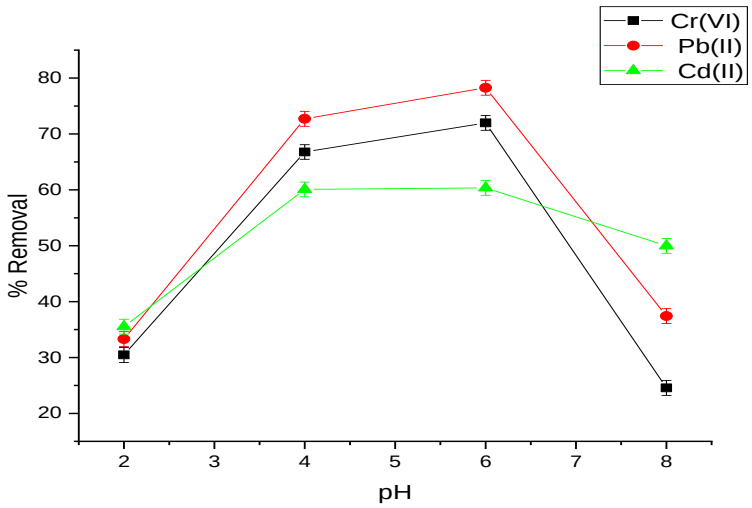

Figure 4.26: Effect of pH on Pb (II), Cd (II), and Cr (VI) removal using NaOH-RHAC

Figure 4.27 shows the effects of variation of pH 2-8 to percentage removal of Pb (II), Cd (II), and Cr (VI) using H_3P0_4 -RHAC.

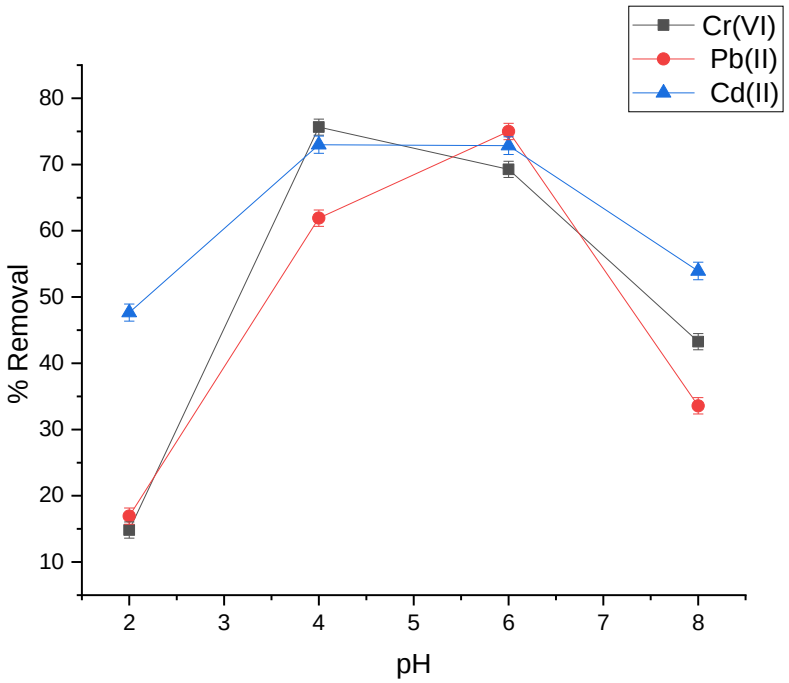

Figure 4.27: Effect of pH on Pb (II), Cd (II), and Cr (VI) removal using H_3P0_4 - RHAC.

Figure 4.26 and **Figure 4.27** show that for Pb (II) removal using NaOH-RHAC, the optimum pH was six (6) with 78.26 % removal while for H_3PO_4-RHAC the optimum pH was six (6) with 74.99 % removal. For Cd (II) optimum pH for both adsorbents was four (4) with 60.73 % and 72.99 % removal for NaOH-RHAC and H_3PO_4-RHAC respectively. For Cr (III) optimum pH was 6 and 4 with 71.98 % and 75.64 % removal for NaOH and H_3PO_4-RHAC respectively. Low Pb (II) and Cd (II) removal at low pH can be attributed to the protonation of H^+, which competes with metal ions onto the adsorbent attachment sites (Kariuki, Kiptoo, & Onyancha, 2017). At slightly acidic pH, both metal ions were at optimum removal. This was due to the deprotonation of H^+ with both metal ions acting as free ions in the solution (Kowanga, Gatebe, Mauti, & Mauti, 2016). At pH greater than seven (7), metal ions, form metal hydroxide precipitates which then interfere with metal ions adsorption thus leading to the reduction in removal efficiency. Optimum pHs for adsorption was used in subsequent experiments.

4.8.2 Effect of sorbent mass on Pb (II), Cd (II), and Cr (VI) removal

The effect of sorbent mass on the removal of Pb (II), Cd (II), and Cr (VI) from aqueous solution was determined at specific optimum pH for each metal ion identified earlier. The results are presented in **Figures 4.28 and 4.29**.

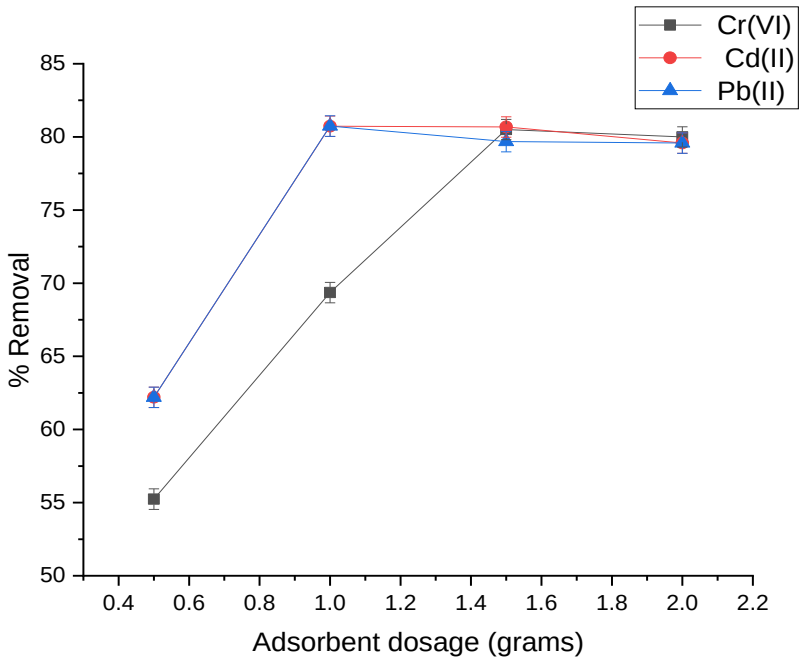

Figure 4.28: Effect of adsorbent dosage on Pb (II), Cd (II), and Cr (VI) removal using NaOH-RHAC

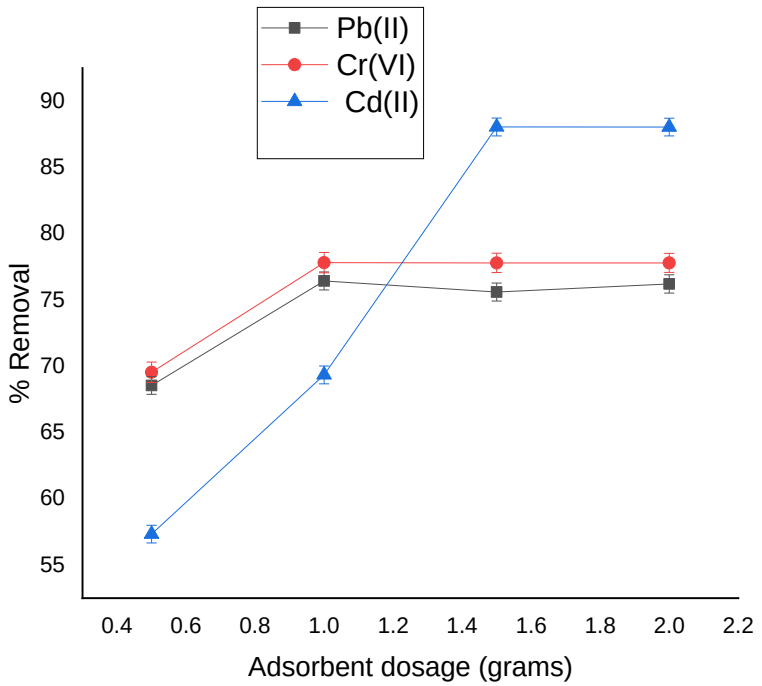

Figure 4.29: Effect of adsorbent dosage on Pb (II), Cd (II), and Cr (VI) removal using H_3P0_4-RHAC

Figure 4.28 and **Figure 4.29** show optimum adsorbents dosages were between 0.5 - 2.0 g. From **Figures 4.28 and 4.29** Pb (II) ions, an optimum dosage for NaOH and H_3P0_4-RHACs was 1.0 grams with 80.73 % and 76.42 % removal respectively. For Cd (II) optimum adsorbent dosages were 1.5 - 2.0 g with 80.15 % and 88.06 % removal for NaOH and H_3PO_4 –RHAC respectively. For Cr (VI) optimum adsorbent dosages were 1.0 grams for both adsorbents with 80.73 % and 76.42 % removal for NaOH and H_3PO_4-RHACs respectively. An increase in percentage metal ions removal with an increase in adsorbent dosages is attributed to increase in the number of binding sites and consequently increased surface area (Pakade, Ntuli, & Ofomaja, 2017).

4.8.3 Effect of contact time on Pb (II), Cd (II), and Cr (VI) removal using NaOH and H3PO4 -RHACs

Optimum contact time determination was carried out by mixing 10 mg/l Pb (II), Cd (II), and Cr (VI) solution at optimum pHs and optimum dosages identified earlier.

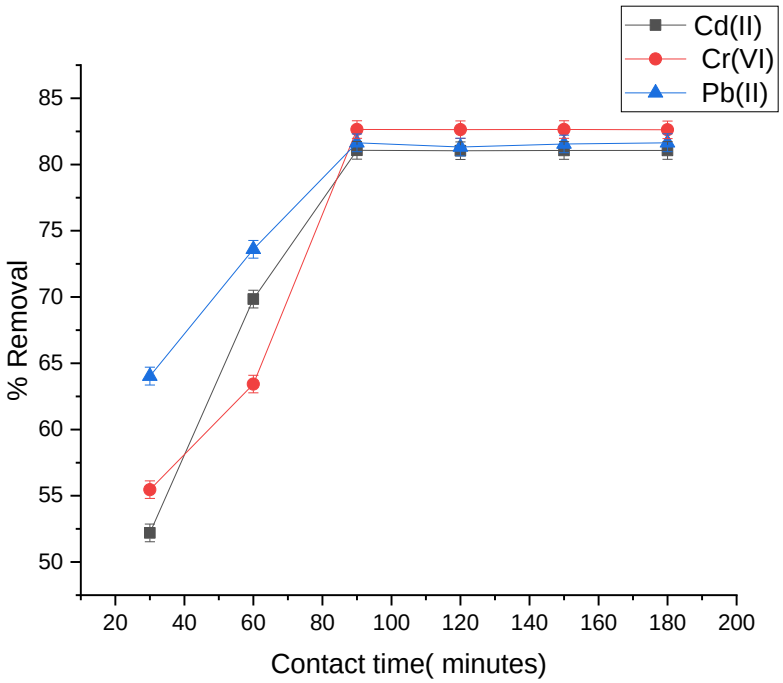

Figure 4.30: Effect of contact time on Pb (II), Cd (II), and Cr (VI) removal using NaOH-RHAC

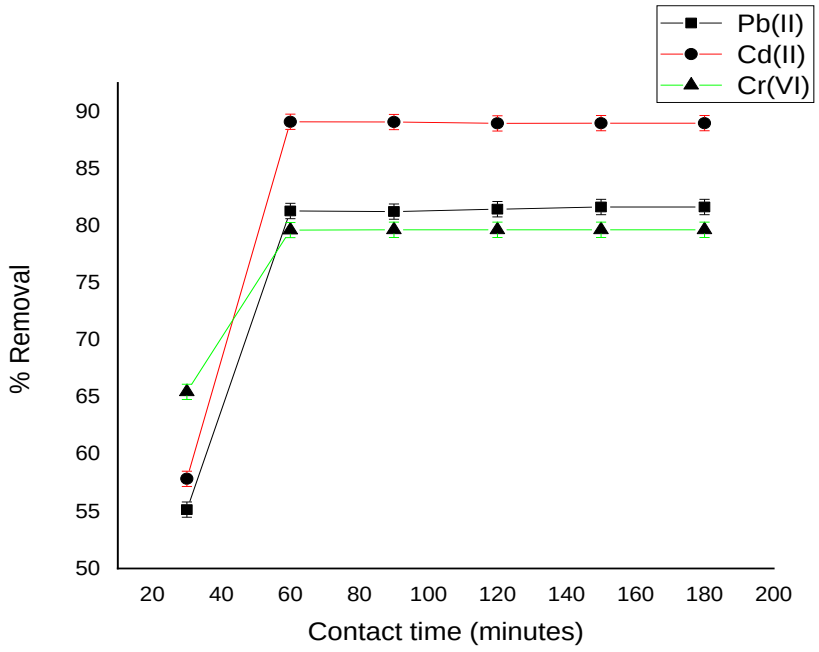

Figure 4.31: Effect of contact time on Pb (II), Cd (II), and Cr (VI) removal using H_3PO_4-RHAC

Figure 4.30 and **Figure 4.31** show Pb (II), Cd (II), and Cr (VI) removal increased with increased contact time. This was due to the increased sufficient time for the interaction between the adsorbent and the adsorbate (Kakoi et al., 2016). The optimum contact time for Pb (II) removal using NaOH and H_3PO_4 RHACs was 60 minutes. For Cd (II) removal, the optimum contact time was 90 minutes for NaOH-RHAC and 60 minutes for H_3PO4-RHAC, with 81.07 % and 89.10 % removal respectively. After that time, the percentage removal remained constant. The optimum contact time for Cr (III) removal using NaOH and H_3PO_4 RHACs was 82.64 % and 79.65 % respectively at 90 minutes. This was because, as the residence time increased the number of adsorbent attachment sites decreased thus leading to a reduction of contact sites between the adsorbent and the adsorbate (Manjuladevi, Anitha, & Manonmani, 2018).

4.8.4 Effect of initial concentration on Pb (II), Cr (VI), and Cd (II) removal using NaOH and H_3PO_4 RHACs

Initial concentrations of Pb (II), Cr (VI), and Cd (II) ranging from 5, 10, 15, and 20mg/l were mixed with RHACs at optimum pH, optimum dosage, and optimum

contact time. Equilibrium concentration remaining at various initial concentrations was then determined using a flame atomic absorption spectrophotometer. Results are shown in **Figures 4.32 and 4.33**

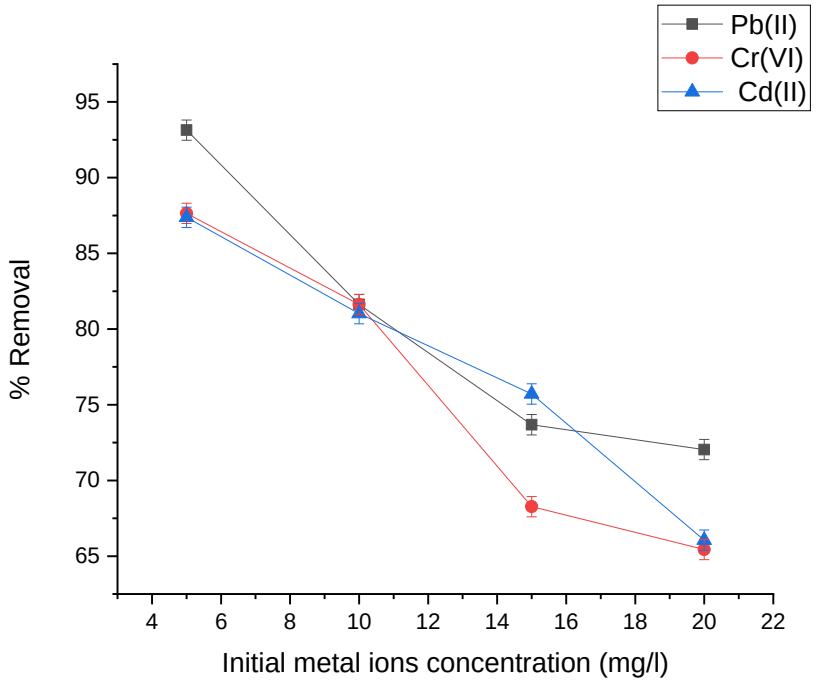

Figure 4.32: Effects of initial metal ions concentration on Pb (II), Cd (II), and Cr (VI) removal using NaOH-RHAC

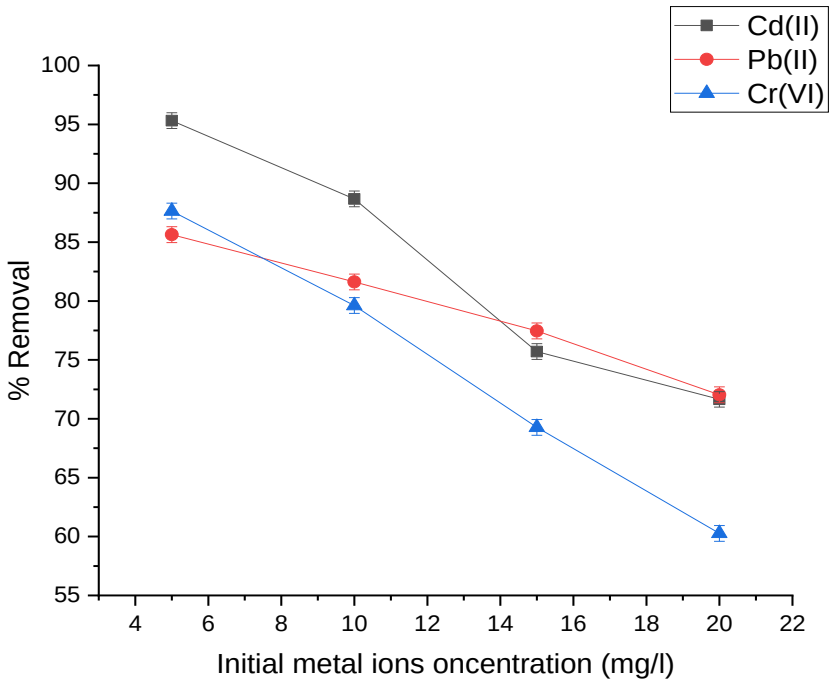

Figure 4.33: Effects of initial metal ions concentration on Pb (II), Cd (II), and Cr (VI) removal using H_3PO_4 –RHAC

From **Figure 4.32** and **Figure 4.33** decreased percentage removal of metal ions with an increase in initial concentration of the metal ions was observed. This was because, at low metal ions concentrations, the ratio of surface-active sites to the total metal ions was high, hence the highest percentage of metal ions removal. However, at high metal ions concentrations, the ratio of surface active sites to the total metal ions reduced hence reduction in the number of metal ions that reacted with the active sites of the adsorbent (Afroze, Sen, & Ang, 2016).

4.9 Adsorption isotherms

4.9.1 Langmuir adsorption isotherms

The linearized form of Langmuir isotherm is shown in **Equation 4.23**;

$$\frac{C_e}{q_e} = \frac{1}{K_L q_m} + \frac{C_e}{q_m} \quad \text{.....Equation 4.23}$$

C_e is the equilibrium concentration in mg/l, q_e is the adsorbed amount in mg/g, K_L is the separation factor which is indicative of the direction of the reaction and q_m is the maximum adsorption capacity in mg/g. Values of K_L and q_m are obtained by plotting ce/qe against ce using **Equation 4.23** (Taha, Dakroury, El-Sayed, & El-Salam, 2010). **Figure 4.34** shows the linearized Langmuir isotherm equilibrium concentration (ce) of Pb (II), Cd (II), and Cr (VI) correlation to the adsorbed amount (ce/qe) for NaOH-RHAC.

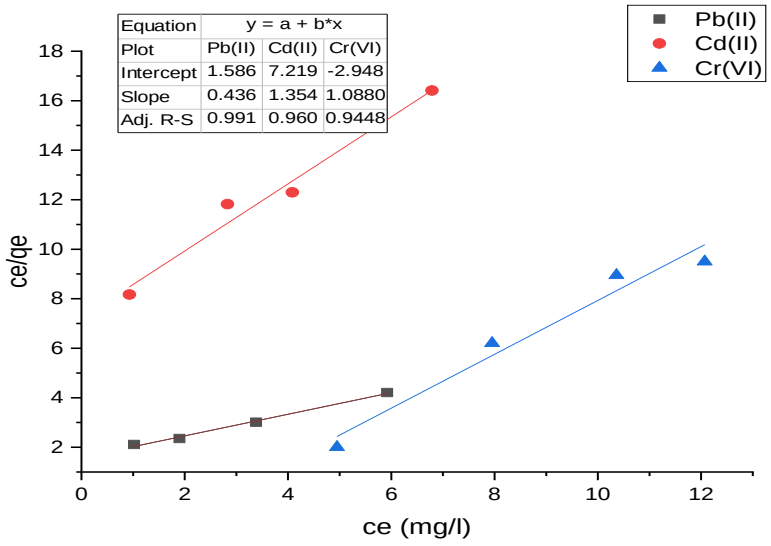

Figure 4.34: Linearized Langmuir isotherm parameters for Pb (II), Cd (II), and Cr (VI) adsorption onto NaOH-RHAC

Figure 4.35 shows the linearized Langmuir isotherm equilibrium concentration (ce) of Pb (II), Cd (II), and Cr (VI) correlation to the adsorbed amount (ce/qe) for H_3PO_4-RHAC.

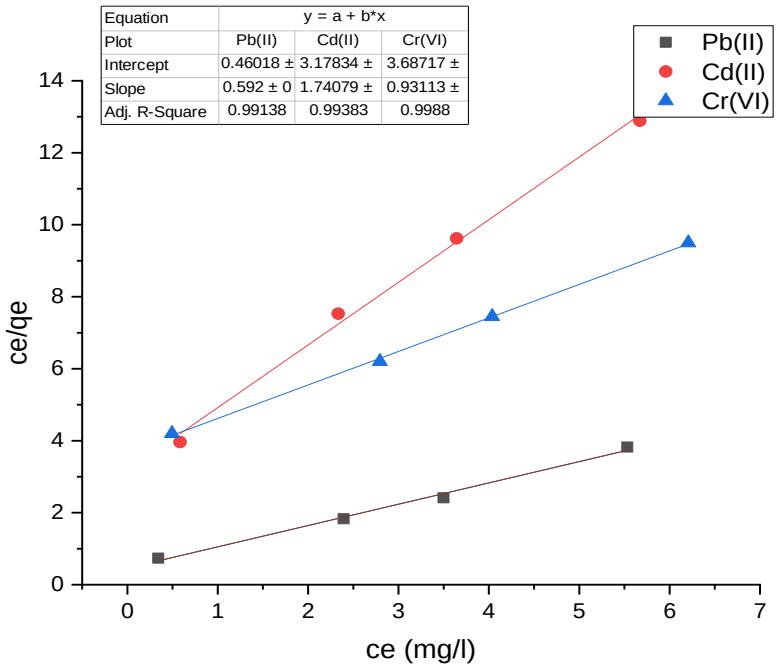

Figure 4.35: Linearized Langmuir isotherm parameters for Pb (II), Cd (II), and Cr (VI) adsorption onto H_3PO_4-RHAC

Freundlich Isotherm

The linearized form of Freundlich isotherm is shown in **Equation 4.24**;

$$\log q_e = \log K_f + \frac{1}{n} \log C_e \quad \text{..... Equation 4.24}$$

Where q_e is the adsorbed amount in mg/g, K_f is the Freundlich constant. Values of K_f and 1/n are obtained by plotting log q_e vs log C_e (Rasmey, Aboseidah, & Youssef, 2018).

Figure 4.36 shows the linearized Freundlich isotherm (log qe) of Pb (II), Cd (II), and Cr (VI) correlation to (log ce) for NaOH-RHAC.

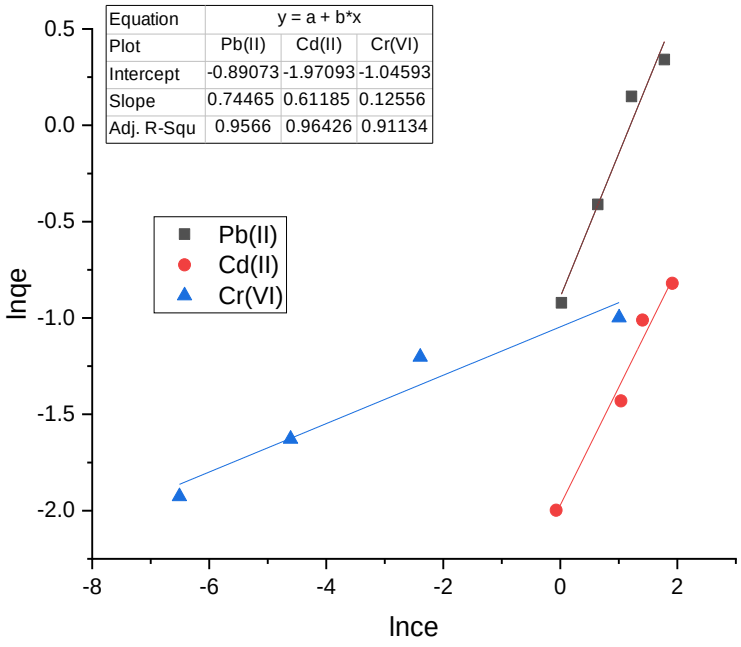

Figure 4.36: Linearized Freundlich isotherm for Pb (II) Cd (II) and Cr (VI) adsorption onto NaOH-RHAC

Figure 4.37 shows the linearized Freundlich isotherm concentration (log qe) of Pb (II), Cd (II), and Cr (VI) correlation to (log ce) for NaOH-RHAC.

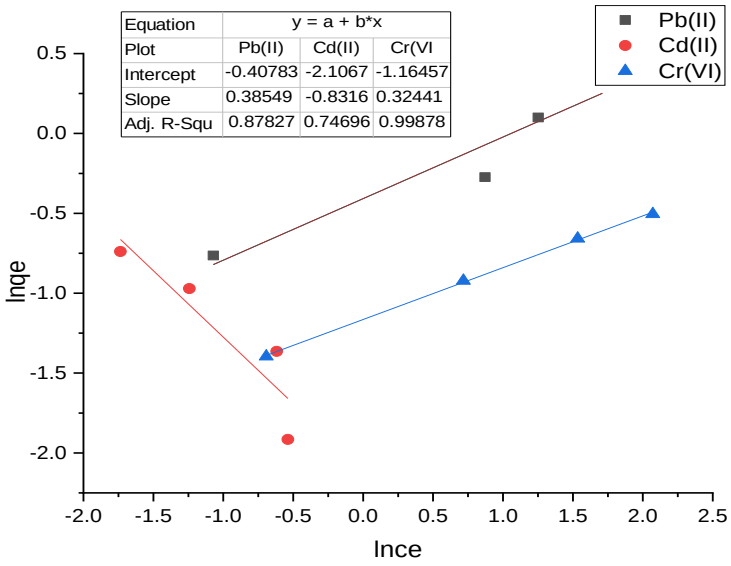

Figure 4.37: Linearized Freundlich isotherm for Pb (II) Cd (II) and Cr (VI) adsorption onto H_3PO_4-RHAC

Figures 4.33-4.36 show the Langmuir and Freundlich isotherms models applied to estimate the adsorption capacity of adsorbents used. The data suggest that uptake occurred on a homogeneous surface by monolayer sorption with the interaction between adsorbed molecules. Results of the modeling of the isotherms of Pb (II), Cd (II), and Cr (VI) according to Langmuir and Freundlich models are summarized in **Table 4.23**

Table 4.23: Comparison of various isotherm parameters for Pb (II), Cd (II), and Cr (VI) adsorption

A: Langmuir isotherm

	NaOH-RHAC				**H_3P0_4 -RHAC**		
	1/qm	K_L	R2		1/qm	K_L	R2
Pb(II)	0.436	1.586	0.9910	Pb(II)	0.592	0.461	0.9914
Cd(II)	1.354	7.129	0.9600	Cd(II)	1.740	3.178	0.9938
Cr(VI)	1.088	2.948	0.9448	Cr(VI)	0.931	3.680	0.9998

B: Freundlich isotherm

	NaOH-RHAC				H_3P0_4 -RHAC		
	1/n	K_F	R2		1/n	K_F	R2
Pb(II)	0.745	0.891	0.9566	Pb(II)	0.3855	0.4078	0.9566
Cd(II)	0.612	1.971	0.9643	Cd(II)	0.8316	2.1067	0.7470
Cr(VI	0.126	1.0460	0.9113	Cr(VI)	0.3244	1.6457	0.9988

Table 2.23 show the correlation coefficient (R2) for Langmuir for Pb (II) removal using NaOH and H_3P0_4-RHACs was over 0.99. Additionally, the value of (R2) for Langmuir for Cd (II) using NaOH-RHAC was over 0.99. Additionally, the value of (R2) for Langmuir for Cd (II) removal using H_3PO_4 –RHAC was over 0.99. This was an indication monolayer adsorption on the homogenous surfaces of the adsorbent was prevalent. Cd (II) removal correlation coefficient R2 for Freundlich was 0.7470 using NaOH-RHAC implying adsorption on a heterogeneous surface was prevalent.

4.10 Kinetics studies

Kinetic studies were conducted at various time intervals using the optimum pH, adsorbent dosage, and initial metal ions concentrations. The purpose of kinetic studies is to determine the rate and the mechanism of adsorption reaction mechanisms. The linear form of pseudo-first-order reaction is as shown in **Equation 4.25** (Sahu & Chatterjee Mitra, 2018);

$$\mathbf{Ln\ (q_e - q_t) = lnq_e - K_1 t \ldots\ldots\ldots\ldots\ldots\ldots\ Equation\ 4.25}$$

Where; q_e amount of metal ions adsorbed at equilibrium, q_t is the adsorption capacity at equilibrium, and K_1 is the pseudo-first-order constant. Values of K_1 and qe are obtained from the slope and intercept respectively by plotting ln (qe-qt) against time t (Sadeek, Negm, Hefni, & Wahab, 2015). **Figure 4.38 and Figure 4.39** show the first-order kinetic graph for adsorption onto NaOH-RHAC and H_3P0_4-RHAC from experimental data listed in Appendix 9

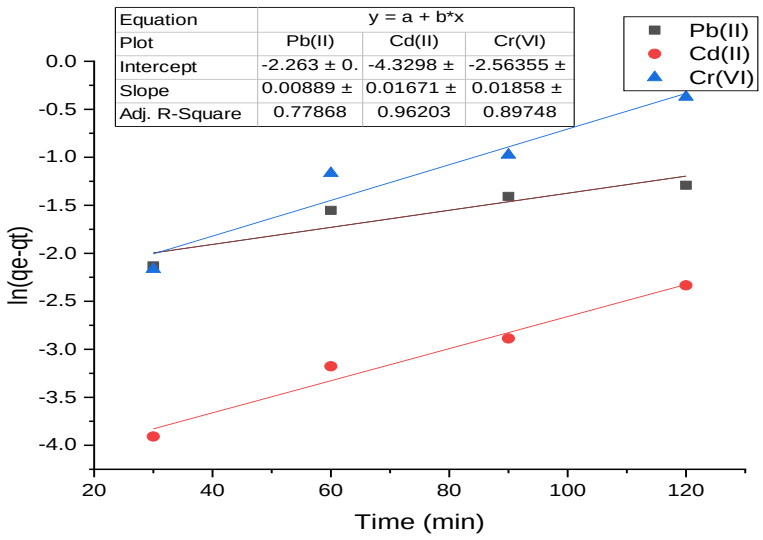

Figure 4.38: Pseudo first-order kinetics for Pb (II), Cd (II), and Cr (VI) adsorption onto NaOH-RHAC

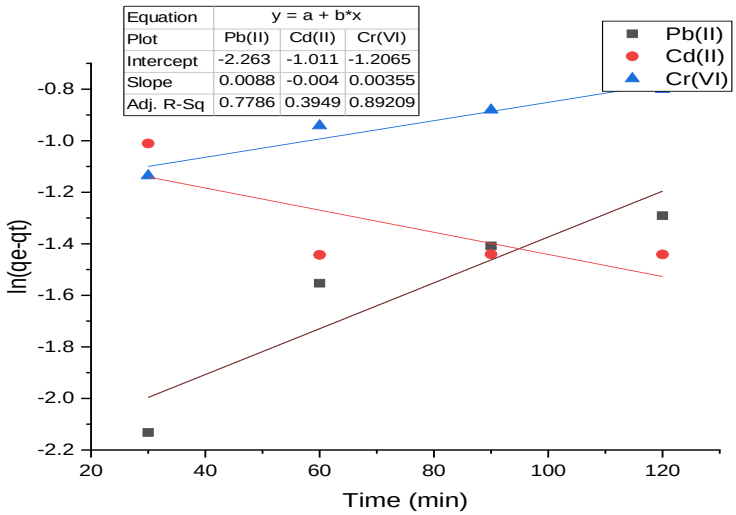

Figure 4.39: Pseudo first-order kinetics for Pb (II), Cd (II), and Cr (VI) adsorption onto H_3P0_4-RHAC

Figure 4.38 and **Figure 4.39** show the values of (R2) for the pseudo-first-order plots were less than 0.90. This was an indication that the rate of metal ions uptake by the adsorbent with time was not linearly proportional to the number of attachment sites which are located on the adsorbent surface (Kołodyńska, Krukowska, & Thomas, 2017). The majority of the interactions between adsorbent and metal ions have been explained by either pseudo-first-order or second-order kinetics based on the best fit

obtained by various groups of workers, although second-order kinetics is the most predominant one (Hubbe, Park, & Park, 2014).

The pseudo-second-order is based on the assumption that the rate-limiting step in Pb (II), Cd (II), and Cr (VI) accumulation onto activated carbon is through the exchange of valence electrons leading to the formation of a new chemical bond (Simonin, 2016). The linearized form of pseudo-second-order is shown in **Equation 4.26** (Moussout, Ahlafi, Aazza, & Maghat, 2018) ;

$$\frac{t}{q_t} = \frac{1}{K_2 q_{e2}} + \frac{1}{q_e} t \quad \text{..... Equation 4.26}$$

Where K_2 is the pseudo-second-order rate constant (g/mg/min). The values of q_{e2} and K_2 are obtained from the slope and intercept respectively after a plot of t/qt against time (t) (Farouq & Yousef, 2015).

Figure 4.40 and Figure 4.41 show the second-order kinetic graphs for adsorption onto NaOH-RHAC and H_3P0_4-RHAC from experimental data listed in Appendix 7.

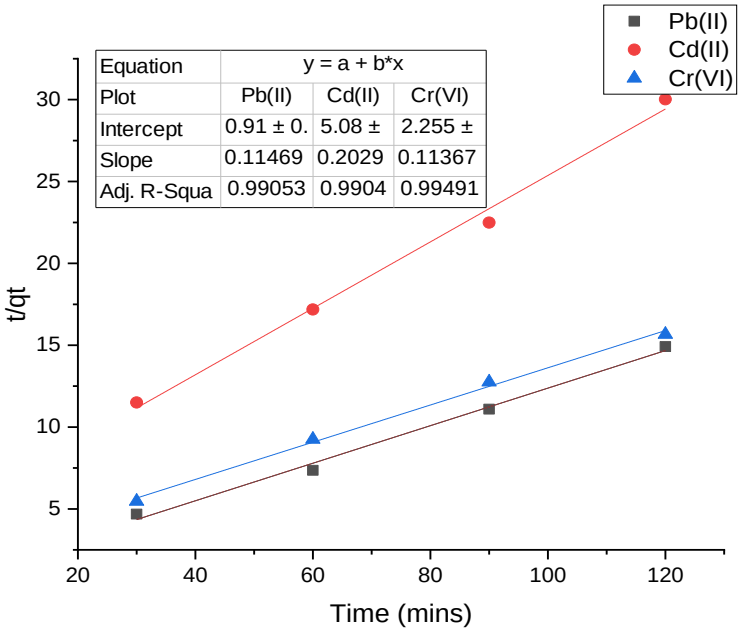

Figure 4.40: Pseudo second-order kinetics for Pb (II), Cd (II), and Cr (VI) adsorption onto NaOH-RHAC

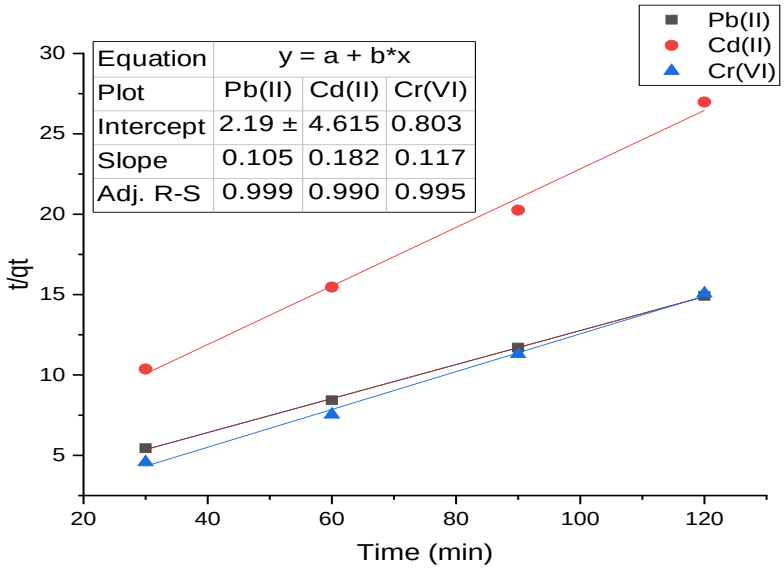

Figure 4.41: Pseudo second-order kinetics for Pb (II), Cd (II), and Cr (VI) adsorption onto H_3P0_4-RHAC

Comparison of the various kinetic parameters for Cd (II), Cr (VI), and Pb (II) adsorption for first and second-order pseudo kinetics are shown in **Table 4.24**.

Table 4.24: Comparison of various kinetic parameters for Cd (II), Cr (VI), and Pb (II) adsorption

A. Pseudo first order

	NaOH-RHAC				**H_3P0_4 -RHAC**		
	qe	K_1	R^2		qe	K_1	R^2
Pb(II)	-2.263	0.0089	0.7787	Pb(II)	0.0088	2.923	0.7787
Cd(II)	-4.330	0.0167	0.9620	Cd(II)	-0.004	1.011	0.3949
Cr(VI)	-2.564	0.0186	0.8975	Cr(VI)	0.0036	1.207	0.8921

B. Pseudo second order

	NaOH-RHAC				**H_3P0_4 -RHAC**		
	qe	K_2	R^2		qe	K_2	R^2
Pb(II)	0.115	0.91	0.9906	Pb(II)	0.105	2.190	0.990
Cd(II)	0.2209	5.08	0.9905	Cd(II)	0.182	4.165	0.9900
Cr(VI)	0.114	2.225	0.9950	Cr(VI)	0.117	0.803	0.9950

Table 4.24 shows the values of (R^2) for the pseudo-second-order plots were greater than (0.90). This was an indication that the mechanism of metal ions adsorption onto the adsorbent was through the exchange of electrons between the metal ions and the adsorbents leading to the formation of a chemical bond (Nethaji, Sivasamy, & Mandal, 2013).

CHAPTER FIVE

CONCLUSIONS AND RECOMMENDATIONS

5.1 Conclusions

Despite efforts in using rice husks as a heating source, briquettes, cement additives, mountains of RH are still visible in rice-growing areas. Openly burning rice husks produces rice husk ash (RHA), which is a valuable source of industrial chemical products. RHA has 87-97% silica, is highly porous, lightweight with a high external surface area. Rice husks ash (RHA) have 80% silica content that is convertible to sodium silicate and other silica-related products (Albert, Werhane, & Rolph, 2014). Sodium silicate produced from RHA has many applications in the chemical industry especially in detergent manufacture and soap production. Silica gel produced from silica is also widely used in the chemical industry.

Sampled rice husks from Kirinyaga County had average moisture of 7.07 % after 3½ hours of drying. About 74 % of the sampled rice husks had diameters ranging from 2.00-1.00 mm. Only about 1.74 % of rice husk had a diameter within a range of 1.00-0.710 mm. The average ash content of the sampled rice husks was 22.65 %. Major components of rice husk include 75-90 % organic materials such as hemicellulose, cellulose, and lignin.

A small-scale oxidation reactor was designed and fabricated with stainless steel, with an inner-core diameter of 0.22 metres and a height of 0.30 metres. The inner-core reactor was insulated with high-temperature refractory cement (Hi-Castable cement). When testing the maximum temperature attained at the reactor cylinder was 432 °C. The starting time was 2 minutes. The fuel consumption rate was 2.26 kg/h, and the time required to bring to boil 2 kg of water was 7-8 minutes. Starting time from the ignition of rice husk by pieces of paper to burn was 1.4 minutes. The average operating time of the oxidation reactor was 13.4 minutes.

Hydrochloric acid leached rice husks produced more Silica (SiO_2), 99.173 % at 500 ºC, 98.899% at 600 ºC, and 98.999% at 700 ºC respectively. Acid leaching removed

metallic impurities more efficiently. SiO_2 yield obtained from water-leached rice husks was 97.37% compared to 99.17% (HCl-leached) and 99.02% (H_2SO_4 -leached respectively. Statistical analysis of the three treatments indicated significant differences at a 95 % confidence level (F=0.0286278 less F critical 5.143253). The implication is that acid-leaching causes a significant difference in % Silica (SiO_2) yield.

In a trial to study the effects of leaching and temperature on Silica availability from rice husk ash (RHA), there were indications that temperatures at which the RHA was generated were not significant. Statistical analysis of the effect of temperatures on Silica content yield from RHA found no significant effect (F critical 5.143253 more than F-value 2.695752). Leaching of rice husk ash (RHA) with H_2O, HCl, and H_2SO_4 had no significant difference at a 95 % confidence level. We can therefore produce Silica from Rice husks by leaching obtained RHA with water thus ensuring synthesized industrial chemicals are green products.

Sodium silicate samples from rice husks were taken to the Kenya Bureau of Standards (KEBS) to verify compliance to KEBs standard (KS 2350: 2012). It was observable that several sodium silicate samples (Openly burnt & 1 M, 2 M NaOH-Treated, Incineration at 600 °C & 3 M NaOH-Treated) complied with KS 2350:2012 specifications**.** Statistical analysis of the chemical properties of sodium silicate from rice husks indicated no significant differences with conventional industry Sodium Silicate as per KS 2350-2012 Standard (Liquid neutral).

Farmers burning rice husk wastes in the field can use the RHA to produce Silica gel and other valuable chemicals. Thirty (30) % of silica gel samples from rice husks had Silica (SiO_2) of over 95%. Further purification could result in marketable Silica gel.

NaOH-RHAC had 35 times more efficiency in total phenols removal. 72-77 % efficiency was recorded using NaOH-RHAC with 2.6 % for H_3PO_4-RHAC. FTIR analysis indicated the RHACs have similar active sites (1740, 1365, 1217cm^{-1}). Since there are no FTIR SiO_2 absorption peaks at 1101, 944, 789, and 470 cm^{-1} we can conclude that that the RHAC samples are activated carbons without silica.

For metallic removal (Pb (II), Cd (II), Cr (VI)) using NaOH-RHAC and H_3PO_4-RHAC, the optimum pH was six (6) with 78.26% and 74.99% removal respectively. For Pb (II), Cd (II) and Cr (VI) ions removal optimum adsorbent dosages for NaOH and H_3P0_4-RHACs were 1.0-2.0 grams. Optimum contact time for Pb (II), Cd (II) and Cr (VI) removal using NaOH and H_3PO_4 RHACs were 60-81.16 minutes.

The correlation coefficient (R^2) for Langmuir for Pb (II), Cd (II) removal using NaOH and H_3P0_4-RHACs was over 0.99. This was an indication monolayer adsorption on the homogenous surfaces of the adsorbent was prevalent.

The values of (R2) for the pseudo-second-order plots were greater than (0.90). This was an indication that the mechanism of metal ions adsorption onto the adsorbent was through the exchange of electrons between the metal ions and the adsorbents leading to the formation of a chemical bond.

Synthesizing and characterizing sodium silicate (Na_2SiO_3), silica gel, and carbonized husk (activated carbon) from rice husk-derived agro-waste has created data useful for the possible creation of small industries. Evaluation of the use of activated carbons from rice husks (RHAC) to control wastewater environmental pollution has been positive. This will create a low-cost solution to environmental pollution control. Proper and effective utilization of rice husks will lead to a cleaner environment, an improvement in the industrial sector, and offer employment to the youth in the rural areas thereby boosting the overall economic growth for the country.

5.2 Recommendations

5.2.1 Recommendations from this study

It is recommended farmers in Coast (Tana delta, Msambweni), Nyanza provinces (Ahero, West Kano, Migori and Kuria), Central (Mwea), Western (Bunyala), and other areas are made aware of these technologies of rice husk waste conversion to valuable green industrial chemicals. Small industrial centres can be set up locally to consume the mountains of rice husk wastes. The activity would also result in less air pollution in the areas. Local rice mills could use this technology to convert the rice

husks they generate to produce extra energy for their plants and earn income from the green industrial chemicals.

5.2.2 Areas of further studies

It is also recommended that studies be done in the following areas

1. Global air pollution continues to harm people's health and the environment. Indoor air pollution and its control are a major health concern. Silica gel and activated carbons have been used for removal of the indoor air pollutants. RHACs can be used for the removal of indoor air pollutants in the form of granules or fibers. Studies on the removal efficiency of RHACs as an indoor air purifier should be undertaken. It is recommended that studies on the use of RHACs in indoor and outdoor air pollution control be undertaken.
2. This study was limited to synthesizing rice husk-derived novel chemicals, there is a need to test the chemicals in field studies as well assess their use.
3. Rice husk (RH) can be a source for several silicon compounds, including silicon carbide, silica, silicon nitride, silicon tetrachloride, zeolite, and pure silicon (Sun et al., 2001). The applications of such materials derived from rice husks are many. It is recommended that studies on other novel products from rice husks be undertaken in Kenya.
4. Economic studies for feasible commercialization of the use of rice husks to produce novel chemicals is an area that needs to be studied.
5. Removal efficiencies and kinetics of removal of Priority Pollutants with RHACs were limited to lead (II), cadmium (II), and chromium (IV) metallic ions, other metallic priority pollutants should be included in an expanded study.

REFERENCES

Abdel, N., Hefny, M., & Chaghaby, G. (2007). Removal of lead from aqueous solution using low cost abundantly available adsorbents. *International Journal Environmental Science Technology, 1*, 67-73.

Abdo, M. (2002). *Environmental studies on Rosetta branch and some chemical applications at the area extends from El-Kanater-Khyria to Kafr El-Zyat City*. Ain Shams University, Faculty of Science. Cairo, 464pp, Egypt: unpublished. Retrieved March 20, 2018

Adam, F., & Iqbal, A. (2010). The oxidation of styrene by chromium-silica heterogeneous catalyst prepared from rice husk. *Chemical Engineering Journal,, 160*(2), 742-750.

Adam, F., Appaturi, J. N., & Iqbal, A. (2012). The utilization of rice husk silica as a catalyst: review and recent progress. *Catalysis Today, 190*(1), 2-14.

Afroze, S., Sen, T. K., & Ang, H. M. (2016). Adsorption removal of zinc (II) from aqueous phase by raw and base modified Eucalyptus sheathiana bark: Kinetics, mechanism and equilibrium study. *Process Safety and Environmental Protection,, 102*, 336-352.

Ahmaruzzaman, M., & Sharma, D. K. (2005). Adsorption of phenols from wastewater. *Journal of Colloid and Interface Science, 287*(1), 14-24.

Alalwan, H. A., Kadhom, M. A., & Alminshid, A. H. (2020). Removal of heavy metals from wastewater using agricultural byproducts. *Journal of Water Supply: Research and Technology-Aqua, 69*(2), 99-112.

Albert, P. J., Werhane, P., & Rolph, T. (2014). *Environmentally Sustainable Projects. In Global Poverty Alleviation: A Case Book ().* Dordrecht: Springer.

Aleixandre-Tudo, J. L., & Du Toit, W. (2018). The role of UV-visible spectroscopy for phenolic compounds quantification in winemaking. In *Frontiers and new trends in the science of fermented food and beverages* (pp. 1-21).

Allen, T. (2015). *Microscopy: a very short introduction* (Vol. Vol. 430). USA: Oxford University Press.

Alothman, Z. A. (2012). A review: fundamental aspects of silicate mesoporous materials. *Materials, 5*(12), 2874-2902.

Alweendo, S. T., Johnson, O. T., Shongwe, M. B., Kavishe, F. P., & Borode, J. O. (2019). Synthesis, optimization and characterization of silicon carbide (SiC) from rice husk. *Procedia Manufacturing, 35*, 962-967.

Anastas, P. T., & Warner, J. C. (1998). *Green chemistry.* Frontiers.

Andreola, F., Barbieri, L., & Lancellotti, I. (2020). The environmental friendly route to obtain sodium silicate solution from rice husk ash: a comparative study with commercial silicates deflocculating agents. *Waste and Biomass Valorization, 11*(11), 6295.

Anisuzzaman, S. M., Joseph, C. G., Taufiq-Yap, Y. H., Krishnaiah, D., & Tay, V. V. (2015). Modification of commercial activated carbon for the removal of 2, 4-dichlorophenol from simulated wastewater. *Journal of King Saud University-Science, 27*(4), 318-333.

AOAC. (2019). *Official Methods of Analysis, 21st Edition (2019).* Rockville, USA: AOAC International.

Asavapisit, S., & Ruengrit, N. (2005). The role of RHA-blended cement in stabilizing metal-containing wastes. *Cement and Concrete Composites, 27*(7-8), 782-787.

ASTM, D. (2009). 2854-09. Standard test method for apparent density of activated carbon. *ASTM Standard, 96*, 1-3.

Atera, E. A., Onyancha, F. N., & Majiwa, E. B. (2018). Production and marketing of rice in Kenya: Challenges and opportunities. *Journal of Development and Agricultural Economics,, 10*(3), 64-70.

Awika, J. M. (2011). Major cereal grains production and use around the world. In Advances in cereal science: implications to food processing and health promotion. *American Chemical Society*, 1-13.

Bailis, P. R., Ogle, D. N., From, D. S., Smith, K. R., Edwards, R., & Energy, H. (2007). *The water boiling test (WBT).* Berkeley, California: University of California-Berkeley.

Bajwa, D. S., Peterson, T., Sharma, N., Shojaeiarani, J., & Bajwa, S. G. (2018). A review of densified solid biomass for energy production. *Renewable and Sustainable Energy Reviews, 96*, 296-305.

Bakar, R. A., Yahya, R., & Gan, S. N. (2016). Production of high purity amorphous silica from rice husk. *Procedia chemistry, 19*, 189-195.

Balamurugan, M., & Saravanan, M. (2012). Producing Nano silica from Sorghum vulgare seed heads. *Powder Technology, 224*, 345-350.

Banerjee, S., Barman, S., & Halder, G. (2017). Sorptive elucidation of rice husk ash derived synthetic zeolite towards deionization of coalmine waste water: a comparative study. *Groundwater for Sustainable Development, 5*, 137-151.

Bank, R. K. (2009). *rice husks.* Los Baños, Philippines: International Rice Research Institute.

Basuki, B. (2015). Eco-efficiency and sustainable development as efforts to produce environmentally friendly product: an exploratory case study. *Issues in Social and Environmental Accounting, 9*(3), 199-218.

Beach, E. S., Cui, Z., & Anastas, P. T. (2009). Green Chemistry: A design framework for sustainability. *Energy & Environmental Science, 2*(10), 1038-1049.

Beagle, E. (1978). *Rice Husk Conversion to Energy.* FAO Agricultural Bulletin *31*.

Belonio, A. T. (2005). *Rice husk gas stove handbook.* (C. o. Department of Agricultural Engineering and Environmental Management, Ed.) Iloilo City, Philippines: Central Philippine University,.

Belonio, A. T., Ramos, J. A., Regalado, M. J., & Ocon, V. B. (2013). An Overview of the Downdraft Rice Husk Gasifier Technology for Thermal and Power Applications. *Journal of Technology Innovations in Renewable Energy, 2*(3), 246-258.

Bergqvist, M. M., Wårdh, S., Das, A., & Ahlgren, E. (2007). A techno-economic assessment of rice husk based heat and power generation in the mekong river delta of vietnam. *In Proceedings of the IGEC-III international, green energy conference.* Västerås, Sweden.

Berlin, M., Allen, J., Kailasam, V., Rosenberg, D., & Rosenberg, E. (2011). Nano porous silica polyamine composites for metal ion capture from rice hull ash. *Applied Organometallic Chemistry, 25*(7), 530-536.

Bie, R. S., Song, X. F., Liu, Q. Q., Ji, X. Y., & Chen, P. (2015). Studies on effects of burning conditions and rice husk ash (RHA) blending amount on the mechanical behavior of cement. *Cement and Concrete Composites, 55*, 162-168.

Bioenergiesysteme GmbH. (2017). *Basic process steps of a biomass gasification plant.* Graz, Austria. Retrieved march 2, 2017, from https://www.bios-bioenergy.at/index.php/en/technology-info/biomass-gasification

Blissett, R., Sommerville, R., Rowson, N., Jones, J., & Laughlin, B. (2017). Valorisation of rice husks using a TORBED® combustion process. *Fuel Processing Technology, 159*, 247-255.

Bogert, J. (2015). Choosing an X-Ray Fluorescence (XRF) Instrument Choosing an X-Ray. *Quality*, 15NDT.

Breeze, P. (2017). *Energy from waste.* Academic Press.

Brouwer, P. (2006). *Theory of XRF.* Almelo, Netherlands: PANalytical BV.

Brumitt, G. (2015). *Waste management: Appropriate technologies for developing countries (Ethiopia's case).* Addis Ababa: Addis Ababa University. Retrieved june 20, 2017, from https://slideplayer.com/slide/4018677/

Bryant, R., Proctor, A., Hawkridge, M., Jackson, A., Yeater, K., Counce, P., . . . Fjellstrom, R. (2011). Genetic variation and association mapping of silica concentration in rice hulls using a germplasm collection. *Genetica, 139*(11-12), 1383-1398.

Calvillo, C. F., Sánchez-Miralles, A., & Villar, J. (2016). Energy management and planning in smart cities. *Renewable and Sustainable Energy Reviews, 55*, 273-287.

Campbell, D. T., & Stanley, J. C. (2015). *Experimental and quasi-experimental designs for research.* Ravenio Books.

Carmona, V. B., Oliveira, R. M., Silva, W. T., Mattoso, L. H., & Marconcini, J. M. (2013). Nanosilica from rice husk: extraction and characterization. *Industrial Crops and Products, 43*, 291-296.

Casaca, C., & Costa, M. (2009). NOx control through reburning using biomass in a laboratory furnace: Effect of particle size. *Proceedings of the Combustion Institute, 32*(11), 2641–2648.

Chandrasekhar, S. A., Satyanarayana, K. G., Pramada, P. N., Raghavan, P., & Gupta, T. N. (2003). Review processing, properties and applications of reactive silica from rice husk—an overview. *Journal of materials science,, 38*(15), 3159-3168.

Chandrasekhar, S., & Pramada, P. N. (2006). Rice husk ash as an adsorbent for methylene blue—effect of ashing temperature. *Adsorption, 12*, 27-43.

Chandrasekhar, S., Pramada, P., & Praveen, L. (2005). Effect of organic acid treatment on the properties of rice husk silica. *Journal of material science, 40*, 6535–6544.

Chareonpanich, M., Nanta-Ngern, A., & Limtrakul, J. (2007). Short-period synthesis of ordered mesoporous silica SBA-15 using ultrasonic technique. *Materials Letters, 61*(29), 5153-5156.

Chen, G., Du, G., Ma, W., Yan, B., Wang, Z., & Gao, W. (2015). Production of amorphous rice husk ash in a 500 kW fluidized bed oxidation reactor. *Fuel, 144*, 214-221.

Chen, H. (2013). *Biogenic silica nanoparticles derived from rice husk biomass and their applications.*

Chen, H. R., Wang, W. X., Martin, J. C., Oliphant, A. J., Doerr, P. A., Xu, J. F., . . . Sun, L. Y. (2013). Extraction of Lignocellulose and Synthesis of Porous Silica Nanoparticles from Rice Husks: A Comprehensive Utilization of Rice Husk Biomass. *Acs Sustainable Chemistry & Engineering, , 1*(2), 254-259.

Chen, X.-G., Lv, S.-S., Zhang, P.-P., Zhang, L., & Ye, Y. .. (2011). Thermal destruction of rice hull in air and nitrogen: A systematic study. *Journal of thermal analysis and calorimetry, 104*(3), 1055-1062.

Chenier, P. J. (2012). *Survey of industrial chemistry.* Springer Science & Business Media.

Chiarakorn, S., Areerob, T., & Grisdanurak, N. (2007). Influence of functional silanes on hydrophobicity of MCM-41 synthesized from rice husk. *Science and Technology of Advanced Materials, 8*(1-2), 110-115.

Childs, N. (2019). *Rice outlook April 11, 2019.* New york, USA: USDA, Economic Research Service. Retrieved from https://downloads.usda.library.cornell .edu/usda-esmis/files/dn39x152w/9s161f273/37720m91r/rcs-19d.pdf

Christensen, L. B., Johnson, B., Turner, L. A., & Christensen, L. B. (2011). *Research methods, design, and analysis.*

Ciannamea, E. M., Marin, D. C., Ruseckaite, R. A., & Stefani, P. M. (2017). Particleboard based on rice husk: effect of binder content and processing conditions. *Journal of renewable materials, 5*(5), 357-362.

Coates, J. (2000). Encyclopedia of analytical chemistry. *Interpretation of infrared spectra, a practical approach. Wiley, Chichester*, 10815-10837.

Conradt, R., Pimkhaokham, P., & Leela-Adisorn, U. (1992). Nano-structured silica from rice husk. *Journal of non-crystalline solids, 145*, 75-79.

Contributors, W. C. (2020, May 5). ActivatedCharcoalPowder BrightField.jpg. *Wikimedia Commons, the free media repository*, p. 417429951. Retrieved from https://commons.wikimedia.org/w/index.php?title=File:ActivatedCharcoalPowder_BrightField.jpg&oldid=417429951

Creswell, J. W. (2014). *Qualitative, quantitative and mixed methods approaches.* Sage.

Danish, M., Naqvi, M., Farooq, U., & Naqvi, S. (2015). Characterization of South Asian Agricultural Residues for Potential Utilization in Future “energy mix.”. *In Energy Procedia, 75*, 2974–2980.

De Sousa, A. M., Visconte, L., Mansur, C., & Furtado, C. (2009). Silica sol obtained from rice husk ash. *Chemistry & chemical technology*, *3*(4).

Debnath, B., Haldar, D., & Purkait, M. K. (2021). Potential and sustainable utilization of tea waste: A review on present status and future trends. *Journal of Environmental Chemical Engineering*, 106179.

Deiana, C., Granados, D., Venturini, R., Amaya, A., Sergio, M., & Tancredi, N. (2008). Activated carbons obtained from rice husk: Influence of leaching on textural parameters. *Industrial and Engineering Chemistry Research., 47*(14), 4754–4757.

Della, V. P., Kühn, I., & Hotza, D. (2002). Rice husk ash as an alternate source for active silica production. *Materials letters, 57*(4), 818-821.

Demirbas, A. (2007). Combustion systems for biomass fuel. *Energy Sources Part A, 29*(4), 303-312.

Dey, K. P., Ghosh, S., & Naskar, M. K. (2013). Organic template-free synthesis of ZSM-5 zeolite particles using rice husk ash as silica source. *Ceramics International, 39*(2), 2153-2157.

Doorvasan, M., Sathiyamurthy, S., Jayabal, S., & Chidambaram, K. (2014). Moisture content of rice husk particulated natural fiber polymer composites. *OSR Journal of Mechanical and Civil Engineering, 24*, 17-21.

Durand-Morat, A., & Bairagi, S. (2021). International Rice Outlook: International Rice Baseline Projections 2020-2030.

Dutta, A. (2017). Fourier transform infrared spectroscopy. *Spectroscopic methods for nanomaterials characterization*, 73-93.

Ephantus, M., Robert, K., Nemoto, Y., & Njogu, P. (2016). *Energy Content Estimation in Waste Saw Dust, Maize Cobs and Rice Husks Using Multiple Regression Analysis.*

Farouq, R., & Yousef, N. S. (2015). Equilibrium and kinetics studies of adsorption of copper (II) ions on natural biosorbent. *International Journal of Chemical Engineering and Applications, 6*(5), 319.

Fernandes, I. J., Calheiro, D., Sánchez, F. A., Camacho, A. L., Rocha, T. L., Moraes, C. A., & Sousa, V. C. (2017). Characterization of silica produced from rice husk ash: comparison of purification and processing methods. *Materials research, 20*, 512-518.

Fidalgo, A., & Ilharco, L. M. (2001). The defect structure of sol–gel-derived silica/polytetrahydrofuran hybrid films by FTIR. *Journal of Non-Crystalline Solids, 283* (1-3), 144-154.

Foletto, E. L., Gratieri, E., Oliveira, L. H., & Jahn, S. L. (2006). Conversion of rice hull ash into soluble sodium silicate. *Materials Research, 9*(3), 335-338.

Gakungu, N. U. (2011). Solid Waste Management: a case study of Public Technical Training Institutions in Kenya. *Unpublished Doctoral dissertation, University of Nairobi, Kenya*.

Gewona, G. K. (2018). *Comparative Gasification Process Studies for Prosopis (P. Juliflora) and Rice Husks (Oryza Sp.) into Renewable Energy Resources in Kenya* (Unpublished Doctoral dissertation, JKUAT-IEET, Jomo Kenyatta University of agriculture and Technology, Kenya).

Gherasim, C. V., Cuhorka, J., & Mikulášek, P. (2013). Analysis of lead (II) retention from single salt and binary aqueous solutions by a polyamide nanofiltration membrane: Experimental results and modelling. *Journal of Membrane Science,, 436*, 132–144.

GOK. (2009). National Rice Development Strategic Plan (2008-2018). *Ministry of Agriculture, Nairobi*, Kenya.

GOK. (2013). National development plan vision 2030. *National Planning Commission, Nairobi*, Kenya.

Govorushko, S. M. (2013). Environmental problems of extraction, transportation, and use of fossil fuels. *Fossil fuels: sources, environmental concerns and waste management practices*, 1-84.

Greenwood, N. N., & Earnshaw, A. (1984). Chemistry of the Elements. Pergamon Press. Oxford. *Chap*, *10*, 435.

Grisdanurak, N., Chiarakorn, S., & Areerob, T. (2007). Influence of functional silanes on hydrophobicity of MCM-41 synthesized from rice husk. *Science and Technology of Advanced Materials*, *8*(1-2), 110.

Gu, S., Zhou, J., Luo, Z., Wang, Q., & Ni, M. (2013). A detailed study of the effects of pyrolysis temperature and feedstock particle size on the preparation of nanosilica from rice husk. *Industrial crops and products,*, *50*, 540-549.

Gummert, M., & Rickman, J. F. (2006). Rice: Drying. *International Rice Research*.

Guo, Y., Jiang, J. Q., Yang, S., Wang, Z., & Hongding, X. (2003). Performance of electrical double layer capacitors with porous carbons derived from rice husk. *Materials Chemistry and Physics*, *80*(3), 704-709.

Gupta, V. K., & Saleh, T. A. (2013). Sorption of pollutants by porous carbon, carbon nanotubes and fullerene-An overview. *Environmental Science and Pollution Research*, *20*(5), 2828-2843.

Gupta, V. K., Nayak, A., & Agarwal, S. (2015). Bio adsorbents for remediation of heavy metals: status and their future prospects. *Environmental Engineering Research*, *20*(1), 1-18.

Gyftopoulos, E. P. (2003). Cogeneration and wood/biomass fueled power sistems. *Combined Production of Heat and Power*, *12714*, 22.

Hadipramana, J., Riza, F. V., Rahman, I. A., Loon, L. Y., Adnan, S. H., & Zaidi, A. M. A. (2016, November). Pozzolanic characterization of waste Rice husk ash

(RHA) from Muar, Malaysia. In *IOP Conference Series: Materials Science and Engineering*, *160*(1), 012066..

Hamouda, A. A., & Amiri, H. A. (2014). Factors affecting alkaline sodium silicate gelation for in-depth reservoir profile modification. *Energies, 7*(2), 568-590.

Hanum, F., Bani, O., & Wirani, L. I. (2017). Characterization of activated carbon from rice husk by HCl activation and its application for Lead (Pb) removal in car battery wastewate. *In IOP Conference Series: Materials Science and Engineering. 180*(1), 012151

Haslinawati, M. M., Matori, K. A., Wahab, Z. A., Sidek, H. A., & Zainal, A. T. (2009). Effect of temperature on ceramic from rice husk ash. *International Journal of Basic Applied Science*, *9*(9), 111-117.

Hegazi, H. A. (2013). Removal of heavy metals from wastewater using agricultural and industrial wastes as adsorbents. *HBRC Journal, 9*(3), 276-282.

Hemalatha, M., Hemasruthi, P., Priya, S. G., Gayathri, N., & Kavinilavu, K. S. (2018). Formulation of Ecofriendly Detergent Powder Using Paddy Husk Ash. *Asian Journal of Applied Science and Technology (AJAST), 2*(4), 70-78.

Holleman, A. F., & Wiberg, E. (2001). *Inorganic Chemistry*. San Diego/Berlin: Academic Press/De Gruyter Wiberg, Nils (edition).

Hossain, M. S., Islam, M. R., Rahman, M. S., Kader, M. A., & Haniu, H. (2017). Biofuel from co-pyrolysis of solid tire waste and rice husk. *Energy Procedia*, *110*, 453-458.

Housecroft, C. E., & Constable, E. C. (2010). *Chemistry: an introduction to organic, inorganic and physical chemistry*. Pearson education.

Hubbe, M. A., Park, J., & Park, S. (2014). Cellulosic substrates for removal of pollutants from aqueous systems: A review. Part 4. Dissolved petrochemical compounds. *BioResources*, *9*(4), 7782-7925.

Ibrahem, S., & Ibrahem, H. (2014). Synthesis and study the effect of H2O/TEOS ratio of the silica xerogel by sol-gel method. *International Archive of Applied Sciences & Technology, 5*(1), 5.

Iler, K. R. (1979). *The chemistry of silica. Solubility, polymerization, colloid and surface properties and biochemistry of silica.* John Wiley and Sons Inc.

Inoue, Y., Sakai, M., Yao, Q., Tanimoto, Y., Toshima, H., & Hasegawa, M. (2013). Identification of a novel casbane-type diterpene phytoalexin, ent-10-oxodepressin, from rice leaves. *Bioscience, biotechnology, and biochemistry*, 120891.

Ismail, H., Nizam, J., & Abdul, H. (2001). The effect of a compatibilizer on the mechanical properties and mass swell of white rice husk ash filled natural rubber/linear low-density polyethylene blends. *Polymer Testing, 20*, 125-133.

Ismail, O., Urbanus, M., Murage, H., & Francis, O. (2016). Conversion of Rice Husks into an Energy Source through Gasification Technology. *International Journal of Science and Research (IJSR), 5*(9), 1264-1268.

James, J. O., & Rao, M. S. (1992). Rice-husk-ash cement. *A review. Journal of Scientific & Industrial Research (JSIR), 51*(5), 383-393.

Jang, H. T., Bhagiyalakshmi, M., Yun, L. J., & Anuradha, R. (2010). Utilization of rice husk ash as silica source for the synthesis of mesoporous silicas and their application to CO2adsorption through TREN/TEPA grafting. *Journal of Hazardous Materials, 175* (1-3), 928-938.

Jantzen, C. M., Brown, K. G., & Pickett, J. B. (2010). Durable glass for thousands of years. *International Journal of Applied Glass Science, 1*(1), 38-62.

Jayamani, E., Hamdan, S., Rahman, M. R., & Bakri, M. K. (2015). Study of sound absorption coefficients and characterization of rice straw stem fibers reinforced polypropylene composites. *BioResource, 10*(2), 3378-3392.

Jung, C. F., de Jesus Pacheco, D. A., Sporket, F., do Nascimento, C. A., & Ten Caten, C. S. (2020). Design from waste: A novel eco-efficient pyramidal microwave absorber using rice husks and medium density fibreboard residues. *Waste Management, 119*, 91-100.

Kabir, M. A., Shabbir, M. S. A., & Elahi, A. F. (2014). Feasibility Study on Power Generation in Bangladesh using Rice Husk as an Alternative Source of Fuel. In *International Conference on Mechanical, Industrial and Energy Engineering*.

Kakoi, B., Kaluli, J. W., Ndiba, P., & Thiong'o, G. (2016). Banana pith as a natural coagulant for polluted river water. *Ecological engineering*, *95*, 699-705.

Kalapathy, U., Proctor, A., & Shultz, J. (2000). A simple method for production of pure silica from rice hull ash. *Bioresource technology, 73*(3), 257-262.

Kalapathy, U., Proctor, A., & Shultz, J. (2002). An improved method for production of silica from rice hull ash. *Bio resource Technology 2, 85*(3), 285-289.

Kalderis, D., Bethanis, S., Paraskeva, P., & Diamadopoulos, E. (2008). Production of activated carbon from bagasse and rice husk by a single-stage chemical activation method at low retention times. *Bioresource Technology, 99*(15), 6809–6816.

Kang, S. H., Hong, S. G., & Moon, J. ,. (2019). The use of rice husk ash as reactive filler in ultra-high performance concrete. *Cement and Concrete Research, 115*, 389-400.

Kariuki, Z., Kiptoo, J., & Onyancha, D. (2017). Biosorption studies of lead and copper using Rogers mushroom biomass 'Lepiota hystrix. *South African Journal of Chemical Engineering, 23*, 62-70.

Kariuki, Z., Kiptoo, J., & Onyancha, D. (2017). Biosorption studies of lead and copper using rogers mushroom biomass 'Lepiota hystrix.'. *South African Journal of Chemical Engineering, 23*, 62-70.

Kaupp, A. (2013). *Gasification of rice hulls: theory and praxis*. Springer-Verlag.

Kealey, D., & Haines, P. J. (2004). *BIOS Instant Notes in Analytical Chemistry*. Taylor & Francis, Farnham, UK.

Kennedy, L., Vijaya, J., & Sekaran.G. (2005). Electrical conductivity study of porous carbon composite derived from rice husk. *Materials chemistry and physics, 91*(2-3), 471-476.

Khoshbin, R., Oruji, S., & Karimzadeh, R. (2018). Catalytic cracking of light naphtha over hierarchical ZSM-5 using rice husk ash as silica source in presence of ultrasound energy: Effect of carbon nanotube content. *Advanced Powder Technology, 29*(9), 2176.

Klunk, M. A., Das, M. D., Impiombato, A. N., Caetano, N. R., Wander, P. R., & Moraes, C. A. (2020). Comparative study using different external sources of aluminum on the zeolites synthesis from rice husk ash. *Materials Research Express, 7*(1), 015023.

Kołodyńska, D., Krukowska, J. A., & Thomas, P. (2017). Comparison of sorption and desorption studies of heavy metal ions from biochar and commercial active carbon. *Chemical Engineering Journal,, 307*, 353-363.

Kontor, S. (2013). *Potential of biomass gasification and combustion technology for small-and medium-scale applications in Ghana.* International Energy Technology and Management Program.

Kook, J. W., Choi, H. M., Kim, B. H., Ra, H. W., Yoon, S. J., Mun, T. Y., & Seo, M. W. (2016). Gasification and tar removal characteristics of rice husk in a bubbling fluidized bed reactor. *Fuel, 181*, 942-950.

Kowanga, K. D., Gatebe, E., Mauti, G. O., & Mauti, E. M. (2016). Kinetic, sorption isotherms, pseudo-first-order model and pseudo-second-order model studies of Cu (II) and Pb (II) using defatted Moringa oleifera seed powder. *The*

Journal of Phytopharmacology, 5(2), 71–78. Retrieved from http://www.phytopharmajournal.com.

Krishnarao, R. V., Subrahmanyam, J., & Kumar, T. J. (2001). Studies on the formation of black particles in rice husk silica ash. *Journal of the European Ceramic Society, 21*(1), 99-104.

Kshirsagar, M. P., & Kalamkar, V. R. (2014). A comprehensive review on biomass cookstoves and a systematic approach for modern cookstove design. *Renewable and Sustainable Energy Reviews, 30*, 580-603.

Kumagai, S., Shimizu, Y., Toida, Y., & Enda, Y. (2009). Removal of dibenzothiophenes in kerosene by adsorption on rice husk activated carbon. Fuel,. *Fuel, 88*(10), 1975-1982.

Kumar, A., & Jena, H. M. (2016). Preparation and characterization of high surface area activated carbon from Fox nut (Euryale ferox) shell by chemical activation with H3PO4. *Results in Physics, 6*, 651-658.

Kumar, A., Roy, A., Priyadarshinee, R., Sengupta, B., Malaviya, A., Dasguptamandal, D., & Mandal, T. (2017). Economic and sustainable management of wastes from rice industry: combating the potential threats. *Environmental Science and Pollution Research, 24*(34), 26279-26296.

Kungu, Raphael & Njogu, Paul & Kinyua, Robert. (2019). Development of Novel Products from Agro-Wastes (Rice Husks) and Characterization in Kenya. *Journal of Environmental Science and Engineering A. 8*.

Kungu, R., Njogu, P., Kinyua, R., & Kiptoo, J. (2019). Green Chemistry Preparation and Characterization of Rice Husk Derived Silica Gel in Kenya. Journal of Environmental Science and Engineering A.

Kurama, H., & Kurama, S. K. (2003). The effect of chemical treatment on the production of active silica from rice husk. In *18th international mining congress and exhibition of Turkey-IMCET* (pp. 431-435).

Lata, S., & Samadder, S. (2014). Removal of heavy metals using rice husk: a review. *International Journal of Environmental Research and Development, 4*(2), 165-170.

Le Van, K., & Thi, T. T. (2014). Activated carbon derived from rice husk by NaOH activation and its application in supercapacitor. *Progress in natural science: materials international, 24*(3), 191-198.

Li, D. W., Chen, D. Y., & Zhu, X. F. (2011). Reduction in time required for synthesis of high specific surface area silica from pyrolyzed rice husk by precipitation at low pH. *Bio resource Technology*, *102*(13), 7001-7003.

Lima, S. P., Vasconcelos, R. P., Paiva, O. A., Cordeiro, G. C., Chaves, M. R., Toledo Filho, R. D., & Fairbairn, E. D. (2011). Production of silica gel from residual rice husk ash. *Química Nova, 34*(1), 71-75.

Liou, T. H., & Wu, S. J. (2009). Characteristics of microporous/mesoporous carbons prepared from rice husk under base- and acid-treated conditions. *Journal of Hazardous Materials, 171*(1-3), 693–703 .

Liou, T. H., & Yang, C. C. (2011). Synthesis and surface characteristics of nanosilica produced from alkali-extracted rice husk ash. *Materials Science and Engineering B , 176*(7), 521-529.

Liu, B., Gu, J., & Zhou, J. (2016). High Surface Area Rice Husk-Based Activated Carbon Prepared by Chemical Activation with ZnCl2-CuCl2 Composite Activator. *Environmental Progress & Sustainable Energy, 35*(1), 133–140.

Liu, Z., Zhu, J., Wakihara, T., & Okubo, T. (2019). Ultrafast synthesis of zeolites: breakthrough, progress and perspective. *Inorganic Chemistry Frontiers, 6*(1), 14-31.

Lu, Y., Song, S., Wang, R., Liu, Z., Meng, J., Sweetman, A. J., . . . Wang, T. (2015). Impacts of soil and water pollution on food safety and health risks in China. *Environment International, 77*, 5-15.

Lubis, H. (2018). Renewable Energy of Rice Husk for Reducing Fossil Energy in Indonesia. *Advanced Research in Applied Sciences and Engineering Technology, 11*(1), 17-22.

Luo, Y., Guo, W., Ngo, H. H., Nghiem, L. D., Hai, F. I., Zhang, J., & Wang, X. C. (2014). A review on the occurrence of micro pollutants in the aquatic environment and their fate and removal during wastewater treatment. *Science of the Total Environment, 473*, 619-641.

Ma, X., Zhou, B., Gao, W., Qu, Y., Wang, L., Wang, Z., & Zhu, Y. (2012). A recyclable method for production of pure silica from rice hull ash. *Powder Technology, 217*, 497-501.

Ma, X., Zhou, B., Gao, W., Qu, Y., Wang, L., Wang, Z., & Zhu, Y. (2012). A recyclable method for production of pure silica from rice hull ash. *Powder Technology, 217*, 497-501.

Macchiarola, K., Koenig, U., Gobbo, L., Campbell, I., McDonald, A. M., & Cirelli, J. (2007). Modern x-ray diffraction techniques for exploration and analysis of ore bodies. *International 5th. December. International Conference 0f Minerals Exploration*, (pp. 1007-11).

Maghanga, J. K., Segor, F. K., Etiégni, L., & Lusweti, J. (2009). Electrocoagulation method for colour removal in tea effluent: A case study of Chemomi tea factory in rift valley, Kenya. *Bulletin of the chemical society of Ethiopia, 23*(3).

Mahmud, A., Megat-Yusoff, P., Ahmad, F., & Farezzuan, A. (2016). Acid leaching as efficient chemical treatment for rice husk in production of amorphous silica nanoparticles. *ARPN Journal of Engineering Applied Science., 11*, 13384–13388.

Maiti, S., Banerjee, P., Purakayastha, S., & Ghosh, B. (2008). Silicon–doped carbon semiconductor from rice husk char. *Materials chemistry and physics, 109*(1), 169-173.

Majiwa, E. L. (2018). A network data envelopment analysis (NDEA) model of post-harvest handling: the case of Kenya's rice processing industry. *Food Security,, 10*(3), 631-648.

Manjuladevi, M., Anitha, R., & Manonmani, S. (2018). Kinetic study on adsorption of Cr (VI), Ni (II), Cd (II) and Pb (II) ions from aqueous solutions using activated carbon prepared from Cucumis melo peel. *Applied water science, 8*(1), 1-8.

Manocha, S. M. (2003). Porous carbons. *Sadhana, 28*(1-2), 335-348.

Mansary, K. G., & Ghaly, A. E. (1997). Physical and Thermochemical Properties of Rice Husk. *Energy Sources, 19*(9), 989–1004.

Maremeni, L. C., Modise, S. J., Mtunzi, F. M., Klink, M. J., & Pakade, V. E. (2018). Adsorptive Removal of Hexavalent Chromium by Diphenylcarbazide-Grafted Macadamia Nutshell Powder. *Bioinorganic Chemistry and Applications,, 2018*(i).

Marrugo, G., Valdés, C. F., & Chejne, F. (2016). Characterization of Colombian agroindustrial biomass residues as energy resources. *Energy & Fuels, 30*(10), 8386-8398.

Marsh, H. (2006). Activated carbon/Marsh H., Rodriguez-Reinoso F. *Amsterdam: Eslevier, 542*.

Martin, K. R. (2007). The chemistry of silica and its potential health benefits. *Journal of Nutrition Health & Aging, 11*(2), 94-98.

Masoud, M. S., El-Saraf, W. M., Abdel-Halim, A. M., Ali, A. E., Mohamed, E. A., & Hasan, H. M. (2016). Rice husk and activated carbon for waste water treatment of El-Mex Bay, Alexandria Coast, Egypt. *Arabian Journal of Chemistry, 9*, S1590-S1596.

Menya, E., Olupot, P. W., Storz, H., Lubwama, M., & Kiros, Y. (2018). Production and performance of activated carbon from rice husks for removal of natural organic matter from water: a review. *Chemical Engineering Research and Design*, *129*, 271-296.

Mhilu, C. F. (2014). Analysis of Energy Characteristics of Rice and Coffee Husks Blends. *ISRN Chemical Engineering*, *1*, 1-6.

Mishra, P. C., & Patel, R. K. (2009). Removal of lead and zinc ions from water by low cost adsorbents. *Journal of Hazardous Materials,*, *168*(1), 319–325.

Mohamed, R. M., Mkhalid, I. A., & Barakat, M. A. (2015). Rice husk ash as a renewable source for the production of zeolite NaY and its characterization. *Arabian Journal of Chemistry*, *8*(1), 48-53.

Mohanty, A. K., Misra, M. A., & Hinrichsen, G. I. (2000). Biofibres, biodegradable polymers and biocomposites: An overview. *Macromolecular materials and Engineering*, *276*(1), 1-24.

Mohanty, K., Naidu, J. T., Meikap, B. C., & Biswas, M. N. (2006). Removal of crystal violet from wastewater by activated carbons prepared from rice husk. *Industrial & engineering chemistry research*, *45*(14), 5165-5171.

Moraes, C. A., Fernandes, I. J., Calheiro, D., Kieling, A. G., Brehm, F. A., Rigon, M. R., & Osorio, E. (2014). Review of the rice production cycle: By-products and the main applications focusing on rice husk combustion and ash recycling. *Waste Management & Research*, *32*(11), 1034-1048.

Moussout, H., Ahlafi, H., Aazza, M., & Maghat, H. (2018). Critical of linear and nonlinear equations of pseudo-first order and pseudo-second order kinetic models. *Karbala International Journal of Modern Science*, *4*(2), 244-254.

Muniandy, L., Adam, F., Mohamed, A. R., & Ng, E. P. (2014). The synthesis and characterization of high purity mixed microporous/mesoporous activated

carbon from rice husk using chemical activation with NaOH and KOH. *Microporous and Mesoporous Materials, 197*, 316-323.

Nagrale, S. D., Hajare, H., & Modak, P. R. (2012). Utilization of rice husk ash. *Carbon, 2*(6), 42.

Naqvi, S. R., Uemura, Y., Osman, N., & Yusup, S. (2015). Production and Evaluation of Physicochemical Characteristics of Paddy Husk Bio-char for its C Sequestration Applications. *Bioenergy Research, 8*(4), 1800-1809.

Nayak, A., & Bhushan, B. (2019). An overview of the recent trends on the waste valorization techniques for food wastes. *Journal of environmental management, 233*, 352-370.

Ndazi, B., Karlsson, S., Tesha, J., & Nyahumwa, C. (2007). Chemical and physical modifications of rice husks for use as composite panels. *Composites Part A: applied science and manufacturing, 38*(3), 925-935.

Nematollahi, B., Sanjayan, J., & Shaikh, F. U. (2015). Synthesis of heat and ambient cured one-part geopolymer mixes with different grades of sodium silicate. *Ceramics International*, *41*(4), 5696-5704.

Nethaji, S., Sivasamy, A., & Mandal, A. B. (2013). Preparation and characterization of corn cob activated carbon coated with nano-sized magnetite particles for the removal of Cr (VI). *Bioresource technology, 134*, 94-100.

Njogu, P., Kinyua, R., Muthoni, P., & Nemoto, Y. (2015). Thermal Gasification of Rice Husks from Rice Growing Areas in Mwea, Embu County, Kenya. *Smart Grid and Renewable energy*, 113-119. doi:10.4236/sgre.2015.65010. Accessed 20 March 2018

Nwidu, L. L., Oveh, B., Okoriye, T., & Vaikosen, N. A. (2008). Assesment of the water quality and prevalence of water borne diseases in Amassoma, Niger Delta, Nigeria. *African Journal of Biotechnology, 7*(17).

Oladejo, J., Shi, K., Luo, X., Yang, G., & Wu, T. (2019). A review of sludge-to-energy recovery methods. *Energie, 12*(1), 60.

Olupot, P. W., Candia, A., Menya, E., & Walozi, R. (2016). Characterization of rice husk varieties in Uganda for biofuels and their techno-economic feasibility in gasification. *Chemical Engineering Research and Design, 107*, 63–72.

Ong, S. T., Ha, S. T., Keng, P. S., Lee, C. K., & Hung, Y. T. (2012). Removal of dyes from wastewaters by low-cost adsorbents. 929-977.

Otieno, D. O., Kumar, A., Onyango, M. S., & Aoyi, O. (2014). Treatment of Tea Industry Wastewater Using a Combined Adsorption and Advanced Oxidation Process. *International Proceedings of Sustainable Research and Innovation Conference.*, (pp. 100-103).

Pakade, V. E., Ntuli, T. D., & Ofomaja, A. E. (2017). Biosorption of hexavalent chromium from aqueous solutions by Macadamia nutshell powder. *Applied Water Science, 7*(6), 3015-3030.

Pandey, S., & Ramontja, J. (2016). Turning to nanotechnology for water pollution control: applications of nanocomposites. *Focus On Medical Sciences Journal, 2*(3).

Patil, R., Dongre, R., & Meshram, J. (2014). Preparation of silica powder from rice husk. *Journal of Applied Chemistry, 27*, 26-29.

Patwardhan, S. V., Maheshwari, R., Mukherjee, N., Kiick, K. L., & Clarson, S. J. (2006). Conformation and assembly of polypeptide scaffolds in templating the synthesis of silica: an example of a polylysine macromolecular “switch”. *Biomacromolecules,, 7*(2), 491-497.

Pijarn, N., Jaroenworaluck, A., Sunsaneeyametha, W., & Stevens, R. (2010). Synthesis and characterization of nanosized-silica gels formed under controlled conditions. *Powder Technology, 203*(3), 462-468.

Pode, R. (.-1. (2016). Potential applications of rice husk ash waste from rice husk biomass power plant. *Renewable and Sustainable Energy Reviews, 53*, 1468-1485.

Prakash, P., & Sheeba, K. N. (2016). Prediction of pyrolysis and gasification characteristics of different biomass from their physico-chemical properties. *Energy Sources, Part A: Recovery, Utilization, and Environmental Effects, 38*(11), 1530-1536.

Prasad, R., & Pandey, M. (2012). Rice husk ash as a renewable source for the production of value added silica gel and its application: an overview. *Bulletin of Chemical Reaction Engineering and Catalysis, 7*(1), 1-25.

Radi, S., Basbas, N., Tighadouini, S., & Bacquet, M. (2014). New polysiloxane surfaces modified with ortho-, meta-or para-nitrophenyl receptors for copper adsorption. *Journal of Surface Engineered Materials and Advanced Technology, 4*, 21-28.

Rao, B., Dalinaidu, A., & Singh, D. (2017). Accelerated diffusion test on the intact rock mass. *Journal of Testing and Evaluation, 35*(2), 111-117.

Rasmey, A. H., Aboseidah, A. A., & Youssef, A. K. (2018). Application of Langmuir and Freundlich Isotherm Models on Biosorption of Pb2+ by Freez-dried Biomass of Pseudomonas aeruginosa. *Egyptian Journal of Microbiology, 53*(1), 37-48.

Razmovski, R., & Šćiban, M. (2008). Biosorption of Cr (VI) and Cu (II) by waste tea fungal biomass. *Ecological Engineering, 34*(2), 179-186.

Real, C., Alcala, M. D., & Criado, J. M. (2006). Preparation of silica from rice husks. *Journal of the American Ceramic Society, 79*(8), 2012-2016.

Reichenauer, G., & Scherer, G. W. (2001). Extracting the pore size distribution of compliant materials from nitrogen adsorption. *Colloids and Surfaces A: Physicochemical and Engineering Aspects, 187*, 41-50.

Riffat, S., Hanley, N., Pavel, C. E., Pullin, A. S., Van Leeuwen, C. J., & Xu, Y. (2016). Environmental Pollution and Control. *Environmental Pollution and Control, 314*.

Rivera-Muñoz, E. (2011). Hydroxyapatite-based materials: synthesis and characterization. *Biomedical Engineering-Frontiers and Challenges*, 75-98.

Riveros, H., & Garza, C. (1986). Rice husks as a source of high purity silica. *Journal of Crystal Growth, 75*(1), 126-131.

Rozainee, M., Ngo, A., Salema, K., Tan, M. S., & Zainura, Z. (2008). Effect of fluidising velocity on the combustion of rice husk in a bench-scale fluidised bed oxidation reactor for the production of amorphous rice husk ash. *Bioresource Technology*, *99*(4), 703-713.

RRI. (2014). *The Knowledge Bank: Milling -By products.* Retrieved 2 June, 2016, from http://www.knowledgebank.irri.org/step-by-step-production/

Sadeek, S. A., Negm, N. A., Hefni, H. H., & Wahab, M. M. (2015). Metal adsorption by agricultural biosorbents: adsorption isotherm, kinetic and biosorbents chemical structures. *International journal of biological macromolecules, 81*, 400-409.

Sahu, A., & Chatterjee Mitra, J. (2018). C. Preparation of Thermo-Modified Tea waste and Its Use to Study the Heavy Metal Adsorption from Waste Water. *IOSR Journal of Applied Chemistry (IOSR-JAC), 11*(7), 40-46.

Salavati-Niasari, M., Javidi, J., & Dadkhah, M. (2013). Ball milling synthesis of silica nanoparticle from rice husk ash for drug delivery application. Combinatorial chemistry & high throughput screening. *National Library of Medicine, 16*(6), 458-462.

Sankar, S., Sharma, S. K., Kaur, N., Lee, B., Kim, D. Y., Lee, S., & Jung, H. (2016). Biogenerated silica nanoparticles synthesized from sticky, red, and brown

rice husk ashes by a chemical method. *Ceramics International, 42*(4), 4875-4885.

Santiaguel, A. F. (2013). A second life for rice husk. Rice Today,. *12*(2), 12-13.

Seck, P. A.-2. (2012). Crops that feed the world. *Rice. Food security, 4*(1), 7-24.

Selvakumar, K. V., Umesh, A., Ezhilkumar, P., Gayatri, S., Vinith, P., & Vignesh, V. (2014). Extraction of silica from burnt paddy husk. *International Journal of ChemTech Research, 6*(9), 4455-4459.

Sereda, L., López-González, M. M., Visconte, L. L., Nunes, R. C., Furtado, C. R., & Riande, E. (2003). Influence of silica and black rice husk ash fillers on the diffusivity and solubility of gases in silicone rubbers. *Polymer, 44*(10), 3085-3093.

Shamsollahi, Z., & Partovinia, A. (2019). Recent advances on pollutants removal by rice husk as a bio-based adsorbent: A critical review. *Journal of environmental management, 246*, 314-323.

Shanmugavalli, R., Madhavakrishnan, S., Kadirvelu, K., Rasappan, K., Mohanraj, R., & Pattabhi, S. (2007). Adsorption studies on removal of Cr (VI) from aqueous solution using silk cotton hull carbon. *J. Industrial Pollution Control,, 23*(1), 65-72.

Sharif, S. (2018). *Fabrication of water glass adhesive silicate from amorphous silica of rice husk ASH.*

Shen, J., Liu, X., Zhu, S., Zhang, H., & Tan, J. (2011). Effects of calcination parameters on the silica phase of original and leached rice husk ash. *Materials Letters, 65*(8), 1179-1183.

Shen, Y. (2018). Rice Husk-Derived Activated Carbons for Adsorption of Phenolic Compounds in Water. *Global Challenges, 2*(12), 1800043.

Shen, Y., Zhao, P., & Shao, Q. (2014). Porous silica and carbon derived materials from rice husk pyrolysis char. *Microporous and Mesoporous Materials*, *188*, 46-76.

Simonin, J. P. (2016). On the comparison of pseudo-first order and pseudo-second order rate laws in the modeling of adsorption kinetics. *Chemical Engineering Journal*, *300*, 254-263.

Singh, R., Srivastava, P., Singh, P., Sharma, A. K., Singh, H., & Raghubanshi, A. S. (2019). Impact of rice-husk ash on the soil biophysical and agronomic parameters of wheat crop under a dry tropical ecosystem. *Ecological indicators*, *105*, 505-515.

Singh, V. K., Solanki, P., Ghosh, A., & Pal, A. (2020). Solid Waste Management and Policies Toward Sustainable Agriculture. Sustainability through Circular Economy. *Handbook of Solid Waste Management*, 1-22.

Singhania, R. R., Agarwal, R. A., Kumar, R. P., & Sukumaran, R. K. (Eds.). (2017). *Waste to wealth*. Springer.

Siqueira, E., Yoshida, I., Pardini, L., & Schiavon, M. (2009). Preparation and characterization of ceramic composites derived from rice husk ash and polysiloxane. *Ceramics international*, *35*(1), 213-220.

Skorbiansky, S. R. (2018). Rice Outlook. *Economic Research Service*, 1-33.

Sluiter, A., Hames, B., Ruiz, R., Scarlata, C., Sluiter, J., & Templeton, D. (2008). Determination of Ash in Biomass (Technical Report No. NREL/TP-510-42622). *Golden, CO: National Renewable Energy Laboratory*, 1-8.

Soltani, N., Bahrami, A., Pech-Canul, M. I., & González, L. A. (2015). Review on the physicochemical treatments of rice husk for production of advanced materials. *Chemical engineering journal*, *264*, 899-935.

Sridhar, G., Sridhar, H. V., Dasappa, S., Paul, P. J., Rajan, N. K., & Mukunda, H. S. (2005). Development of producer gas engines. *Proceedings of the Institution of Mechanical Engineers, Part D:, 219*, pp. 423-438.

Stavland, A., Jonsbråten, H. C., Vikane, O., Skrettingland, K., & Fischer, H. (2011). In-depth water diversion using sodium silicate–Preparation for single well field pilot on Snorre. *In IOR 2011-16th European Symposium on Improved Oil Recovery* (p. 230). European Association of Geoscientists & Engineers.

Stosnach, H. (2006). On-site analysis of heavy metal contaminated areas by means of total reflection X-ray fluorescence analysis (TXRF). *Spectrochimica Acta Part B: Atomic Spectroscopy, 61*(10-11), 1141-1145.

Sun, L., & Gong, K. (2001). Sil Sun, L., & Gong, K. (2001). Silicon-based materials from rice husks and their applications. *Industrial & engineering chemistry research, 40*(25), 5861-5877.

Suvarnakuta, P., & Suwannakuta, P. (2006). Biomass cooking stove for sustainable energy and environment. *In The 2nd Joint International Conference on "Sustainable Energy and Environment (SEE 2006)",* (pp. 1-5). Bangkok, Thailand.

Szymańska, E., Gerretzen, J., Engel, J., Geurts, B., Blanchet, L., & Buydens, L. M. (2015). Chemometrics and qualitative analysis have a vibrant relationship. *TrAC Trends in Analytical Chemistry, 69*, 34-51.

Taha, A. W., Dakroury, A. M., El-Sayed, G. O., & El-Salam, S. A. (2010). Assessment removal of heavy metals ions from wastewater by cement kiln dust (CKD). *Journal of American Science, 6*(12), 910-917.

Todkar, B. S., Deorukhkar, O. A., & Deshmukh, S. M. (2016). Extraction of silica from rice husks. *International Journal of Engineering Research and Development, 12*(3), 69-74.

Toniazzo, L., Fierro, V., Braghiroli, F., Amaral, G., & Celzard, A. (2013). Biosorption of model pollutants in liquid phase on raw and modified rice husks. *Journal of Physics: Conference series, 416*, 12026.

Treviño-Cordero, H.-A. L., Mendoza-Castillo, D. I., Hernández-Montoya, V., Bonilla-Petriciolet, A., & Montes-Morán, M. A. (2013). Synthesis and adsorption properties of activated carbons from biomass of Prunus domestica and Jacaranda mimosifolia for the removal of heavy metals and dyes from water. *Industrial Crops and Products,, 42*, 315-323.

Ugheoke, B. I., Mamat, O., & Ari-Wahjoedi, B. (2013). A direct comparison of processing methods of high purity rice husk silica. *Asian Journal of Scientific Research*, *6*(3), 573-580.

Ugheoke, I. B., & Mamat, O. (2012). A critical assessment and new research directions of rice husk silica processing methods and properties. *Maejo international journal of science and technology*, *6*(3), 430.

Uhrlandt, S. (2006). Silica in Kirk-Othmer Encyclopedia of Chemical Technology. *John Wiley & Sons, Inc.: Hoboken, New Jersey*, *22*, 365-379.

Umeda, J., & Kondoh, K. (2008). High-purity amorphous silica originated in rice husks via carboxylic acid leaching process. *Journal of materials science, 43*(22), 7084-7090.

Umeda, J., & Kondoh, K. (2010). High-purification of amorphous silica originated from rice husks by combination of polysaccharide hydrolysis and metallic impurities removal. *Industrial crops and products, 32*(3), 539-544.

Van Nguyen, N., & Ferrero, A. (2006). Meeting the challenges of global rice production.

Viswanathan, B., Neel, P. I., & Varadarajan, T. K. (2009). Methods of activation and specific applications of carbon materials. *India, Chennai*.

Wang, J., & Zhuang, S. (2017). Removal of various pollutants from water and wastewater by modified chitosan adsorbents. *Critical Reviews in Environmental Science and Technology*, *47*(23), 2331-2386.

Wang, X., Ouyang, Y., Li, X., Wang, H., Guo, J., & Dai, H. (2008). Room-temperature all-semiconducting sub-10-nm graphene nanoribbon field-effect transistors. *Physical review letters*, *100*(20), 206803.

Wanja, D. W., Mbuthia, P. G., Waruiru, R. M., Mwadime, J. M., Bebora, L. C., Nyaga, P. N., & Ngowi, H. A. (2019). Bacterial pathogens isolated from farmed fish and source pond water in Kirinyaga County, Kenya. *International Journal of Fisheries and Aquatic Studies*, *7*(2), 34-39.

Wannapeera, J., Worasuwannarak, N., & Pipatmanomai, S. (2008). Product yields and characteristics of rice husk , rice straw and corncob during fast pyrolysis in a drop-tube/fixed-bed reactor. *Songklanakarin Journal Science and Technology.*, *30*(3), 393–404.

Waswa-Sabuni, B., Syagga, P. M., Dulo, S. O., & Kamau, G. N. (2003). Rice husk ash cement–an alternative pozzolana cement for Kenyan building industry. *Journal of civil Engineering, JKUAT, 8*, 13-16.

Yalcin, N., & Sevinc, V. (2001). Studies on silica obtained from rice husk. *Ceramics International*, *27*(2), 219-224.

Yuvakkumar, R., Elango, V., Rajendran, V., & Kannan, N. (2014). High-purity nano silica powder from rice husk using a simple chemical method. *Journal of experimental nanoscience*, *9*(3), 272-281.

Zemnukhova, L. A., & Nikolenko, Y. M. (2011). Study by X-ray photoelectron spectroscopy of rice husk and the products of its processing. *Russian Journal of General Chemistry*, *81*(4), 694-700.

Zhao, Q. J., Tao, R., Yam, A., Mok, R., & Song, C. (2008). Biodegradation behavior of polycaprolactone/rice husk ecocomposites in simulated soil medium. *Polymer Degradation and Stability*, *93*(8), 1571-1576.

APPENDICES

Appendix I: Process patent application

FORM IP 4

Regulation 12

THE INDUSTRIAL PROPERTY ACT, 2001

The Managing Director,

Kenya Industrial Property Institute.

STATEMENT JUSTIFYING APPLICANT'S RIGHT TO PATENT/ UTILITY MODEL CERTIFICATE

Name and address of applicant(s)	**Jomo Kenyatta University of Agriculture and Technology** **P.O Box 62000-00200, Nairobi, Kenya** **Tel:** 067-22124/5202 **Ext. 2319** or **4062** dipuil@jkuat.ac.ke
Name and address of agent (if any)	**N/A**
Title of invention	**System and Process for Production of sodium silicate, Silica gel and Activated carbon from Waste rice husks.**

The derivation of my/our right to be granted a patent upon the said application is as follows-

(iii) We consent to the publication of the details contained herein to each of the inventors named above.

Dated at **Juja** this **28th day** of **June, 2017**.....

Applicant's Signature .....……

Appendix II: Fabrication method

1. Cut 2 flat bar length 500, Cut 2 flat bar length 270, Cut 45^{o} at the ends of each and join the corners

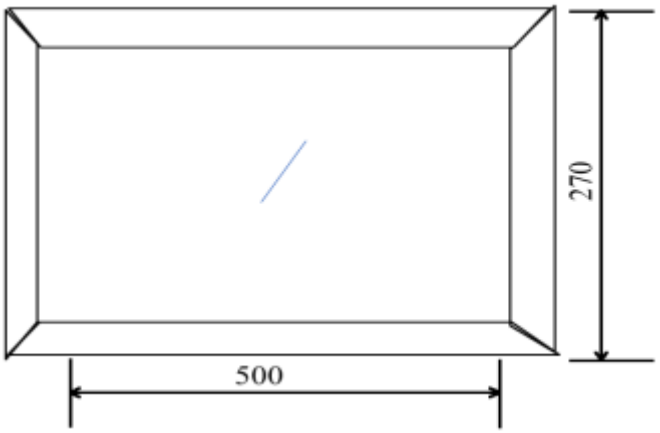

2. Weld a sieve inside the formed framework for allowing air into the stove.

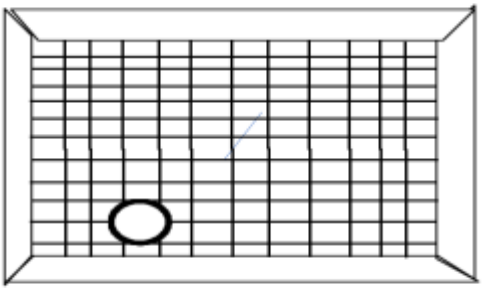

3. Weld made part of onto front of drawer

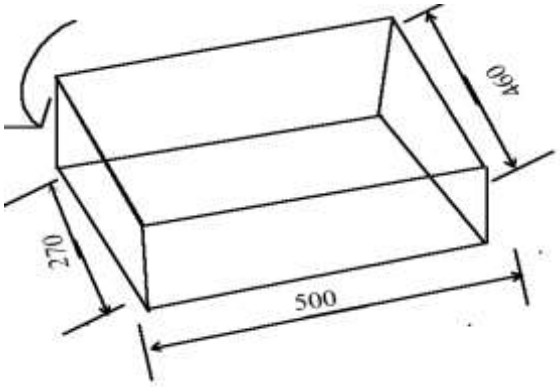

4. Make a hole for blowpipe filling into the stove e.g. welding a 450mm thick pipe at bottom of front sieve.
5. Place a 240 at the Center of cover plate and would it on the cover, Weld in a 44mm hole sieve below cylinder

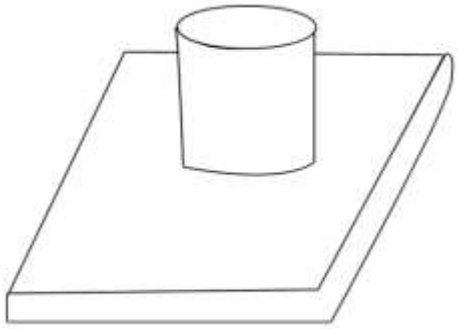

6. Weld a hole pipe at the center of the sieve. Place a 300-cylinder connectivity around the 240 cylinder and weld it all around. Place folded cortex on made framework. Pour refractory material between both cylinders

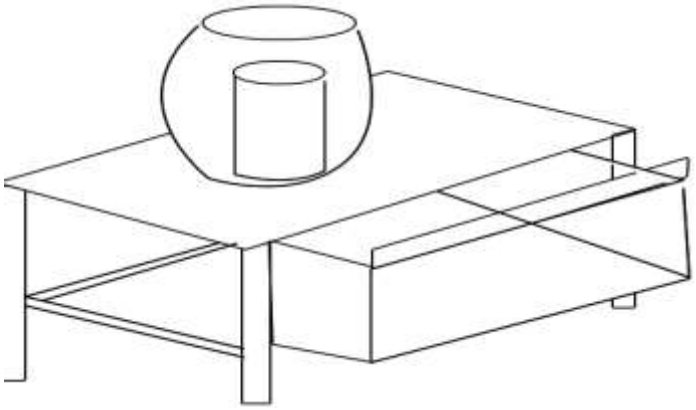

7. Do painting and testing of the stove

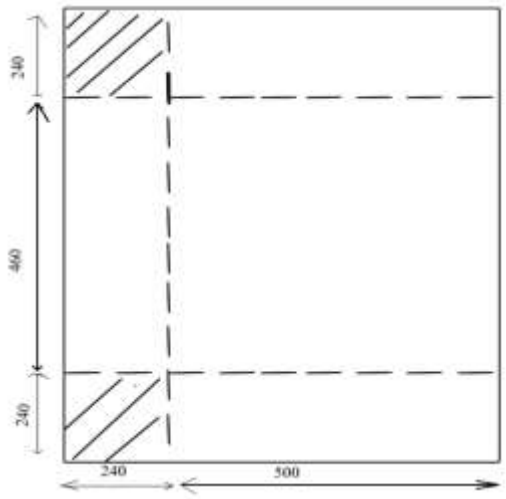

8. Knock and cut the two corners, Fold the sheet along material lines

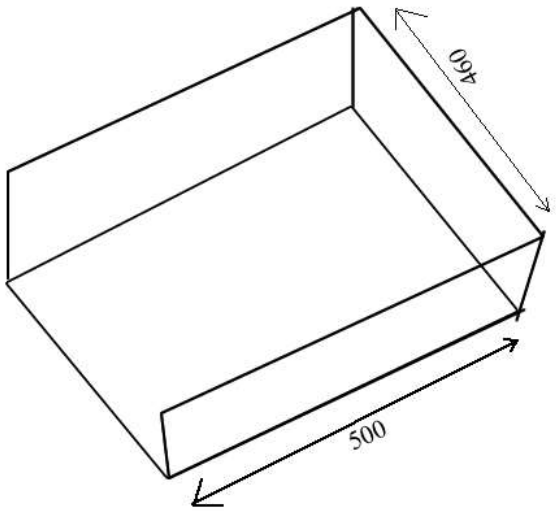

9. Join the corners by welding

10. Weld the four flats 30mm from the bottom of the stands

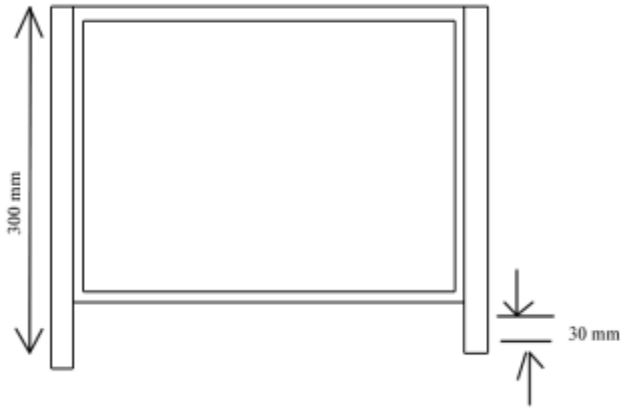

11. Cut sheets measuring 500x270 and weld them on sides of the stove.

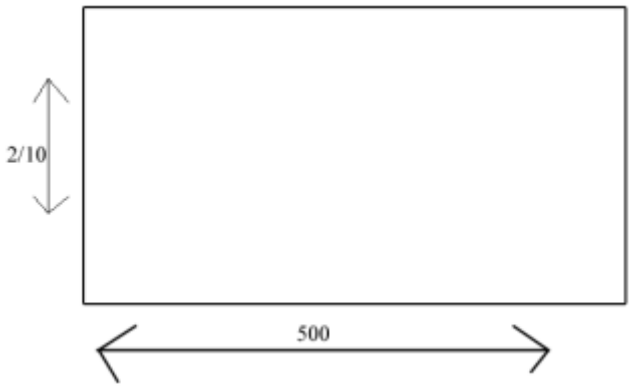

12. Cut a sheet measuring 940x 740 and mark out folding lines.

13. Weld the joint to form a cylinder

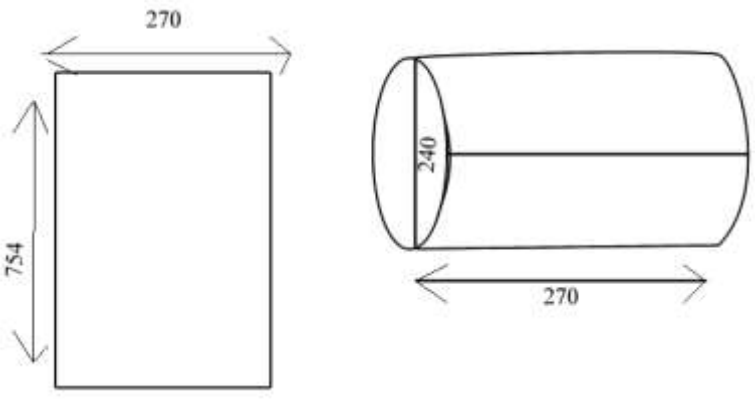

14. Cut a sheet measuring 943x300

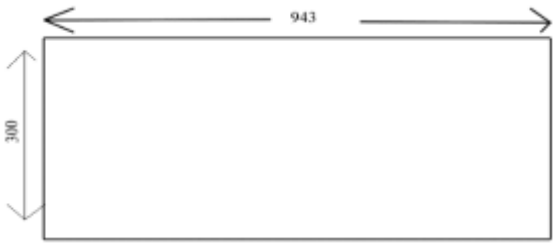

15. Roll it to form a cylinder

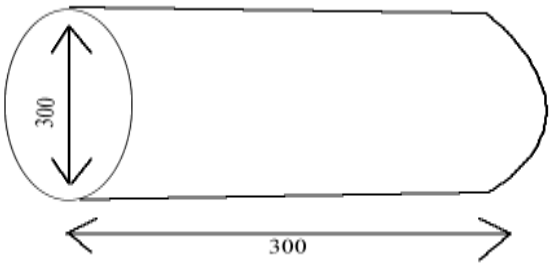

16. Cut two pieces of flat bar length

17. Weld 30m grooves each

18. Cut the center of each flat bar 500x500

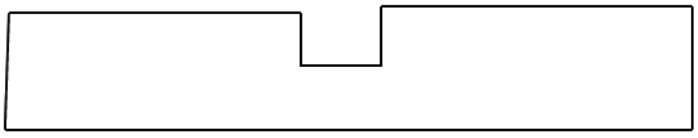

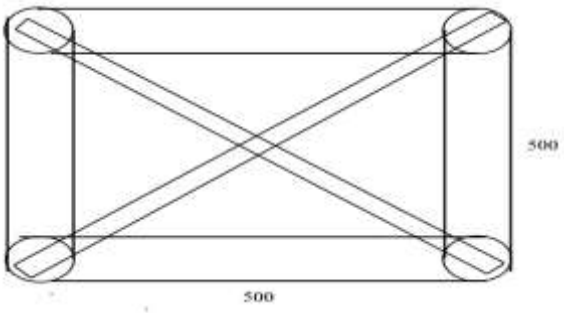

19. Weld the flat bars to corners of slotted round pipe.

20. Weld the centers of flat bars where they meet each other.

21. Cut 4 pieces of flat bars, of length 480mm

Appendix III: KEBS laboratory results

Kenya Bureau of Standards
Standards for Quality life

Fax: +254 (0) 20 6009660
E-Mail: info@kebs.org
Website: www.kebs.org

KEBS Centre, Popo Road
P.O. Box 54974, 00200 Nairobi
Tel.: +254 (0) 20 6005490, 6005506

Laboratory Test Report

Page 1 of 1

PRIVATE SAMPLE

REPORT UID: 20201005104546-V4
KEBS Sample Ref. No: BS202031899
Date : 5 October, 2020
1. Description of Sample: SODIUM SILICATE SOLUTION
2. Sample Submitted by: RAPHAEL EMMANUEL KUNGU
3. Customer Contact: RAPHAEL
4. Customers Ref No: PRIVATE
5. Customer's Address:
6. Lab Ref: KEBS/TES/INO-NAR/I/20
7. Date of Receipt: 10 September, 2020
8. Date Analysis Started: 20 September, 2020
9. Sample Submission Form No: 237996
10. Additional information provided by the customer:

11. Acceptance criteria-title and number of specification against which it is tested:
KS 2350:2012 Kenya Standard Specification for Sodium Silicate

12. Parameters tested and Method(s) of test: as listed in the report below:

LABORATORY TEST REPORT

No.	Parameters		Results	Requirements	Test Method No.	LOD
1.	Appearance		Opaque	-	Visual Inspection	
2.	Density	g/mL	1.53	1.25-1.7	KS2350:2012	
3.	Ratio of SiO2:Na2O		4.5:1	Not Specified	BS 6092	
4.	Silica as SiO2	% m/m	28.4	Not Specified	BS 6092	
5.	Sodium Oxide as Na2O	% m/m	6.4	Not Specified	BS 6092	
6.	Specific Gravity		1.53	-	TZS 219	
7.	Total Alkalinity	% m/m	6.35	5-20.2	KS 2350:2012	
8.	Total Solids Content	% m/m	45	Not Specified	KS 2350:2012	

CAUTION: ... submitted sample and all details in respect of the ... products are not verified or confirmed

This report refers to a privately ... source and test results of ...

COMMENTS/REMARKS:
The sample performed as shown
NB: This test report supersedes the earlier Report UID Number: 20201005100001-V3

Tom O. Okumu - Manager Inorganic Chemistry Laboratory — 5 October, 2020
FOR: MANAGING DIRECTOR — **Date of Issue**

The results contained herein apply only to the particular sample(s) tested whose sample submission form serial number is herein quoted, and to the specific tests carried out, as detailed in this Test Report. No extract, abridgement or abstraction from a Test Report may be published or used to advertise a product without the written consent of the Managing Director, KENYA BUREAU OF STANDARDS. If undelivered, please return to the address written above.

Appendix IV: Provisional patent application

JOMO KENYATTA UNIVERSITY OF AGRICULTURE AND TECHNOLOGY

P.O. BOX 62000(00200) **NAIROBI**, Tel:(067) 52124/52028 ext. 2319 or 4062
Main Campus, Juja, Thika Road
Directorate of Intellectual Property Management and University-Industry Liaison

Our Ref: JKU/2/111/07/P

Your Ref: New

Date: 30th August, 2018

The Managing Director
Kenya Industrial Property Institute
P.O. Box 51648-00200,
Nairobi

Dear Sir,

RE: REQUEST FOR PROVISIONAL PATENT APPLICATION

We would like to file the above application for our invention entitled *"Process for Manufacture of Liquid Sodium Silicate and High Purity Grade Silica Gel for Industrial Use from Rice Husk Ash"*.

Attached herewith please find Provisional Patent Disclosure, Form IP 3, Form IP 4 and payment of **Kshs. 1,000/-** for your necessary action.

We look forward to receiving a priority date and number as soon as possible.

Eng. B. K. Kariuki, P. Eng, MIEK, MNQI, MAEE, CEM.
Director, Intellectual Property Management and University-Industry Liaison
Encls.

DIPUIL
Jomo Kenyatta University Of
Agriculture & Technolgy, Juja

Appendix V: Research license

REPUBLIC OF KENYA

NATIONAL COMMISSION FOR SCIENCE,TECHNOLOGY & INNOVATION

Ref No: **970825**

Date of Issue: **10/October/2019**

RESEARCH LICENSE

This is to Certify that Mr.. RAPHAEL KUNGU of jomo kenyatta university college of agriculture and technology, has been licensed to conduct research in Embu on the topic: SYNTHESIS AND CHARACTERIZATION OF INDUSTRIAL CHEMICALS FOR APPLICATION IN ENVIRONMENTAL POLLUTION CONTROL FROM RICE HUSKS for the period ending : 10/October/2020.

License No: **NACOSTI/P/19/1075**

970825

Applicant Identification Number

Director General
NATIONAL COMMISSION FOR SCIENCE,TECHNOLOGY & INNOVATION

Verification QR Code

NOTE: This is a computer generated License. To verify the authenticity of this document, Scan the QR Code using QR scanner application.

Appendix VI: Abstracts

ABSTRACT ONE

Green Chemistry Preparation and Characterization of Rice Husk Derived Silica Gel in Kenya

Raphael Kungu[1], Paul Njogu[1], Robert Kinyua[2] and Jackton Kiptoo[3]

1. *Institute for Energy and Environmental Technology, Jomo Kenyatta University of Agriculture and Technology, Nairobi 62000-00200, Kenya*
2. *Department of Physics, Jomo Kenyatta University of Agriculture and Technology, Nairobi 62000-00200, Kenya*
3. *Chemistry Department, Jomo Kenyatta University of Agriculture and Technology, Nairobi 62000-00200, Kenya*

Abstract: Rice is a grass seed from *Oryza glaberrima* species also known as the African rice. In Kenya, rice is mostly grown in Central (Mwea) and Nyanza (Ahero, West Kano, Migori and Kuria) areas. Milling rice produces rice husks as by-products which can be sources of valuable chemical products (silica gel, sodium silicate). In trials to produce silica gel from rice husks, rice husks were charred in a combustion chamber (30 min) then ashed in a Muffle furnace (Advantec KL-420) at different temperatures. The ashes were then leached with distilled water/acids to remove metal oxides. Sixty grams (60 g) of the leached RHA (Rice Husk Ash) was mixed with 300 mL of 3 M NaOH solution in a Pyrex 500 mL beaker and boiled at 100 °C (1 h). The silica gel samples were characterized using several methods. Elemental analysis was done using TXRF (Total X-Ray Fluorescence), while FTIR (Fourier-Transform Infrared Spectroscopy) was used to obtain an infrared spectrum of absorption of the silica sample. Results of the analysis conform to local and international quality standards. The rice husks had an average moisture content of 7.07% and 1.00-2.00 mm diameter. And 1.74% of the rice husk had pore sizes of about 0.710 mm. The average ash content was 22.65%. At 600 ℃ ,leaching with water yielded 98.2% silica compared with 99.1% (H_2SO_4) and 96.9% (HCl). At 500 ℃, leaching with HCl/H_2SO_4 causes a decrease. At 500 ℃, the availability of SiO_2 is more for water leached samples. At 400 ℃, water leaching gave 98.49% silica while HCl leaching was 97.85% silica and H_2SO_4 was 99.41%. Silica is a precursor of silica gel. Statistical analyses imply water leaching RHA instead of acid leaching at 500 ℃ will produce a significant amount of silica gel. The open burn samples produced equal or better SiO_2 (silica gel precursor) yields compared with the incineration samples. FTIR analysis of the silica gel sample compared well with adsorption peaks of silica gel in literature. XRD (X-Ray Diffraction) analysis produced a pattern consistent with other XRD patterns of silica gel published by other researchers.

Key words: Rice husk conversion, silica gel synthesis, green chemistry, ideal conditions.

ABSTRACT TWO

Development of Novel Products from Agro-Wastes (Rice Husks) and Characterization in Kenya

Raphael Kungu[1], Paul Njogu[1] and Robert Kinyua[2]

1. Institute for Energy and Environmental Technology, Jomo Kenyatta University of Agriculture and Technology, Nairobi 62000-00200, Kenya

2. Academy Division, Jomo Kenyatta University of Agriculture and Technology, Nairobi 62000-00200, Kenya

Abstract:

Rice growing is a popular agricultural activity in some areas in Kenya. The challenge is in the disposal of RH (Rice Husks). Rice production results in 20% RH as byproduct. Simple incineration of RH results in RH ash which is a source of valuable chemical products. The ash is 87-97% silica, highly porous and light weight, with a very high external surface area. The end product of RHA (Rice Husk Ash) after chemical treatment, sodium silicate, is a precious commodity that has myriad applications especially in detergent manufacture and soap production. The objective was to determine the best conditions to synthesize silica from agro-wastes (RH) in Kenya. The yield (% SiO_2) of the HCl (Hydrochloric Acid) leached RH at 500 °C was the highest at 99.2%. Overall these conditions were the best in producing silicate. Percentage (%) removal of each metal is different due to its chemical form in RH. The removal percentage of K is especially remarkable. And 0.5 M HCl leaching followed by thermal treatment of 600 °C gave the best increase in % silica dioxide. The same process removed the most metallic impurities (P_2O_5, K_2O, CaO, Mn and Zn). Leaching with 0.5 M HCl followed with thermal treatment of 500 °C gave the best overall yield in % silica dioxide. An increase in temperature from 600 °C slightly reduced the % silica dioxide content. The 0.5 M HCl used in these trials was able to produce 99.17% silica content from the Mwea RH. The SiO_2 obtained with the water washed RH sample is 97.37% as compared 99.17% (HCl-washed) and 99.02% (H_2SO_4 (Sulphuric Acid)-leached). The FTIR (Fourier Transform Infrared Spectroscopy) spectra indicates HCl leaching avails more silica content than H_2SO_4 leaching.

Key words: RH conversion, acid leaching, silicate, sodium silicate, ideal conditions.

ABSTRACT THREE –SRI conference paper

Removal of Color from Tea Processing-Industrial Effluents Using Low-Cost Novel Activated Carbon Derived from Agro-Wastes

[1]Raphael kungu, [1]Paul Njogu, [2]Robert Kinyua

[1] Institute of Energy and Environmental Technology, Jomo Kenyatta University of Agriculture and Technology, P.O. Box 62000- 00200 Nairobi, Kenya

[2]Academic Division, Jomo Kenyatta University of Agriculture and Technology, P.O. Box 62000- 00200 Nairobi, Kenya

***Abstract*—** Rice is grown globally as a food crop. Rice husks are products of rice milling. Disposal of rice husks creates health and environmental problems. The carbon contained in rice husks can be activated with sodium hydroxide (NaOH) and phosphoric acid (H_3PO_4) to produce efficient liquid pollutant adsorbents. The objective of this study was to study the application of Rice husk-derived Activated Carbon (AC) in wastewater pollution control. Samples of rice husks were collected from Mwea, Kenya. Rice husks were washed; oven-dried, portions were treated with NaOH, digested, and dried in the furnace. The process was repeated with Phosphoric acid. Resultant Activated carbon was tested for adsorption of organic compounds in tea processing wastewater using UV and FTIR spectroscopy. Tea Processing-Industrial Effluents were collected from Tea Factories in Nyeri County, Kenya. Results indicated that NaOH-activated carbon had 35 times more efficiency in total phenols removal. 72-77% efficiency was recorded compared with 2.6% for H_3PO_4-activated carbon. FTIR analysis showed peaks at 1737, 1369, and 1226 cm^{-1} representing sites associated with Esters, Carboxylate, and Aromatic CH in-plane bond. Sodium hydroxide activated rice husks (RH) carbon had similar active sites at 1740, 1365 and1217cm^{-1}. Results reveal that RH-derived activated carbon can be employed as low-cost alternatives to commercial activated carbon in effluent treatment. Due to its low cost and renewability, it is an excellent adsorbent material for organic pollutant removal.

***Keywords*—** activated carbon, pollution, wastewater.

Appendix VII: Experimental data

1. Equilibrium data from experimental trials for Pb (II), Cd (II) and Cr (IV)

Pb(II)					**Cd (II)**				
Ce	**qe**	**t/qt**	**qt**	**ln(qe-qt)**	**Ce**	**qe**	**t/qt**	**qt**	**ln(qe-qt)**
0.420	0.531	0.389	-1.366	-0.311	0.182	1.512	0.087	-1.461	0.363
0.291	0.432	0.581	-1.274	-0.210	0.147	1.677	0.203	-1.223	0.324
0.421	1.513	0.497	-0.129	0.178	0.224	2.042	0.119	-1.532	0.717
1.214	1.932	0.581	0.116	0.549	0.319	2.532	0.112	-1.363	0.997
Cr(VI)									
Ce	**qe**	**t/qt**	**qt**	**ln(qe-qt)**					
0.287	2.114	0.772	0.833	0.661					
0.438	3.139	0.117	-0.889	1.134					
0.712	3.432	0.169	- 0.209	1.374					
0.598	4.339	0.151	-0.305	1.398					

2. Kinetics data from experimental trials for Pb (II), Cd (II) and Cr (IV)

Pb(II)					**Cd (II)**				
Ce	**qe**	**t/qt**	**qt**	**ln(qe-qt)**	**Ce**	**qe**	**t/qt**	**qt**	**ln(qe-qt)**
0.451	0.9673	4.686	0.249	-0.6666	0.1301	1.3116	11.46	0.3545	-0.085
0.234	0.9711	7.36	0.3771	-0.5432	0.0771	1.3205	17.48	0.3642	-0.079
0.167	0.9773	11.09	0.413	-0.5324	0.0472	1.3255	22.45	0.39644	-0.075
1.158	0.9799	14.912	0.3884	-0.5198	0.0415	1.3264	30.52	0.39642	-0.074
Cr(VI)									
Ce	**qe**	**t/qt**	**qt**	**ln(qe-qt)**					
0.0359	1.2280	5.41	0.3567	-0.0720					
0.0139	1.4284	9.45	0.3678	-0.0719					
0.0177	1.4277	11.61	0.3796	-0.0610					
0.0180	1.4279	14.71	0.3996	-0.0558					